STUDIES IN: (A) RECYCLING POLYESTERS & NYLONS BY DEPOLYMERIZATION TO ITS CONSTITUENT MONOMERS USING PHASE TRANSFER CATALYSTS & (B) SYNTHESIS AND COMPOSTABILITY OF NEWLY DESIGNED POLYESTER MOLECULES

By

Shrirang Sabde

A DISSERTATION

Submitted to
Michigan State University
in partial fulfillment of the requirements
for the degree of

Chemical Engineering – Doctor of Philosophy

2024

ABSTRACT

Plastic waste management is a colossal problem for modern society, that has resulted into several legislations and technological solutions across the world. Waste plastic can be part of the circular economy by their catalytic conversion into monomers and useful products. This work presents development and design of technologies to solve plastic waste issues using depolymerization, re-polymerization and composting. In the first part, depolymerisation of polyethylene terephthalate (PET) and Nylon 6 waste was studied using 2-L high pressure autoclave reactor at molten state and autogenous pressure in the presence of excess of water under subcritical conditions for various time intervals. Operation parameter such as reaction temperature, time, and concentration for both catalysts were studied. The obtained monomers (terephthalic acid (TPA) and ethylene glycol) were characterised by qualitative and quantitative analysis. In comparison with zinc acetate (used before), PEG 400 was the best catalyst. Concentration profiles were developed for PET, oligomer and terephthalic acid (TPA) using HPLC. A new mechanism of solid (polymer)-liquid(melt)-liquid (water) phase transfer catalysis (PTC) for hydrolysis was proposed and validated. This work is published in the Journal of cleaner production[1](doi.org/10.1016/j.jclepro.2023.138312).

A similar approach was used for depolymerization of nylon 6 into 6-aminocaproic acid (ACA) in the first stage using PEG as the phase transfer catalyst and the aqueous phase containing ACA and PEG was subjected to dehydration and cyclization to caprolactam in the second stage. The hydrolytic depolymerization method was applied to nylon 6 by using pure water as depolymerization agent, reacting under subcritical water 230-250 °C and autogenous pressure, the reaction time was 60 min. PEG 400 was discovered as efficient phase transfer catalyst for hydrolysis of nylon 6. A new theory was developed to interpret dehydration of nylon 6 to 6-

aminocproic acid (ACA) where the reaction takes place in subcritical water phase. The highest yield of caprolactam reached 96% in reaction time of 60 min. plastic.

There is challenge of separation of plastic waste (i.e PET or Nylon) from organic waste. Our next approach was to prepare biobased and biodegradable/compostable polyester which can be used for preparation compostable bags. For this, the polymer must have a high molecular weight for processing conditions. So, this study aims to prepare high molecular weight biobased and biodegradable polyester. The polymerization synthesis methodology was developed to synthesize high molecular weight polymers (60-80 kg/mol) namely polybutylene adipate co-terephthalate (PBAT), polybutylene sebacate co-terephthalate (PBSeT), and polybutylene azelate co-terephthalate (PBAzT) were synthesized using a developed methodology. The polymers obtained were characterized by intrinsic viscosity, acid number, and molecular weight and compared with a commercial polymer. The extent of reaction was determined by monitoring acid group in the reaction mixture.

Next step, the food waste and compostable bags were mixed with a composition of brown and green. The reactor feed composition was maintained the same for all experiments. Various runs were conducted at different temperatures. The percent loss of dry mass was calculated by ASTM-D2974 method. The compostable bags were observed by visual inspection and pictures were recorded for it. It was observed that within 8-10 days all bags disintegrated and disappeared from the mixture.

Overall, this work contributes to the concepts of circular economy and developing sustainable technology. Study of depolymerization using solvolysis, repolymerization for redesigning polymer for end of life will help to solve the issues of menace by plastic waste.

Dedicated to my parents, and almighty God

ACKNOWLEDGMENTS

I would like to express my sincere gratitude to my advisors, Dr. Ganapati D. Yadav, Institute of Chemical Technology (ICT), India and Dr. Ramani Narayan, Michigan State University (MSU), USA for providing me with Dual Ph.D. degree opportunity as part of a collaboration between ICT and MSU to pursue Ph.D. in Department of Material Science and Chemical Engineering. It was my pleasure working under such eminent scientists. They always motivated me to work hard, be smart, be creative, and keep work standards high. I extend my gratitude to all my committee members (Prof. Andre Lee, Prof. Scott Barton, Prof. Muhammad Rabnawaz, Prof. Robert Ferrier, and Prof. Lakshmi Kantham) for the questions and comments that lead me to think more deeply about my experiment and results. I want to thank Sean Barton from MSU Recycling center and Brody Dinning Hall for providing food waste for a composting study. Natur-Tech, USA for providing compostable bin liner samples. I want to thank Roger Cargill, founder of Finite Phoneix's, for his support in repairing and maintaining the bioreactor system. I heartily acknowledge ground-level help in the laboratory of my lab mate (Badal Lodaya), visiting scholar (Dr. Neha Mulchandani and Dr. Shehla Mushtaq), and undergraduate students (Carmen Rose, Ryan Stearns, Olga Stathis, Darian Mason, and Nicole Hanshaw)

TABLE OF CONTENTS

Chapter 1

Introduction

1.1 Polymer waste

Polymers are essential in everyday life because they are a broad and friendly application. Thus, the mass production of polymers has increased over the last few decades. United States (EPA) report from 1960 to 2015 mentioned that the waste developed percentage has risen to 8 % [2]. The plastic industry has diverse applications in various industries like packaging, automotive, agriculture, etc., which is approximately 41.5 million tons of total plastic consummation(Plastics Europe (PEMRG) / Consultic / ECEBD-2013)[3]. A significant portion of the landfill is shared by plastic waste. There is a need to process the landfill. There are various challenges available for recycling waste plastic to new plastic or value-added materials.

1.2 Challenges and need for polymer recycling

Plastic's diverse application and the product is a significant issue with polymer waste management. Because the collection and segregation become complex altogether for polymer waste [4], as in the case of metal, wood, and glass waste does not have such complex challenges[5]. The recycling of metal is easy because of uniformity in waste, due to which the recycling percentage is high for metal. The principal activity in polymer recycling is the separation of MSW (Municipal solid waste) to PSW (polymer separated waste)[6]. These are divided into two groups- polymer with carbon backbone (i.e., addition polymer-PP.PE, PS) and polymer with heteroatom in the backbone (i.e., condensation polymer-PET, Nylon, PU)[7].

1.3 Polymer recycling approaches

Polymeric waste can be recycled by four main methods such as *primary recycling, mechanical recycling (secondary), chemical recycling (Tertiary), and energy recovery (quaternary)*[8]. Depolymerization is tertiary recycling technique and an axiomatic approach to green sustainability. Among these approaches, solvolysis is an ideal, sustainable, green method for processing polymer waste [9][10]. The Mechanism involves breaking a polymer chain with the help of a solvent. It is called solvolysis, such as ***methanolysis, hydrolysis, glycolysis, and aminolysis*** [11]. Although the chemical recycling process has the potential of a zero-emission recycling technique, many challenges have to be resolved before establishment on a practical scale. These problems can be divided into three categories: 1) Economical and 2) Technical, and 3) chemistry involved.

1.4 Feedstock recycling and challenges

The current approach to recycling polymer is a non-integrated initiative; in other words, technical and economic difficulties have been dealt with independently. However, there is a need for an integrated approach that will give a practical and sustainable process.

1.4.1 Economical challenges

The cost of recovered adipic acid is higher than the virgin, making the entire recycling process unfeasible. Because one of the prime objectives of chemical recycling is to decouple the polymerization with the petroleum-based product.

1.4.2 Technological challenges

Technical challenges associated with chemical recycling are mainly: 1. Segregation of nonpolymeric and olefins from polymer waste 2. Depolymerization 3. Purification of recovered monomer 4. Re-polymerization of recovered monomer (14).

1.5 Present recycling

Condensation polymer was monomerized by solvolysis, mostly with supercritical water or alcohol. Also, the addition polymer successfully decomposed in supercritical and subcritical fluids. For the crosslinked polymer, the supercritical fluid was excellent in recycling. Nylon recycling survey, the depolymerization on a commercial scale, has used hydrolysis and ammonolysis technique. The PET recycling survey lists companies describing depolymerization technology and research activities. The process becomes abortive if depolymerization results in a complex mixture of monomers and their decomposed product.

1.6 The objective of the current proposal

Develop a chemical recycling process that will be robust to polymer waste. Polymer waste consists of additives, olefins, stabilizers, etc., incompatible with the depolymerization process. Recycling plastic into monomers is conventional practice, but there is a need to change this trend. For most of the methods, the recycling cost of the monomer is higher than the virgin monomer, which lacks the process. It is proposed to convert these monomers into value-added products with novel catalytic pathways, which will increase attraction for recycling. Another objective is to integrate the depolymerization and compost process. This integration will convert biodegradable polyester into compost. Depolymerization of polyester waste into compost rector will remove segregation challenges.

Chapter 2

Depolymerization of PET using phase transfer catalyst

2.1. Introduction

It is impossible to conceive of modern life without the use of plastics in one form or the other. The plastic market size in the world was valued at USD 609.1 billion in 2022 which is expected to grow at a compound annual growth rate (CAGR) of 3.7 % up to 2030 [12]. Plastics such as Polyethylene Terephthalate (PET) and Polycarbonates (PC) are employed in the packaging of apparel, beverages, appliances, consumer goods, toys, etc. (Cornago et al., 2021). PET is extensively used in food packaging, fibers, audiotapes, videotape, containers, etc. In particular, the packaging of appliances is likely to offer financial opportunities for market growth. The colossal demand results into massive plastic consumption, resulting in exorbitant amount of waste which is not properly disposed leading to environmental degradation. Plastic recycling, both physical and chemical, has received tremendous attention for two reasons: pollution abatement and valorization of plastic waste which has become part of the circular economy.

PET does not directly pose a hazard to environment and human beings[16]. It is totally recyclable and is the most widely recycled plastic globally ranging from 60-90 % with India topping the list. PET mainly contains high aromatic compounds that are stable and inert, which hinder microbial degradation [17]. However, there are various researchers who have reported microbial degradation of PET [18,19]. Furthermore, enzymatic routes were studied to increase productivity, reaction kinetics and stability of enzyme at high temperature by Biundo et al. (2018) and Castro et al. (2019). Engineered depolymerase showed enzymatic depolymerization of PET to 90 % conversion in 10 h [20]. *Humicola insolens cutinase* (HiC) was used as an enzymatic catalyst for PET depolymerization into terephthalic acid (TPA), ethylene glycol (EG)

and bis(hydroxyethyl)terephthalate (BHET) in 7 days at 70 °C [21]. The foregoing reports not only show microbial catalytic routes for PET depolymerization but also suggest their potential to create a circular economy for polyester recycling. Therefore, an economic and eco-friendly process is needed to create a circular economy for the treatment of plastic waste. Plastic recycling presents a massive economic incentive to get feedstock and environmental protection due to the excessive consumption of non-renewable feedstock. In Europe, 4-6 % of oil and gas is consumed for the production of polymer materials [22]. Plastics should be part of the circular economy since 98% pure feedstock is used to generate 78 million tons of plastics; globally 72 % of plastic is not recovered at all whereas 40 % is landfilled and 30 % is leaked to the environment. As mentioned before PET is the highest among all recycled plastics, in which 14 % is used for energy generation [15], 14 % for cascade recycling and 2 % for circular recycling [17]. Quantities for recycled plastics are very low compared to the global recycling rate of paper (58 %) and iron and steel (70-90 %)[15].

A new realization is that plastic waste should be considered as a resource rather than burden and innovative technologies and policies for recycle must be enacted by local governments. Polymeric waste can be recycled by four main approaches: *Primary Recycling, Mechanical Recycling (Secondary), Chemical Recycling (Tertiary), and Energy Recovery (Quaternary)* [23]. The recycling techniques of primary and secondary, classified as mechanical recycling, vary in the amount of recycling material [24]. Chemical recycling, upcycling and downcycling can be a good strategy to overcome the plastic waste menace. It is also termed as feedstock recycling which can further be categorised in three main approaches: depolymerisation into its monomers, solvolysis, partial oxidation and cracking (thermal, catalytic[25], hydrogenation[26], oxidation [17], etc.).

Thermochemical methods and solvolysis of plastics are both chemical recycling processes. Thermochemical process is carbon renewable technology and hydrolysis is polyester renewable technology. Both processes have their own limitations. Thermochemical process is better for dealing with carbon-carbon backbone polymer recycling. It would be better to design a system which is combination of solvolysis and pyrolysis for mixed plastic (polyester +carbon-carbon backbone polymer) for carbon management. However, thermochemical process requires high temperature (~500-700°C) in comparison to solvolysis for breaking a polymer chain. In thermochemical process[27], the breaking of polymeric chain, whether random or selective, depends upon nature of catalyst. Likewise, in catalytic pyrolysis of plastics, the product is distributed in gas, liquid and solid phases [28]. Also, high entropy alloy is used in thermochemical degradation of plastic banner waste. The yield of benzoic acid and phthalic acid is found to be 70-75 % and 15-20 %, respectively [29]. The major limitation of thermochemical process is yield of desired product and demand for high energy. However, this process is helpful in recycling carbon-carbon backbone polymeric waste. On the other hand solvolysis process uses solvent as agent to break the plastic linkage. Solvolysis has a limitation to deal with carbon-carbon backbone polymeric waste. Treatment of nylon using thermochemical process yields the product which is mixture of Caprolactam, CH_4 ,CO_2 and CO [26,30]. However, it is convenient to convert ester into monomer by solvolysis with less product distribution. The recovered monomer can be further used for polyester synthesis.

Depolymerisation is an axiomatic approach to green sustainability. Among these approaches, solvolysis is the most ideal, sustainable, green method for processing polymer waste. The mechanism involves chain scission of the polymer with the help of solvents. Solvolysis methods are named on the basis of solvents used for depolymerisation such as methanolysis [31],

hydrolysis [32], glycolysis [33], and aminolysis [34] and ammonolysis. These methods are extensively reviewed in the literature [15] and effective depolymerisation is carried out with supercritical or subcritical fluids; for instance, water or carbon dioxide [35], thermolysis [36], and ionic liquid [37]. Most of the techniques consist of acidic [38], alkaline (López-Fonseca et al. 2009) and expensive or hazardous chemicals [40] using harsh reaction conditions. Depolymerization into monomer needs to possess desirable purity to be utilized in the re-polymerisation process. Neutral hydrolysis gives a mild separation process of product (monomer) and catalyst recovery. Depolymerization with volatile organic compounds can be responsible for the greenhouse effect, depletion of ozone layer and global warming. Hence, depolymerization needs to be done by neutral hydrolysis [41].

Polyethylene glycol (PEG) 400 is well known for widespread medical and industrial applications; it is soluble in polar and non-polar compounds. While PEG is generally used as a solvent, it can also be used as a catalyst in phase transfer catalysis (PTC) [42]. Various phase transfer catalysts have been deployed in depolymerization, which may require less severe temperature conditions [43]. However, these phase transfer catalysts are uneconomical because of longer reaction times, non-reusability and environmental liability [44]. Most of PET hydrolytic depolymerisation has been studied in the presence of metal acetate and ionic liquids (Al-Sabagh et al., 2014; Tincu et al., 2022). Depolymerization reaction above melt phase has been studied in reactive extrusion without catalyst. It shows 18-30 % conversion in less than 10 min residence time. In reactive extrusion, the depolymerization conversion prominently depends upon temperature, residence time, pressure, water to PET feed ratio, etc.[49]. Also, alkaline hydrolysis with deep eutectic solvents was used for PET depolymerization in microwave reactor, but the conversion of PET into TPA found to be 80- 82 % (Attallah et al., 2021).

PET depolymerization using acidic, basic or neutral hydrolysis leads to several problems such as monomer instability in the reaction mixture, onset of secondary reactions and need for longer reaction time (de Carvalho et al., 2006;Liu et al., 2012). For example, in neutral hydrolysis, subcritical and supercritical depolymerization with zinc acetate is reported to cause dehydroxylation and dimerization of ethylene glycol (EG) [51]. However, hydrolysis in the presence of PTC has no such undesirable reactions [43]. Depolymerization with PTC is mostly studied below melt phase, because of the lack of stability of ammonium salts based PTC at higher temperature. Although PTC-assisted depolymerizations have been conducted at lower temperature resulting higher yields, they suffer with excessive reaction time because these are solid-liquid (S-L) PTC reactions [43,52].

In alkaline hydrolysis of PET, formation of salt with dimer or timer of terephthalic acid (TPA) was found, which might have affected the yield of TPA[50]. As the breaking of a PET chain is due to a catalytic mechanism (Chen et al., 2013), a mixture with dimers or trimers of TPA may form sodium salt with NaOH [52]. Consequently, it could be measured as TPA, as there is no separation between monomer and dimer. Most of the researchers have studied the extent of PET depolymerization based on a titration method [53]. Indeed, in the case of complete depolymerization, this method may be applicable, but to study depolymerization behaviour, there is a need to have a reliable quantitative analysis such as HPLC and GC.

No research has appeared on using phase transfer catalysis for depolymerizing PET in neutral hydrolysis. In this work, a systematic analysis of the depolymerisation of PET using polyethylene glycol (PEG) 400 as the phase transfer catalysis was done and kinetics of the process reported. It is an interesting case of multiphase transfer catalysis (Yadav 2004, 2021). PEG 400 is stable under reaction condition unlike other ammonium or phosphonium based

catalysts and is inexpensive, readily available and biodegradable. In addition, depolymerisation based on ester linkages (carbonyl to carboxyl group) was studied and compared by HPLC analysis. In depolymerization, polymer chain scission is not necessarily ordered, but mostly random, i.e., formation of various oligomers. The formation of various oligomers limit the analysis process. A new method was thus developed for the analysis of oligomers and monomers. The overall process is an excellent example of circular economy through polymer (chemical) recycling.

2.2. Materials and methods

2.2.1 Material

PET flakes with sizes of 5-0.8mm, were procured from Reliance Industries Ltd (RIL), Mumbai, India and PEG 400 from S. D .Fine Chemical, Mumbai. High purity HPLC grade water was used. All other chemicals used were of analytical grade obtained from reputed vendors.

2.2.2 Experimental

A stainless-steel autoclave (Amar Equipments, Mumbai, India), with internal diam.75 mm, volume 300 mL, standard 4-blade pitch turbine impeller, equipped with proper agitation, heating arrangements and controllers, was used for all hydrolysis experiments. The reactor was preheated to 80- 90 °C and the reactants added. The control experiment was done by using 111 mol H_2O/mol PET, 0.0021 mol of PEG 400/cm3. Typical experiments were done at 240°C. The melting temperature of the resin was calculated to be 240 °C by differential scanning calorimetry (DSC). The polymer melt phase played an important role and the time required for the polymer to melt entirely was governed by the initial water to PET molar ratio (W/P) charged to the reactor. Complete melting occurred at 240 ºC which was achieved in 25-35 min depending on the W/P ratio (**Fig. A1.1**). Once the melting occurred, it was taken as zero time. Since periodic sampling

was not possible, independent experiments were done for different time intervals for the same W/P ratio to study the kinetics. After the desired time interval, heating was stopped, the reactor removed and quenched quickly in an ice bath. The reaction mass temperature dropped immediately to 100 °C within a minute of quenching. It would solidify the unreacted polymer, if any. Subsequently, the reactor was opened, and the product removed. The product was separated into two-phase (solid and liquid) using a sintered glass filter. No further washing was performed with cold water to remove any residual water-soluble components, such as ethylene glycol (EG) monomer. The aqueous phase composed of EG, water, PEG 400. Glycol presence was identified by Agilent 6890 GC (Agilent Technologies, USA) with a DB-5 capillary column (0.25μm×0.25mm×30 m with 5 % diphenyl/95 % dimethyl polysiloxane packing) and an FID (flame ionization detector). The GC method was set starting at 70 °C for 2 min with a ramp rate of 10 °C/min until 210 °C with a H_2 flow rate of 30 mL/min and N_2 as a carrier with a flow rate of 30 mL/min. The injection volume of the sample was 2 μL. The quantification of EG and presence of PEG 400 in liquid was done through HPLC-ELSD analysis. Recovered solid was dried at 80 °C under vacuum to a constant weight. The solid was ground using a mortar and pestle into a fine powder for analysis.

2.2.3 Qualitative analysis of decomposed PET

Solid samples were recovered from hydrolytic reaction at various time intervals and used for the thermal behaviour by DSC and TGA (Perkin Elmer STA 6000) and XRD (Bruker AXS diffractometer, Cu-K radiation of wavelength 154 nm, at gazing angle (10°) 2Θ scan). The weight loss and percent crystallinity from 30 to 350 °C with heating and cooling cycle with rate of 10 °C per min in nitrogen atmosphere provided the thermal history of material. The mass spectra of the products were obtained on an ISQ single quadrupole MS (Thermo Scientific)

instrument with electron ionization (EI). Fourier transform infrared spectroscopy (FTIR) of samples was performed with Perkin Elmer spectra BX spectrophotometer in KBr pellets between 4,000 and 300 cm^{-1}. CP/MAS ^{13}C NMR was conducted to investigate changes in the structure of decomposed PET using a JEOL JNM-ECA 500 spectrometer with an NM-93030 CPM probe. The solvent used for ^{13}C NMR and ^{1}H NMR was DMSO-d6 and the results were compared with the standard TPA pattern.

2.2.4 Quantitative analysis

The foremost difficulty in hydrolytic depolymerisation of PET is to find a method for quantifying the extent of hydrolysis as a function of reaction time. Previous literature on evaluating the extent of hydrolysis covers intrinsic viscosity, infrared analysis, end group analysis and gel permeation chromatography (GPC). However, these techniques are satisfactory for PET hydrolysis below the melt phase [54] since complete depolymerization quantification includes fragmented oligomers to final monomer and unreacted polymer. PET recycling using DMSO and hydrotalcite was studied by [40] to produce a wide range of oligomer formation wherein their structural characterization were achieved by mass spectrometry with complementary NMR analysis. Solvent system used for calculation is required to be such that non-polar and polar oligomers become soluble. The identification of the main product of hydrolysis was done using HPLC with reversed phase C-18 column. The mobile phase was a mixture of acetonitrile: water (0.1 % trifluoracetic acid)-20:80 with flow rate of 1.0 ml/min. Detection was done using UV detector at 280nm. The solid sample was dissolved in DMSO and diluted using methanol. TPA was confirmed by matching commercial TPA residence time (RT). A standard curve was used for HPLC analysis.

$$\%\ yield\ of\ TPA(x) = \frac{n_{TPA}}{n_{TPA0}} \times 100 \quad (1)$$

Where,n_{TPA0} is theoretical concentration (in M (mol L^{-1})) and n_{TPA} is terepthalic acid concentration at any time (M). n_{TPA0} is calculated from degree of polymerisation of the polymer flakes used for experiments.

$$n_{TPA0} = C_{P0} \times n \quad (2)$$

Where, C_{P0} is PET initial concentration in M and n is degree of polymerisation.

In HPLC, two peaks were observed for reaction samples drawn. After more than 3 min whereas after 30 min sample showed only one peak. The first peak was identified as TPA and second peak as oligomer. The complementary analysis using MS-EI showed the molar mass of reaction samples (at 3 ,10, 15 min) 166 and 211-311 Da.

HPLC and end group analyses were done and compared because they correlated with scission of ester linkages, which related to the kinetics of hydrolytic depolymerisation as shown in **Scheme 2.1**.

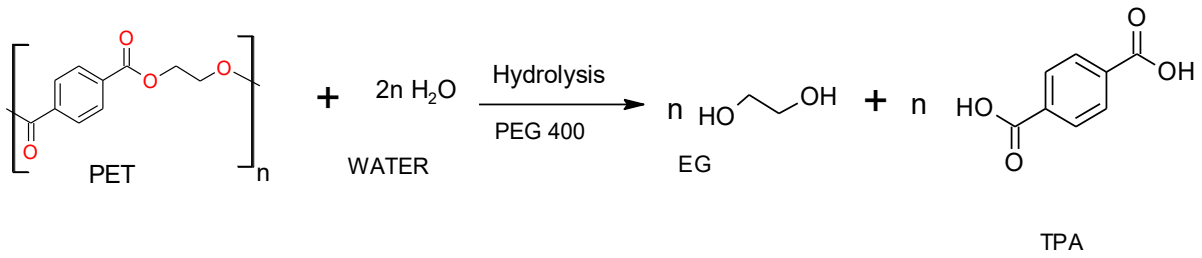

Scheme 2.1. Reaction scheme for PET hydrolysis.

The reaction extent was determined by the analysis of the solid phase for carboxyl group content. Titrimetric method was used for the two solvent system depending upon solid product solubility, i.e. extent of hydrolysis, as described elsewhere (Khalaf and Hasan 2012; Campanelli et al. 1993). Each chain scission gives one carboxyl end group, and hence measuring carboxyl group present at various reaction times gives the extent of depolymerization. The conversion of ester linkages calculated by using following relation:

$$\%\ conversion\ of\ ester\ linkages(Carbonnyl\ to\ carboxyl)(x) = \frac{C_{COOH}}{C_{EL0}} \quad (3)$$

Where,C_{EL0} is Initial ester linkage concentration (mol/g polymer) and C_{COOH} is carboxyl group concentration at any time (mol /g polymer).

The statistical values were reported by taking a mean of three readings of conversion from three acid value for a specimen. Standard deviation in conversion was calculated using following equation:

$$Standard\ deviation = \sqrt{\frac{\sum(\bar{x_i} - x)}{n-1}} \quad (4)$$

Where, $\bar{x_i}$ is average conversion and x is conversion at any time.

The liquid phase was analysed for EG and PEG400 by HPLC and HPLC-ELSD respectively, using an Agilent BDS C8 column (4.6 mm × 250 mm) with DI water (100 %) mobile phase at flow rate of 0.6 mL/min with RI detector. The yield of ethylene glycol was calculated as follows:

$$\%\ yield\ of\ EG(x) = \left(\frac{n_{EG}}{n_{EG0}}\right) \times 100 \quad (5)$$

Where, n_{EG0} is theoretical ethylene glycol concentration (M) and n_{EG} is ethylene glycol concentration at any time (M).

2.3. Results and discussion

Structural identification of products was done by using different analytical methods.

2.3.1 Structural identification of products of hydrolysis of PET using PEG 400

The structural identification of main product (solid phase) in the degradation of PET in water catalysed by polyethylene glycol 400 was performed by using different structural characterization tools such as DSC, TGA, FTIR, XRD, NMR, EI-MS.

2.3.1.1 DSC

Thermal analysis of the product received for various reaction time was performed with heating rate 10 °C/min. The thermal analysis of samples studied by DSC is depicted in **Fig. 2.1** which shows glass transition temperature (75 °C), crystallisation temperature (165 °C), and melting temperature (240 °C) for samples at different times; the variation in these properties provides is clearly seen. (**Table A2.1** (supplementary information, SI) provides the thermal properties and change in crystallinity of PET samples at various reaction time. As the reaction time increases glass transition temperature disappears, which proves the complete scission of the polymeric chain at 30 min. The cleavage of polymeric chain after 15 min reaction time shows melting onset temperature and peak temperature as 110.9 and 150 °C, which are identical with that for BHET. After 15 min reaction time, there was an absence of endothermic peak showing an amorphous nature of the material. After 30 min a sublimation curve is seen which is similar to that of terephthalic acid. Melting endotherm gives an idea about the structure of polymer; as the reaction time increases the endothermic peak broadens and shifts toward lower melting temperature. Broadening of endothermic peak increases the enthalpy of heat of sublimation and it decreases crystallinity [57][58], It is attributed to terephthalic acid, as is seen for reaction at 30 min (**Fig. 2.1**).

2.3.1.2 TGA

The TGA profile for reactant and products at various reaction times are shown in **Fig. A2.2 and A2.3**. The weight loss of ~ 92 % in the range of 390-400 °C for 0 min can be seen, which is caused by the thermal decomposition of PET. The first range of 200-300 °C shows nearly 40-50 % weight loss, for 5-15 min reaction time. For the second range of 390-400 °C, a weight loss in the range of 60-50 % was observed, which is attributed to thermal decomposition PET produced

in TGA process [59]. For the third range of 230-340 °C, weight loss of nearly 94 % can be seen for 30 min reaction time. The third range of temperature is attributed to terephthalic acid, and sublimation occurs before the decomposition temperature [60]. A similar trend is followed by PEG 400 hydrolytic product for 30 min reaction time.

2.3.1.3 XRD

XR diffractogram for different reaction samples is shown in **Fig. A2.4** (supplementary information, SI); due to high degree of crystallinity of PET it exhibits a typical pattern, with broader peaks at 2Θ= 16.4, 17.7, and 23.0. The crystallinity of PET is different from crystallinity of terephthalic acid; progressive decrease in molecular weight of polymer can be seen in Fig. A2 due to breakage of polymer. The JCPDS (Pattern: 00-031-1916) data show excellent match with that of terephthalic acid.

2.3.1.4 FTIR

Figure A2.5 shows FTIR of standard TPA and PET reaction conditioned with PEG 400 at different reaction times, PET shows a typical molecular vibration at 1734 (-C=O stretch, ester), 1,238 C-O, 1043 (–O-(CH_2)-O-), and 969 cm^{-1} C-O peaks of PET. FTIR shows carbonyl peak for all OH- stretch that keep increasing with increase in reaction time. As reaction time increases there was absence of ethylene glycol. These results are akin to the standard terephthalic acid [61] confirms that product as terephthalic acid.

2.3.1.5 ^{1}HNMR

The ^{1}HNMR for samples catalyzed by PEG 400 for 30 min reaction time had the following shifts shown in **Fig. 2.2** at δ 8.21 ppm. These spectra when compared with standard TPA are identical. After 10-15 min reaction the spectra indicates the presence of BHET, which is confirmed by the presence of signal for methylene protons of CH_2-OH, methylene group near –COO-, hydroxyl

group at δ 3.9, 4.4, and 4.1 ppm, respectively. When glycolysis of PET with mixed oxides is carried out in the presence of hydrotalcite, it formed BHET monomer with 50 min at 196°C [62], However, in our work using PEG 400 as a phase transfer catalyst, the hydrolysis of PET led to the formation of BHET monomer along with terephthalic acid within 10-15 min.

2.3.1.6 ^{13}C NMR

In NMR ^{13}C spectra for standard reference spectra for TPA and that for the hydrolysis of PET with PEG 400 at different reaction times as shown in **Fig. A2.6**, the signal at δ 129 ppm indicates aromatic protons of benzene ring, 167 (COOH), 134 (aromatic C adjacent to ester). However, for 15 min reaction time it shows similar spectra; in addition spectra of methylene carbon of COO-CH_2 and CH_2OH indicated signal at 4.963 and 3.73 ppm, respectively. Also, reference spectra for the commercial terephthalic acid when compared with 30 min reaction sample is identical which confirms that the product formed is TPA. NMR spectra of the hydrolysed product also suggests the purity of product formed in reaction is 99.1 %.

2.3.1.7 MS

The structural characterization of long chain high molecular weight molecules can be achieved by mass spectrometry (MS) [63], which is complementary to NMR analysis as a reliable structural identification tool. In recycling of PET with DMSO solvent and hydrotalcite catalyst, Sharma et al. (2013) obtained an oligomer, whose molecular weight was analysed by MS. In the current work, with PEG 400, the MS shown in **Fig. A2.7** shows molecular weight of 216 and 166 gm.mol^{-1}, which are identical to molecular weight of BHET and TPA for reaction times of 15 and 30 min.

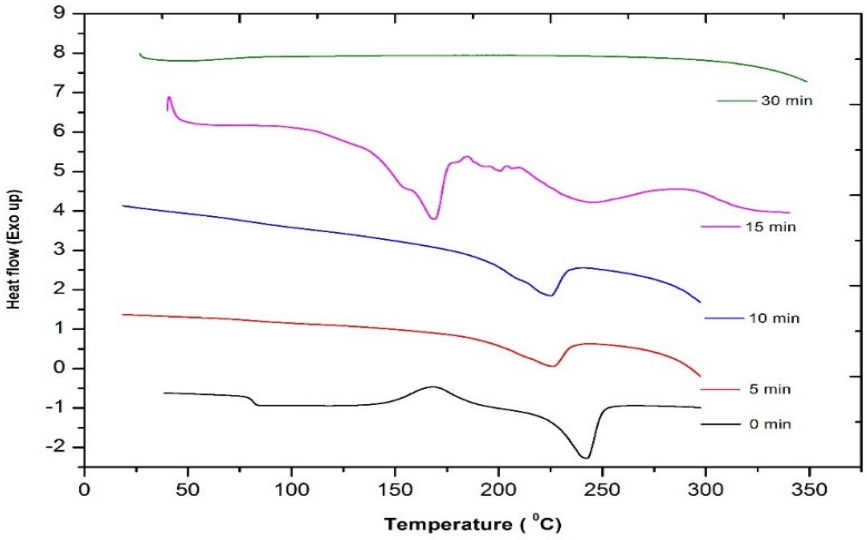

Figure 2.1. DSC plot of PET hydrolysis catalysed by PEG-400 at different times.

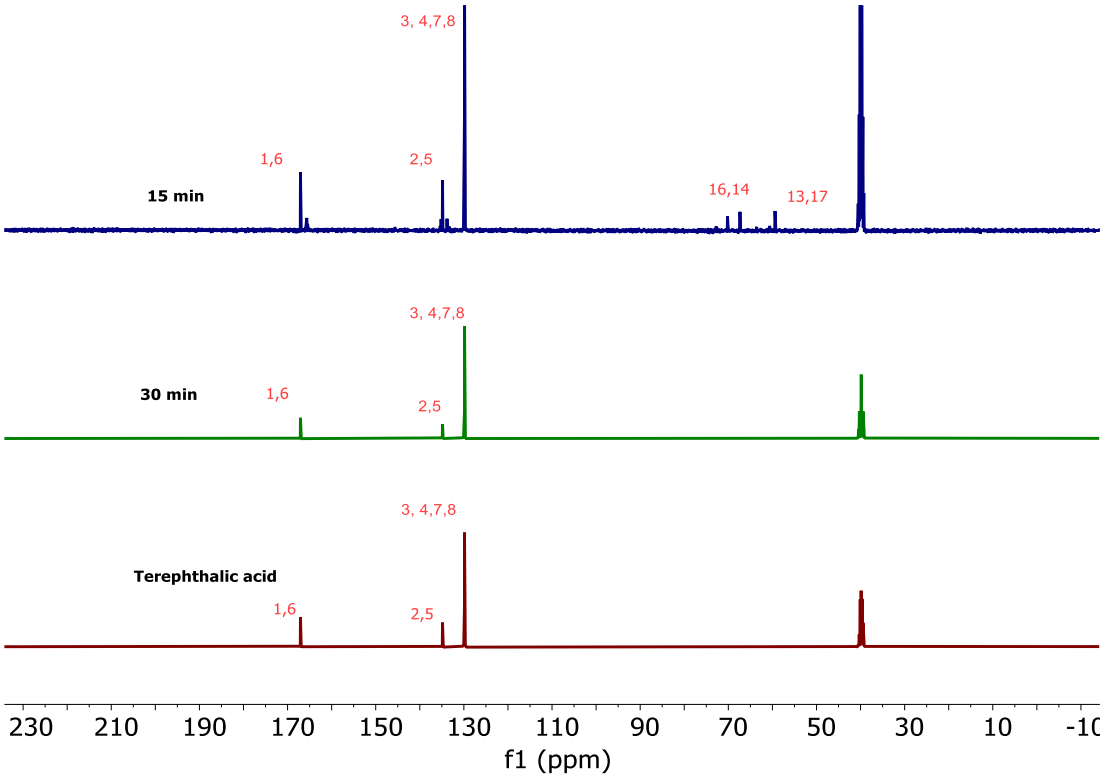

Figure 2.2. [1]HNMR spectra of standard TPA and PET with PEG 400 at different reaction times.

2.3.2 Reaction mechanism: S-L-L-L PTC

The reaction proceeds by solid (polymer)-liquid(melt)-liquid (water) phase transfer catalysis (PTC) as delineated in **Scheme 2.2** at 240 ºC. It ultimately becomes L(aq)-L (interfacial film)-L(org) PTC when all polymer is melted. When the temperature is lowered the liquid TPA becomes solid, EG remains in the aqueous phase along with PEG 400 making it possible to recycle the catalyst.

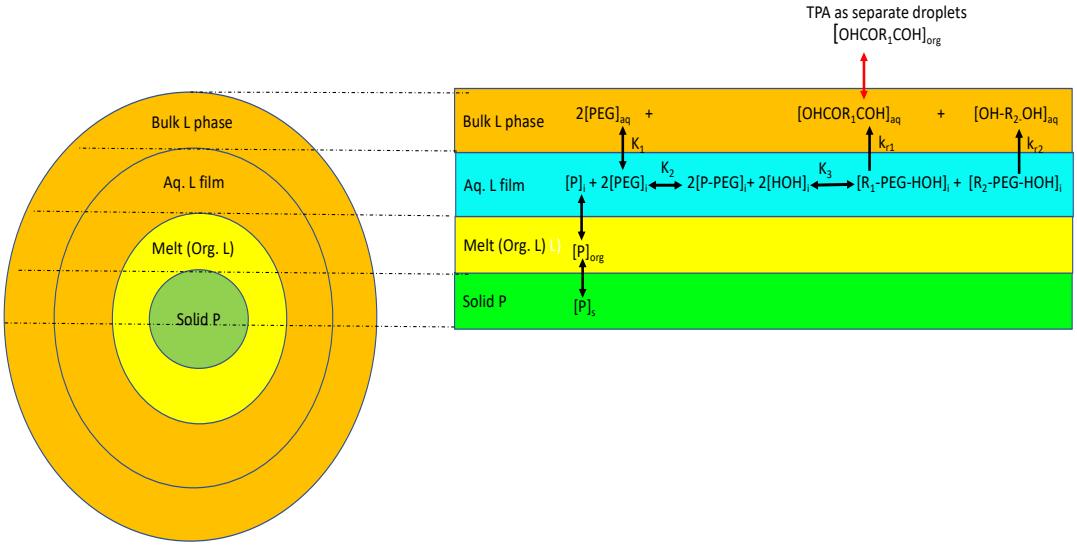

Scheme 2.2. General mechanism for PET depolymerization in the presence of PTC.

Various mechanisms of PTC for L(aq)-L(org), S(reactant)-L(org), L(aq)-L(middle)-L(org), S(cat/reactant)-L(aq)-L(org) and S-L(omega)-L(org) have been discussed and modelled by Yadav (Yadav, 2021;Yadav, 2004). The PET hydrolysis forms an interesting case of S-L-L-L PTC. PEG forms a hydrogen bonding with hydroxyl hydrogen of PEG 400 with carbonyl oxygen of ester linkage and reacts with PEG 400. Instantaneously PET long chain molecules scission takes place randomly. Oligomers with lower molecular weight is characterized by higher solubility in water with high dielectric constant. Such oligomers are then transferred to the aqueous phase, where the hydrolysis takes place, and immediate formation of terephthalic acid takes place.

Oligomers are characterized insoluble in water forms a hydrogen bonding with PEG 400 and transferred to aqueous phase. Furthermore, this active intermediate is easily attacked by protonated water molecule because high dissociation energy of water at 240 ºC. Consequently, all oligomer breaks down into monomer and there is formation of TPA and EG. When all solid PET is in a molten state, it becomes L(melt)-L(interfacial film)-L(aq) PTC. Now the mechanism in the current case can be discussed and modelled.

As discussed before PET melts at 240 ºC and hence the particles are softened from 75 ºC towards the melt phase and there are 4 phases in the reaction mass: polymer PET $[P]_s$ as a solid, softened and later converted into a melt as organic liquid $[P]_{org}$, a thin layer of aqueous film surrounding the organic phase which contains the phase transfer catalyst $[PEG]_i$ and $[P]_i$ which forms a complex $[P\text{-}2PEG]_i$ and reacts with water in that phase. The catalyst is distributed between the aqueous phase and interfacial film. The polymer is hydrolyzed with two moles of water to break it into two portions, giving rise to TPA (as liquid) and EG in the bulk aqueous phase. TPA is transferred out of the film as a separate organic phase and remains as a disperse droplets (Scheme 2). The catalyst in the film is in equilibrium with that in the bulk aqueous phase (equilibrium constant K_1). The solid P goes into a molten phase at 230-240 ºC. Before the molten phase, P is sparingly soluble in the interfacial film and its rate is increased when the entire P is in the molten state. P form a complex with 2 moles of the catalyst PEG and the complex P-2PEG then reacts with 2 moles of water forming a complex P-2PEG-2HOH which is broken into two polymers complexes R_1-PEG-HOH (acid part) and R_2-PEG-HOH (glycol part) which dissociate into TPA and EG and transferred to the aqueous phase. TPA has practically no solubility in water and hence is transferred to the organic phase as a droplet.EG remains in the bulk aqueous phase. The catalyst is regenerated.

The overall reaction for PET depolymerization in the presence of PEG is as follows:

$$\left[\left[\mathrm{P}\right]_n\right]_i + 2n\left[\mathrm{H_2O}\right]_i \xrightarrow[[\mathrm{PEG}]_i]{} n\left[\left[\mathrm{OHCOR_1COH}\right]\right]_s + n\left[\left[\mathrm{OH\text{-}R_2\text{-}OH}\right]\right]_l$$

PET solid particles are dispersed in the liquid phase containing water in large excess and phase transfer catalyst (PEG). When the temperature is raised to melt PET, the solid particles are softened and converted in to globules containing exterior of molten PET and interior of solid PET.

Ultimately, the PET droplets will be form within the aqueous phase. Then it becomes L-L PTC. The ester linkages of PET are broken according to the mechanism as given below.

$$[[\mathrm{P}]_x](s) \overset{K_1}{\rightleftharpoons} [[\mathrm{P}]_x](l) \ldots\ldots (1)$$

$$\mathrm{K}_1 = \frac{\left[\left[\mathrm{P}\right]_x\right]_{org}}{\left[\left[\mathrm{P}\right]_x\right]_s} \ldots\ldots\ldots (2)$$

PET distribution in thin aqueous film (inter-phase)

$$[[P]_x]_{org}(l) \overset{K_2}{\rightleftharpoons} [[\mathrm{P}]_x]_i(l) \ldots\ldots\ldots (3)$$

$$\mathrm{K}_2 = \frac{\left[\left[\mathrm{P}\right]_{\mathrm{x}}\right]_{\mathrm{i}}}{\left[\left[\mathrm{P}\right]_{\mathrm{x}}\right]_{\mathrm{org}}} \ldots\ldots\ldots (4)$$

PET forming complex with PEG

$$[[P]_x]_i(l) + [PEG] \overset{K_3}{\rightleftharpoons} [[\mathrm{P-PEG}]_x]_i \ldots\ldots\ldots (5)$$

$$\mathrm{K}_3 = \frac{\left[\left[\mathrm{P\text{-}PEG}\right]_x\right]_i}{\left[\left[\mathrm{P}\right]_x\right]_i \left[\mathrm{PEG}\right]} \ldots\ldots\ldots (6)$$

When PEG is used as catalyst following complex may formed bonding with water molecule

$$[\mathrm{HOH-PEG}] \overset{1/\mathrm{K}_i}{\rightleftharpoons} [\mathrm{PEG}] + [\mathrm{H-OH}]$$

$$\mathrm{K}_{\mathrm{i}} = \frac{\left[\left[\mathrm{HOH\text{-}PEG}\right]_x\right]_i}{\left[\mathrm{PEG}\right]\left[\mathrm{H\text{-}OH}\right]} \ldots\ldots\ldots (7)$$

PEG distribution in various complexes is given by:

$$\left[\text{PEG}\right]_0 = \left[\left[\text{HOH-PEG}\right]_x\right]_i + \left[\left[\text{P-PEG}\right]_x\right]_i + [\text{PEG}]$$

$$\left[\text{PEG}\right]_0 = \text{K}_\text{i}\left[\text{PEG}\right]\left[\text{H-OH}\right] + \left[\text{P}\right]_x\left[\text{PEG}\right]_i + [\text{PEG}]$$

The concentration of free PEG can be obtained from above equation

$$[\text{PEG}] = \frac{\left[\text{PEG}\right]_0}{\left[1 + \text{K}_\text{i}\left[\text{H-OH}\right] + \left[\left[\text{P}\right]_x\right]_i\right]} \text{.....(8)}$$

Complex (active reactant) reacts with water in thin aqueous film (interphase) and breaks down PET in two fractions

1. Water soluble fraction (oligomer formation)

2. Water insoluble fraction (solid oligomers of higher molecular weight)

Breaking of PET is an instantaneous reaction. It was observed that there was no presence of unreacted PET in less than 3 min. This indicated that PET breaks down instantaneously in to mixture of oligomer as mentioned above (water soluble and insoluble).

$$\left[\left[\text{P-PEG}\right]_x\right]_i + \text{H-OH} \xrightarrow{k_{r1}} \left[\left[\text{P}\right]_{x-n}\right]_s + \left[\left[\text{P}\right]_n\right]_s + \left[\text{PEG}\right] \text{....(9)}$$

$$-\frac{d\left(\left[\text{P-PEG}\right]_x\right)}{dt} = k_{r1}\left[\left[\text{P-PEG}\right]_x\right]\left[\text{H}_2O\right] \text{.....(10)}$$

1. The oligomer fraction which was readily water soluble reacts with water and is converted into monomer due to a very fast reaction. It was confirmed by the analysis of reaction mixture which showed the presence of monomers (TPA and EG).

$$\left[\left[\text{P}\right]_{x-n}\right]_{aq}(l) + \text{H-OH} \xrightarrow{k_{r2}} \left[\left[\text{OHCOR}_1\text{COOH}\right]\right]_{org}(s) + \left[\left[\text{OH-R}_2\text{-OH}\right]\right]_{aq}(l) \text{....(11)}$$

$$-\frac{d\left(\left[\text{P}\right]_{x-n}\right)}{dt} = k_{r2}\left[\text{P}\right]_{x-n}\left[\text{H}_2O\right] \text{.....(12)}$$

2. The solid oligomer fraction which is sparingly soluble in water slowly reacts with water and converts into monomer which is the rate determining step (RDS).

$$\left[\left[\mathrm{P}\right]_n\right]_i + \left[\text{H-OH-PEG}\right]_i \xrightarrow{k_{r3}} n\left[\left[\mathrm{HOOCR_1COOH}\right]\right]_s + n\left[\left[\text{OH-R}_2\text{-OH}\right]\right]_l + \left[\left[\mathrm{PEG}\right]\right]_{aq} \quad ....(13)$$

$$+\frac{d\left(\left[\left[\mathrm{HOOCR_1COOH}\right]\right]_s\right)}{dt} = k_{r3}\left[\left[\mathrm{P}\right]_n\right]_i\left[\text{H-OH-PEG}\right]_i \quad .....(14)$$

The overall rate of reaction is given by Eq. (14).

The concentration of [H-OH-PEG] is unknown, and it is assumed that concentration of [P-PEG] to be the same as the concentration of oligomer found experimentally by HPLC analysis. The solid samples (intermediate) were collected and dissolved in DMSO at different reaction times for analysis.

The measured concentration of solid has been used for determination of kinetics (**Fig. A2.8** HPLC analysis).

Substitution values of unknown concentration of [H-OH-PEG] from equation (7)

$$+\frac{d\left(\left[\left[\left[\mathrm{HOOCR_1COOH}\right]\right]\right]_s\right)}{dt} = k_{r3}\left[\left[\mathrm{P}\right]_n\right]_i\left[\text{H-OH-PEG}\right]_i\left[H_2O\right]$$

$$+\frac{d\left(\left[\left[\mathrm{HOOCR_1COOH}\right]\right]_s\right)}{dt} = k_{r3}\mathrm{K_i}\left[\left[\mathrm{P}\right]_n\right]_i\left[\mathrm{PEG}\right]\left[\text{H-OH}\right]_i\left[H_2O\right] \quad .....(17)$$

The concentration of water is excess and substituting value for catalyst concentration

$$+\frac{d\left(\left[\left[\mathrm{HOOCR_1COOH}\right]\right]_s\right)}{dt} = k_{r3}\mathrm{K_i}\left[\left[\mathrm{P}\right]_n\right]_i\frac{\left[\mathrm{PEG}\right]_0}{\left[1+\mathrm{K_i}\left[\text{H-OH}\right]+\left[\left[\mathrm{P}\right]_x\right]_i\right]}\left[\text{H-OH}\right]_i\left[H_2O\right] \quad .....(18)$$

$$k_{app} = k_{r3}\mathrm{K_i}\frac{\left[\mathrm{PEG}\right]_0}{\left[1+\mathrm{K_i}\left[\text{H-OH}\right]+\left[\left[\mathrm{P}\right]_x\right]_i\right]}\left[\text{H-OH}\right]_i\left[H_2O\right] \quad .....(19)$$

Substituting value for k_{app} equation (18) becomes

$$+\frac{d\left(\left[\left[\mathrm{HOOCR_1COOH}\right]\right]\right)}{dt}=k_{app}\left[\left[\mathrm{P}\right]_n\right]_i \text{.....(20)}$$

The concentration of PET can be written as $\left[\left[P\right]_n\right]_t=\left[\left[P\right]_n\right]_0-\left[\left[\mathrm{OHCOR_1COH}\right]\right]$

Solving equation (20) for time- 0 to t

$$+\frac{d\left(\left[\left[\mathrm{HOOCR_1COOH}\right]\right]\right)}{dt}=k_{app}\left[\left[P\right]_n\right]_0-\left[\left[\left[\mathrm{HOOCR_1COOH}\right]\right]\right]_s \text{.....(21)}$$

$$+\frac{d\left(\left[\left[\left[\mathrm{HOOCR_1COOH}\right]\right]\right]\right)}{\left[\left[P\right]_n\right]_0-\left[\left[\mathrm{HOOCR_1COOH}\right]\right]}=k_{app}dt\text{.....(22)}$$

Integrating the equation 22 for limit time t=0 to t=t

$$\int_{[[\mathrm{OHCOR_1COH}]]_0}^{[[\mathrm{OHCOR_1COH}]]_t}+\frac{d\left(\left[\left[\mathrm{HOOCR_1COOH}\right]\right]\right)}{\left[\left[P\right]_n\right]_0-\left[\left[\mathrm{HOOCR_1COOH}\right]\right]}=k_{app}\int_0^t dt\text{.....(23)}$$

$$\ln\left(\frac{\left[\left[P\right]_n\right]_0-\left[\left[\mathrm{HOOCR_1COOH}\right]\right]_0}{\left[\left[P\right]_n\right]_0-\left[\left[\mathrm{HOOCR_1COOH}\right]\right]_t}\right)=k_{app}t\text{.....(24)}$$

Where conversion can be defined as

$$X=\left(\frac{\left[\left[\mathrm{HOOCR_1COOH}\right]\right]_t-\left[\left[\mathrm{HOOCR_1COOH}\right]\right]_0}{\left[\left[P\right]_n\right]_0-\left[\left[\mathrm{HOOCR_1COOH}\right]\right]_0}\right)\text{.....(25)}$$

Assuming initial concentration of terephthalic acid =0, then

$$X=\left(\frac{\left[\left[\mathrm{HOOCR_1COOH}\right]\right]_t}{\left[\left[P\right]_n\right]_0}\right)\text{.....(26)}$$

$$-\ln\left(1-X\right)=k_{app}t\text{.....(27)}$$

$\left[\left[\mathrm{OHCOR_1OCOH}\right]\right]_t$ = Concentration of TPA (recovered in solid phase was measured by dissolving into DMSO and analysed in HPLC (**Fig. A2.8 and Fig. A2.9**).

$\left[\left[P\right]_n\right]_0$ = Initial concentration of PET (mol/cm^3)

$\left[\left[\mathrm{HOOCR_1COOH}\right]\right]_0$ = Initial concentration of TPA (mol/cm^3)

2.3.2.1 Hydrolysis product analysis

Figure 2.3 shows concentration profiles for PET, TPA and oligomer whereas **Fig. A2.10** shows the yield of TPA. To investigate the effect of water concentrations on the apparent rate constant, experimental data were collected at 240 °C for PEG concentration of 2.11×10^{-5} mol/cm^3 for reaction times up to 10 min. **Figure 2.4** shows data for rate constant calculated using TPA and end group analysis, the difference between two rate constants indicates that end group analysis measures acid group of TPA and dimer or trimer. As predicted the pseudo first order model fits the initial rate data at 240 °C and catalyst concentration 2.11×10^{-5} mol/cm^3, giving reaction rate constant 1.40 min^{-1}. The pseudo first-order kinetics gives a slope of 1.40 min^{-1}. The value for rate constant with PEG 400 is, therefore 1.40 min^{-1}. Campnelli et al. (1993) found with addition of zinc salt, there was 18 % increase of rate constant for a salt concentration 0.1 % (w/w PET). The addition of the PEG 400 leads to 3.88 times increase in rate of hydrolysis reaction. Thus, it is concluded that at 240 ℃ the use of PEG 400 with a very small concentration of 2.11×10^{-5} mol/cm^3 results in to extraordinary increment in the rate of PET hydrolysis.

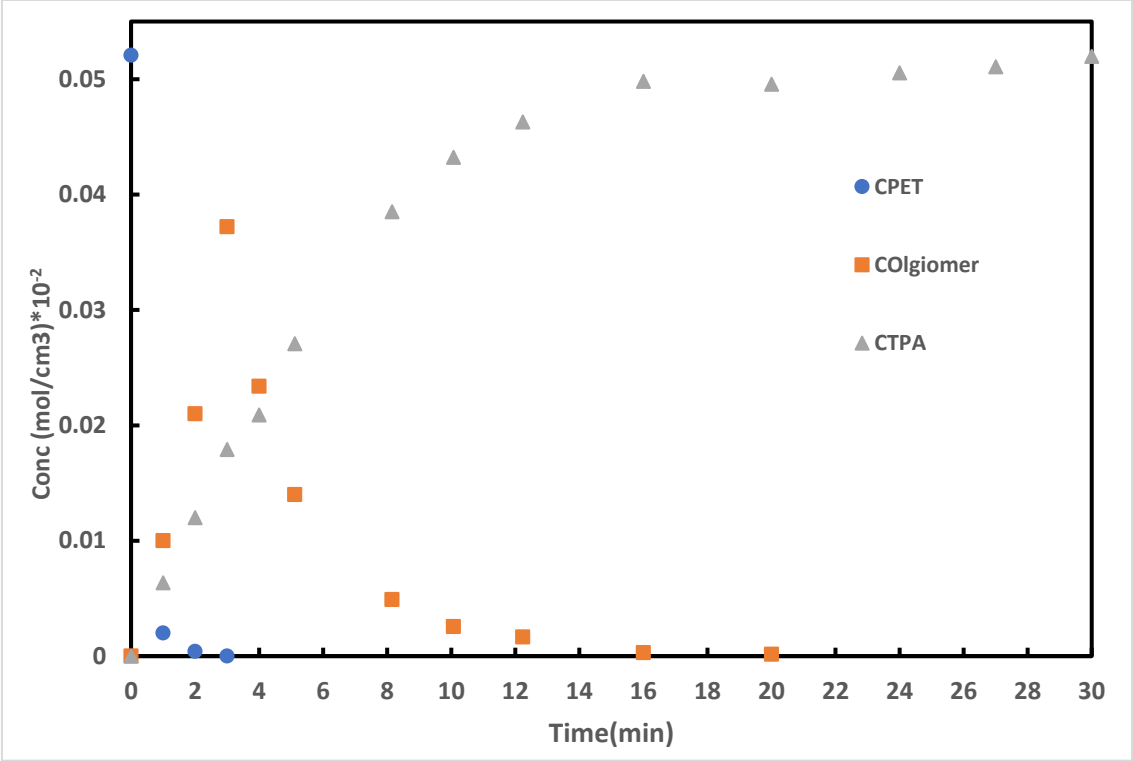

Figure 2.3. Concentration profile for PET, TPA, intermediate oligomer with respect to time at 240 °C with PEG 400 catalytic effect. (Reaction condition- Temperature: 240 °C; Catalyst concentration: 2.11×10^{-5} mol/cm^3; PET concentration :5.27×10^{-4} (mol/cm^3); Water: 100 cm^3; Speed of agitation: 650 rpm) (Analysis based on HPLC Method).

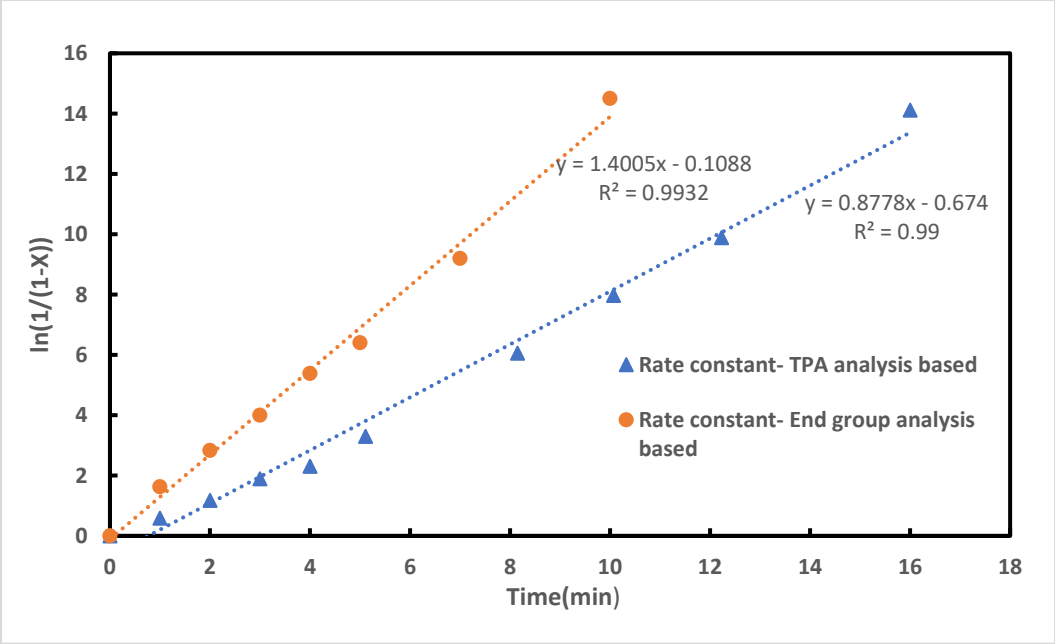

Figure 2.4. Initial rate data based on TPA and end group analysis. (Reaction condition- Temperature: 240°C; Catalyst concentration: 2.11×10^{-5} mol/cm^3; PET concentration: 5.27×10^{-4} (mol/cm^3); Water: 100 cm^3; Speed of agitation: 650 rpm).

2.3.3 Influence of reaction conditions on hydrolysis reaction of PET

The reaction mixture consisted of two phases: solid PET and aqueous phase for all experiments and times of reaction. The solid phase was found stuck on the sides and bottom of the reactor for reaction times less than 15 min at 240 °C for an initial reactor loading 22 mol water/mol PET. Similar trend has been observed by [66] with zinc acetate as catalyst. At lower temperatures it was a slurry of PET and aqueous phase and organic mass upon cooling at all temperatures.

2.3.3.1 Influence of initial molar ratio

The hydrolysis reaction was investigated using PET and water initial charge ratio range of 22-110 mol water/mol PET, **Fig. 2. 5** depicts the conversion of carbonyl to carboxylic group (x) as function of time with reaction condition of 240 °C and autogenous pressure (3.2 MPa) generated by water vapour. The initial molar ratio of 22 mol water/mol PET reaches 80 % conversion

within 10 min and thereafter only additional 10 % increase in conversion was observed. On the other hand, for initial mol ratio 55-111 mol water/mol PET produced approximately 86-88 % conversion in 10 min and reached to 100 % conversion within 20 min. The initial mol ratio 55-111 mol water/mol PET gave complete depolymerization, whereas less than 22 mol water/mol PET initial mol ratio reaction failed to give complete depolymerisation. **Figure 2.6** shows the equilibrium concentration of carboxylic group governed by initial molar ratio of water and PET. The equilibrium concentration of carboxyl group does not have impact of PEG 400 rather by initial mol ratio of water: PET and temperature. Campnelli et al. (1993) had reported equilibrium (carboxyl group) formation below 55 mol water/mol PET and it could not reach complete depolymerisation. There was an autogenous pressure generation since water was used in large excess than stoichiometrically required. It leads to break down of particles into liquid phase which in turn creates larger surface area helps to form reactive polar intermediate. Also, particle size has major influence on heat and mass transfer, which governs the dissolution of PET in PEG 400. PET depolymerization with reactive extrusion shows the pressure has huge impact on conversion [49].

Although hydrolysis is investigated using carbonyl conversion to carboxyl group, there might be formation of dimer or trimer of TPA, which are not the desired products, where the dimers and trimers of carboxyl group are considered as TPA. Thus, **Fig. A2.11 and A2.12** show concentration and percent yield of TPA in reaction mixture, which is the desired product.

2.3.3.2 Influence of reaction time

The complete depolymerization is majorly governed by reaction time for an all-initial reaction conditions. In **Fig. 2.5**, it was observed that within 12 min all ester linkages scission takes place. More than 50 % reaction time was utilized to achieve the desired product terephthalic acid, which

is also confirmed through percent yield of TPA in **Fig. A2.11**. It can also seen from **Fig. 2.5** to reach acid value equivalent to terephthalic acid requires 15-20 min reaction time.

A complete depolymerisation is seen in **Fig. 2.5** is 10 min on the basis of ester linkage whereas, **Fig. A2.11** depicts more than 95 % yield for TPA on the basis of HPLC analysis in 30 min. This indicates that the estimation of conversion based only on ester linkage has limitations and it is required to combine with the analysis of the desired products.

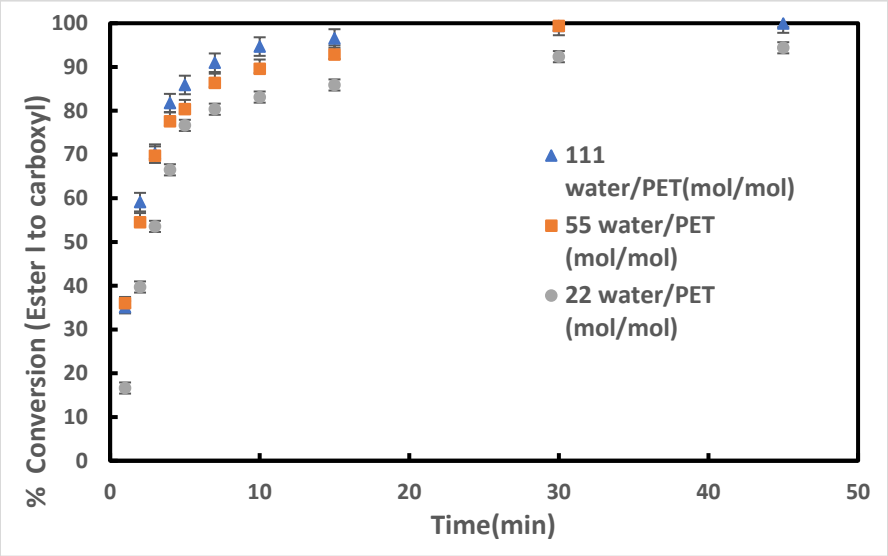

Figure 2.5. Carboxyl group concentration with time for three different initial water to PET charge ratio. (Reaction condition- Temperature: 240°C; Reaction time: 30 min; Catalyst concentration: 2.11×10^{-5} mol/cm^3; Speed of agitation: 650 rpm) (Analysis based on end group).

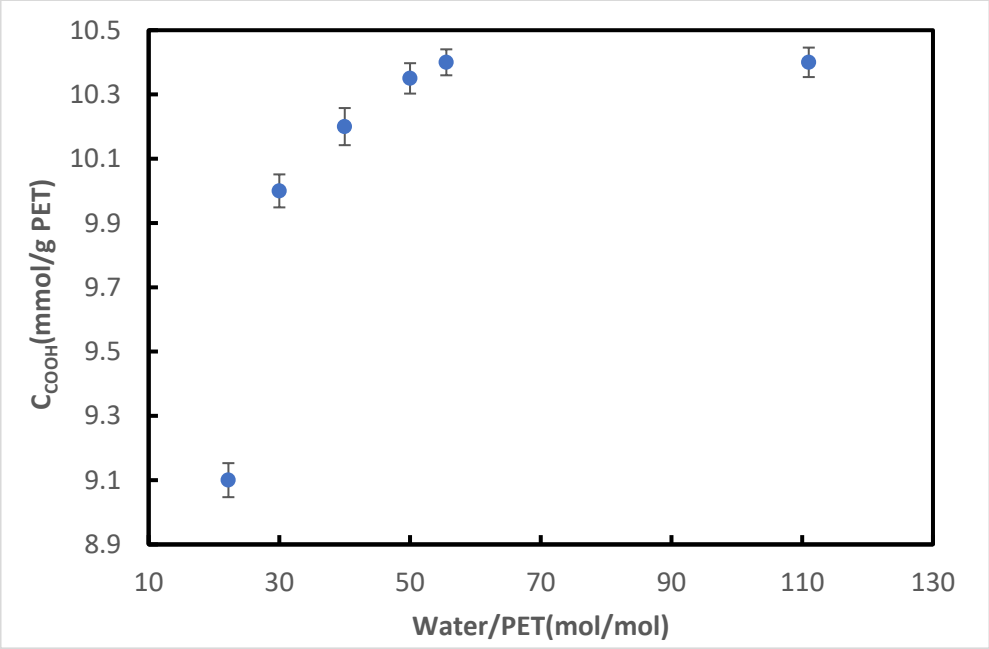

Figure 2.6. Equilibrium values of carboxyl group concentration as function of initial water concentration. (Reaction condition- Temperature: 240°C; Reaction time: 30 min; Catalyst concentration: 2.11×10^{-5} mol/cm^3; Speed of agitation: 650 rpm) (Analysis based on end group).

2.3.3.3 Influence of catalyst concentration on hydrolysis

The influence of PEG 400 concentration on depolymerization was studied in autoclave in the temperature range 230-260 °C, with a reaction time 30 min, for initial reactor loading 111 mol water/mol PET and with 0- 3.0×10^{-5} mol PEG/cm^3. The effect of PEG 400 various concentration on scission of ester linkages to carboxyl group shown in **Fig. 2 7.**

Effect of catalyst concentration was studied in a control experiment without any catalyst under similar conditions. The control of experiment (without PEG 400) showed 48 $\pm$1.65 % conversion of ester linkages to carboxyl group, which was a mixture of oligomers equivalent to 1 min hydrolysed reaction sample. It is clearly observed that change in catalyst concentration from 1.4×10^{-5} mol PEG 400/cm^3 **to** 2.5×10^{-5} mol PEG 400/cm^3 gives sufficient effect about 20 % increase in conversion. However, increase of 40 % molar concentration leads to more than 80 % conversion in scission of ester linkages. Partial increase in conversion does not produce the

desired product (TPA) rather it gives a mixture of oligomers, until it reaches complete conversion (carboxyl concentration approx. 10.4 mmol carboxyl group). Thus, molar concentration of PEG 400 of 2.0×10^{-5} mol/cm^3 is sufficient to give the maximum conversion in breaking of ester linkages. Increase in the amount of PEG 400 beyond that value does not have any effect on breaking of ester linkages (i.e., carboxyl group content).

Figure A2.13 indicates relationship among the yield of TPA at various temperatures using the HPLC basis. The increase in temperature and catalyst concentration increased TPA yield. However, Yu et al. (2012) had reported a decrease in yield above 1.5 %, which might be due to the acidic effect of zinc acetate on the stability TPA at high temperature. Among most of the reported catalysts for the PET hydrolysis, glycolysis has shown decrease in yield of TPA with increase in temperature.

Figure A2.14 shows the EG yield increased with increasing concentration of PEG at 220–240 °C. When PEG 400 concentration increased from 0 to 1.5×10^{-5} mol/cm^3 the yield of EG increased considerably. After $2\text{-}3\times10^{-5}$ mol/cm^3 the yield remained constant. As against our data, the previous literature reports decrease in yield with increase in temperature as well as catalyst concentration [51]. However, EG yield had no such effect with PEG 400 in PET hydrolysis in our case.

2.3.3.4 Effect of catalyst concentration on hydrolysis kinetics

As shown in **Fig. 2.8**, the initial rate of reaction was found to increase with increasing concentration of the catalyst. This is typical of PTC reactions. All further experiments were conducted at a catalyst concentration of 2×10^{-5} mol/cm^3.

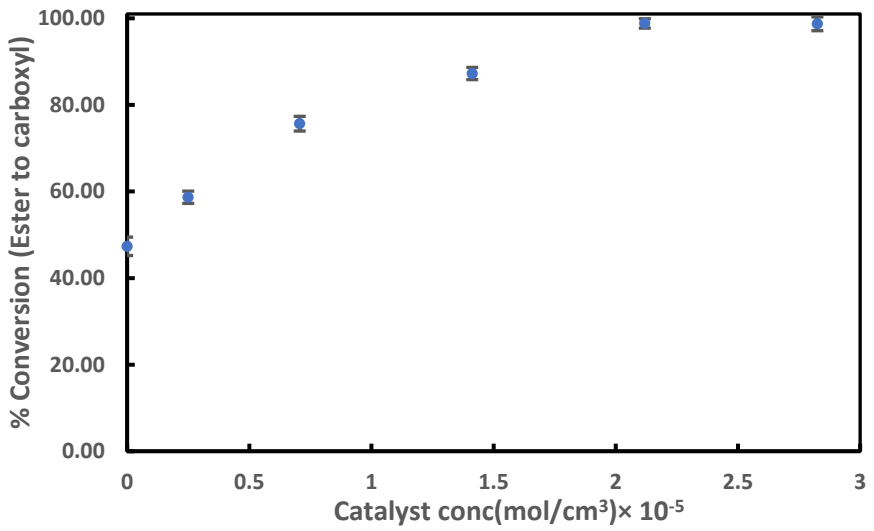

Figure 2.7. Effect of PEG 400 various concentration on percent conversion of ester linkages. (Reaction condition- Temperature: 240°C; PET concentration: 5.27×10^{-4} (mol/cm^3); Water: 100 cm^3; Reaction time: 30 min; Speed of agitation: 650 rpm) (Analysis based on end group).

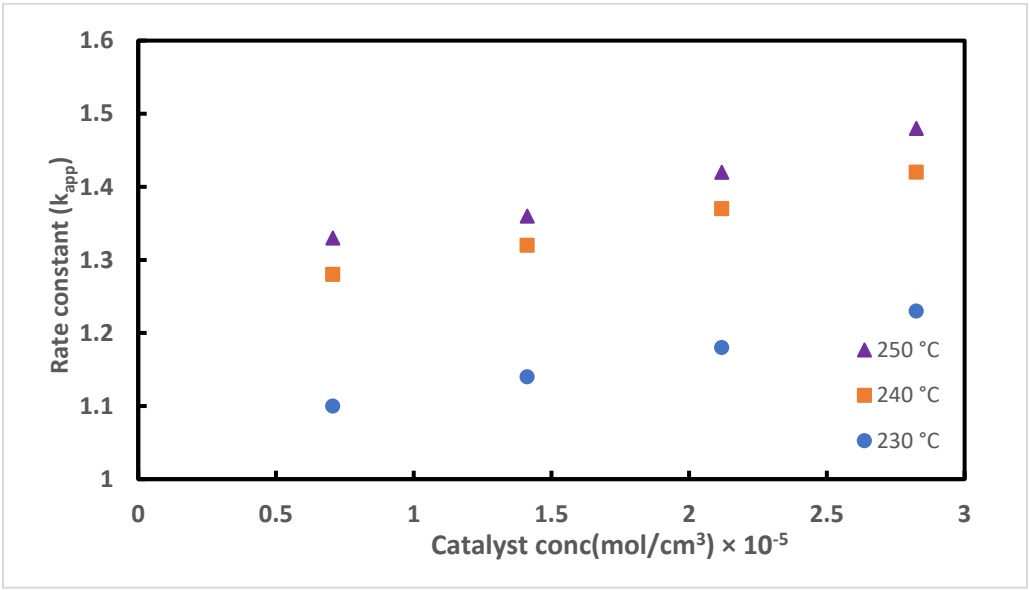

Figure 2.8. Effect of PEG 400 concentration on reaction rate constant at different temperatures. (Reaction condition- Temperature: 240°C; Reaction time: 30 min; PET concentration: 5.27×10^{-4} (mol/cm^3); Water: 100 cm^3; Speed of agitation: 650 rpm) (Analysis based on end group).

2.3.3.5 Influence of temperature on PET hydrolysis

The rate constants for initial charge ratio 55 mol water/mol PET were calculated at different temperatures (**Table 2.1).** There could be an onset of mass transfer effects at higher temperature which was explained in the model which is for an instantaneous reaction for which the activation energy values are on lower side. Increase reaction rate happens in the case of truly kinetically controlled reaction having high activation energy. The Arrhenius plot was made (**Fig. 2.9)** to get an apparent activation energy of 34.4 KJ/mol. The activation energy values can be compared with published literature (**Table 2.2**). Uncatalyzed melt phase hydrolysis is reported to have a activation energy as 55.7 KJ/mol (Campanelli et al., 1993) whereas zinc acetate and zinc chloride catalysed hydrolysis with 47.8(1994) and 64.9 KJ/mol [69] respectively. Uncatalyzed high temperature hydrolytic depolymerization of PET on reactive extrusion activation energy is found to be 74.4KJ/mol [49]. Thus, PEG 400 is the best catalyst in comparison with all previously used catalysts.

Table 2.1 Effect of Temperature on rate constant (based on end group analysis) for PEG 400 catalysed hydrolysis

Temperature (°C)	k (min^{-1})
230	1.2
240	1.40
250	1.624

Reaction conditions: 55 mol water/mol PET with PEG 400 at molar concentration of 2.11×10^{-5} mol/cm^3.

Table 2.2 Actitation energy for different catalyst

Catalyst	Activation energy (kJ/mol)	References
PEG400	34.4	Current study
Autocatalytic	123	Kao et.al 1998
Humicola insolens cutinase (HiC)	98	Eugenio et al. 2021
Autocatalytic	90	Goje et al., 2004
$[(CH_3)N(C_{16}H_{33})][PW_{12}O_{40}]$	68	[70]
Zinc acetate	47.9	[71]
Sulphuric acid	102	[72]
Phosphnium salt	75.3	[39]
Tri-octyl-methyl ammonium bromide	83	[73]
Zinc Chloride	50.55	[69]

The influence of reaction temperature on conversion of carbonyl to carboxyl group was studied, and results are shown in **Fig. A2.15**. The result shows increase in reaction temperature increases carboxylic group concentration; in other words, increases initial rate of reaction. **Fig. A2.16 and Fig. A2.17** depict the effect of temperature for short reaction time, it can be observed an increase in temperature favours the formation of terephthalic acid.

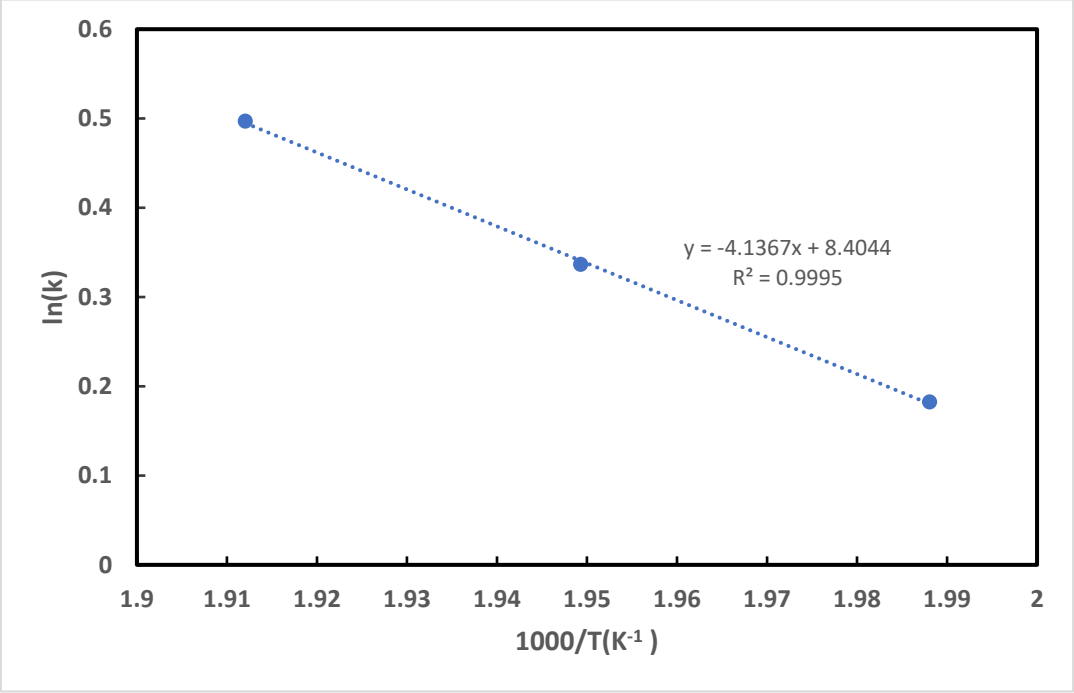

Figure 2.9. Arrhenius plot in presence PEG 400 catalytic depolymerisation. (Reaction condition- Reaction time: 30 min; Catalyst concentration: 2.11× 10^{-5} mol/cm^3; PET concentration: 5.27×10^{-4} (mol/cm^3);; Water: 100 cm^3; Speed of agitation: 650 rpm).

2.3.4 Catalytic mechanism of PET depolymerisation

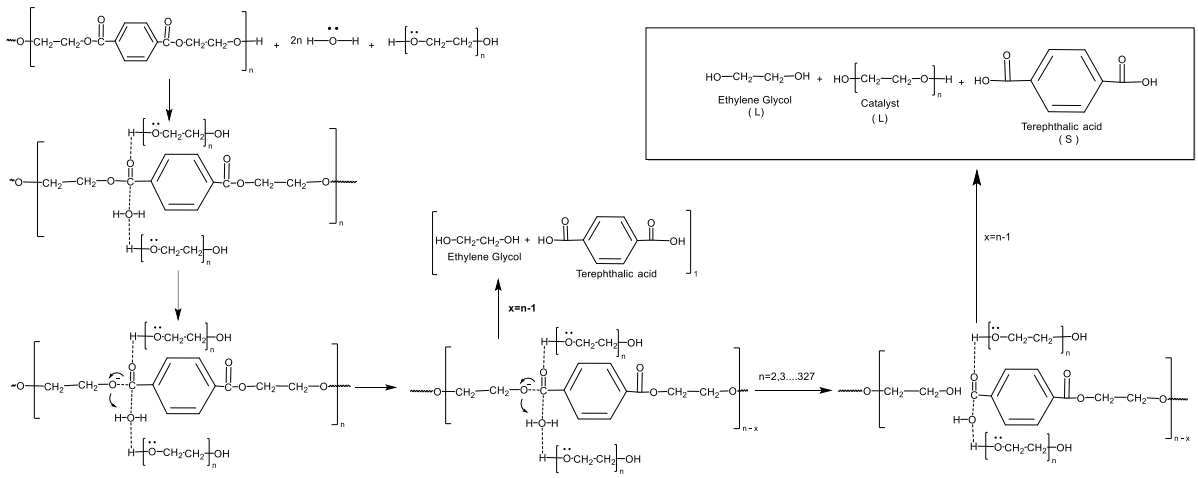

Scheme 2.3. Proposed catalytic mechanism for PET in presence of PEG 400.

Examination of PET by TGA and DSC showed that the PET melting temperature is about 240 °C. Then in the melt liquid phase PET reacted with in the aqueous phase containing PEG 400. There is layer of water around the melt droplets in which the catalyst PEG 400 exits. Water molecule reacts with electron deficient ester linkage which is formed by PEG 400 in repeat unit of PET. PEG 400 hydroxyl group forms a bonding with carbonyl oxygen, which eventually produce electron deficient oxygen ester linkage. Consequently, PET is depolymerised into monomers i.e., TPA and EG. However, the quantitative analysis showed the presence of oligomers or intermediates, which might be dimers or trimers of terephthalic acid. The concentration profile in **Fig. 2.3** indicates that after 3 min the intermediate oligomers is converted to monomers, i.e., TPA and EG in the presence of PEG 400. Moreover, there might have a possibility of PEG 400 reacting with PET in the melt phase. However, HPLC-ELSD analysis **(Fig. 2. 10)** depicted the presence of PEG 400 in the aqueous phase, which showed the PEG 400 acts as a phase transfer catalyst which can be recycled. TPA and EG could be recovered easily after reducing being separate immiscible phases. The aqueous phase containing PEG was recyclable.

2.3.5 Catalyst stability and reusability

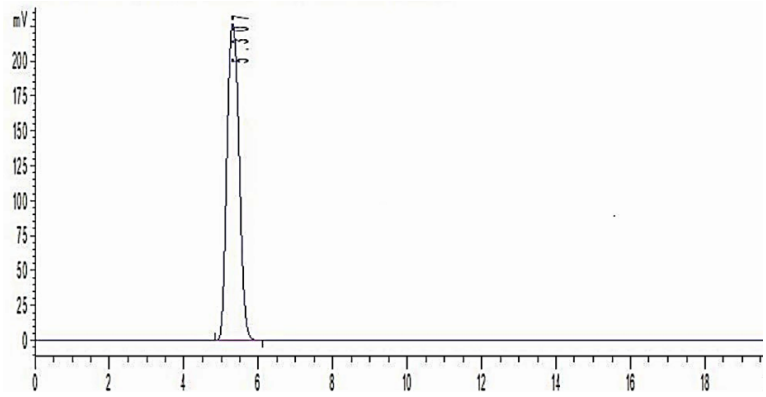

(a)

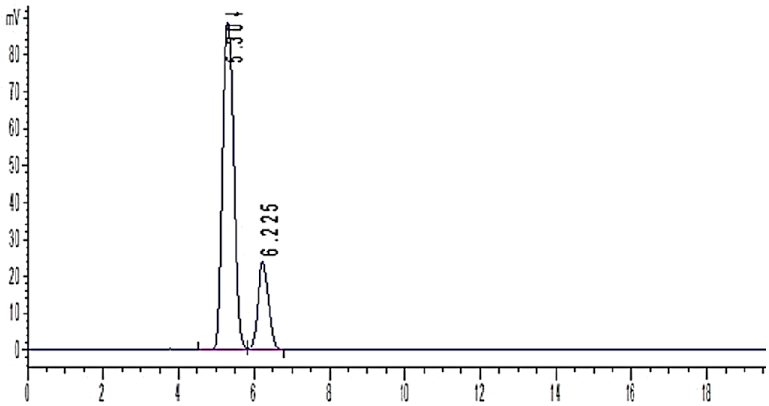

(b)

Figure 2.10. ELSD plot for (a) standard PEG 400 sample (b) reaction liquid sample after reuse. (Reaction condition- Temperature: 240℃; Catalyst concentration: 2.11× 10-5 mol/cm^3; PET concentration:5.27×10^{-4} (mol/cm^3); Water: 100 cm^3; Reaction time: 30 min; Speed of agitation: 650 rpm).

The aqueous phase containing PEG 400 and EG was made up with water to 100 mL and investigated for reusability for 5 times. **Figure 2.10** shows the HPLC-ELSD analysis of the reaction liquid phase, which contains PEG 400. It clearly indicates that the ELSD pattern for the standard and reaction liquid mixture have almost similar spectra. However, there is a presence of an additional peak which might be due to the formation of PEG 400-oligomer complex in scattering effect. In addition, there is a little change in the concentration of PEG 400 after the

reaction, suggesting that the fidelity of the catalyst structure was maintained during the reaction. Moreover, the catalytic activity of PEG 400 was studied with reuse of reaction liquid phase for subsequent run, which is a solution of EG and PEG 400. As, shown in **Fig. A2.18**, recycled liquid phase gave similar activity as that of fresh catalyst for four consecutive recycles.

2.4 Conclusion

Conversion of waste PET plastic into its monomers is highly desirable to achieve circular economy and the net zero goal. A systematic investigation was undertaken to study phase transfer catalysis and a new model for hydrolytic depolymerization of PET was developed. In comparison with the published reports on use of metal acetate and mixed oxide catalysts, PEG 400 exhibited excellent catalytic activity. The limitation of the end group analysis method which was used before is that it does not distinguish among monomer and oligomers. This gap was overcome and the concentration profiles of PET, oligomer, and TPA were developed using the HPLC method. The S-L-L-L PTC hydrolysis reaction of PET at melt phase was studied by using PEG 400 as the catalyst. In fact, in melt phase, the so-called S-L PTC turns out to be L-L PTC reaction where the interfacial film is saturated with active intermediate of PEG with PET, which is transferred to aqueous phase for reaction with water than aqueous phase dissolved in solid mentioned in literature. The reaction conditions with initial molar ratio of 55-110 mol water/mol PET, reaction time 30 min, PEG 400 catalyst concentration 2.0×10^{-5} mol/cm^3 at 240 °C, and 3.2 MPa autogenous pressure gave the best yield and conversion of PET. The yield and purity of TPA were found to be 90 and 99.1 %, respectively. The synergetic effect of catalyst and pressure generated by water helps increase the conversion and yield of TPA. The addition of PEG 400 as catalyst accelerates depolymerisation process by 15 min reaction time in comparison with supercritical and metal acetate depolymerisation. In literature most of the PTC reactions were

studied either below melt phase or low temperature which required either much higher reaction time or resulted in much lower conversion. The PTC results in thee current case are superior to PET depolymerisation using zinc salts or that under microwave irradiation with deep eutectic solvent. In the previous studies more than 10 % of the reaction product was insoluble in DMSO whereas the entire solid phase was soluble in DMSO in the current work. In other words, all PET is converted to either monomer or lower molecular weight oligomer, which is subsequently converted to monomer and thus conversion of the oligomer to monomer helps to achieve complete conversion and yield. A pseudo-first-order rate equation was fitted for PET depolymerization with a rate constant of 1.4 min^{-1} at 240 ^{o}C, and the apparent activation energy was 34.4 KJ/mol. The rate of hydrolysis is very fast, and complete depolymerization takes place within 30 min. NMR showed excellent monomer purity (terephthalic acid) without product purification or downstream processing. The depolymerization of PET using PEG 400 could be viewed as an eco-friendly process for recycling PET and reuse of monomers.

Chapter 3

Hydrolytic Depolymerization of nylon 6 using phase transfer catalyst

3.1 Introduction

The modern society faces enormous problems related to resource depletion, waste generation and energy scarcity and commitment of a majority of nations to the net zero goal by 2050. Amongst all, plastic pollution is a hotly debated topic necessitating several legislations and technology advances including single use plastic (SUP) ban, use of biodgradable bioplastics, hydrogen economy[74] and decarbonization[75]. Thiounn and Smith and Lange et al. have recently reviewed this area covering several different techniques of polymer recycling [76]. Tertiary recycling of waste polymers, also called chemical recycling which use hydrolysis and pyrolysis among others to break down the polymer into value-added products[28]. The product so obtained is typically used as a feedstock for the preparation of fuels and polymers. Recently we provided an interesting case of depolymerization of PET into terephthalic acid (PTA) and ethylene glycol (EG) using phase transfer catalysis (PTC) that also covered an interesting case of mechanism[1]. Polymer recycling also covers incineration for energy recovery which is not the advisable because incineration of many plastics leads to obnoxious hazardous gases and leaves behind toxic residues. Darzi et al.[77] discuss the application of the hydrothermal processing of PET and nylon-6 mixture as a upcycling method. Thus, chemical recycling is the most desirable technology for plastic recycling which consists of recycling, upcycling, and downcycling. This method has two advantages; firstly, it prepares virgin plastic from waste ones, and secondly, it grants a new process to recover carbon resources. Depolymerization reaction transforms polymer into corresponding monomers. Generally, the depolymerization process is endothermic[78]. For example, polyamide can readily be converted into a monomer[79]. However, these are energy intensive processes, i.e.,

harsh reaction conditions. To break the polymer, major approaches are super-critical or subcritical fluids [80]. Many researchers have worked on polyamide depolymerization; for example, Czernik and Hornung et al. mentioned the effective conversion of nylon 6 into caprolactam[81]. Kamipura et al. has extensively worked on nylon 6 depolymerization using sub-critical and super-critical water[82].

However, environmentally friendly super-critical water provokes undesirable side reactions and generates a complex reaction mixture with decomposed monomer products. To solve the above problems, many researchers have focused on using supercritical alcohols. However, processing waste into monomers with alcohol is not economically advisable[83]. Indeed, in the case of waste conversion into value-added products, alcohol may be required which is called alcoholysis. Furthermore, among these methods, hydrolysis is the best technique as regards cost[77]. Depolymerization of waste plastic can be efficiently achieved using phase transfer catalysis (PTC) as was recently demonstrated by Sabde et al. [1] in hydrolysis of waste polyethylene terephthalate [PET] using polyethylene glycol (PEG) 400 as a recyclable catalyst.

In commercial processes, PEG-catalyzed reactions can substantially replace expensive and environmentally harmful PTCs[42]. Well-known applications of PEG in organic synthesis include Williamson ether synthesis, substitution reactions, and oxidation and reduction reactions[65]. PEG has been modified with ammonium salts and crown ethers to enhance phase transfer in a two-phase system. Because of the ease of biodegradability, PEGs are considered as alternative ecofriendly solvents to ionic liquids. Although ionic liquids are regarded as more reactive than PEGs, they are associated with difficulty in biodegradability and separation problems and above all non-green methods of their synthesis. The role of PEG in liquid-liquid (L-L) and solid-liquid(S-L), is studied by Yadav and Motirale[84]. The use of PEG in the depolymerization of nylon 6 seems attractive

from theoretical and practical view points and the current work is in that direction. The theoretical analysis of multiphase transfer catalysis and use of ionic liquids such as PEG is reported by Yadav[85]. Caprolactam is prepared by the cyclization of 6-aminocaproic acid. Caprolactam is the monomer needed for the production of Nylon 6, which is widely used in the textile industry to produce non-woven fabrics, filaments, carpets and plastics. In the global textile industry, chemical fiber accounts for >77% of the total production volume of textile fiber in 2021 at 88.2 million metric tons (MMT). Caprolactam is synthesized from cyclohexanone via its oxime by with acid that induces the Beckmann rearrangement. Also 6-aminocaproic acid can be condensed to make caprolactam by dehydration and cyclization from 210-260 °C[86].

Thus, in this work we decided to use a phase transfer catalysed depolymerization of nylon 6 in subcritcal water into 6-aminocaproic acid which could be cyclized subsequently into caprolactam. A new model was proposed and validated against experimental data. The results are novel and subscribe to circular economy and conversion of waste into wealth.

3.2. Experimental

3.2.1 Material

Nylon 6 flakes, 0.8-5 mm size, were procured from BASF Mumbai, India, polyethylene glycol (PEG 400) from S. D.Fine Chemicals, MumbaiHigh purity HPLC grade water was used. All other chemicals used were of analytical grade.

3.2.2 Decomposition in water

A stainless-steel autoclave (Amar Equipment's, Mumbai, India), equipped with proper agitation, heating arrangements and controllers was used with following specifications: internal diameter 75 mm, volume 300 mL, standard 4-blade pitched turbine impeller, The polymer-water slurry as reactants was preheated in the range 80- 90 °C before charging to the autoclave. Typical

experiments were done at 250°C. The melting temperature of the resin was calculated to be from 230-240 °C which was ascertained by differential scanning calorimetry. Polymer melt phase plays an important role in the reaction which is governed by initial water to nylon 6 charge ratio (12-63 mol water/mol repeat unit nylon 6), and various time as shown by TGA in Fig. 1. After the desired reaction time interval, the reactor heating was stopped the vessel removed from the heating mentle and quenched quickly in an ice bath. The reaction mass mixture temperature dropped immediately to 100 °C within a minute of quenching. Subsequently the reactor vessel was opened, and the product removed. The product was filtered using a sintered glass filter containing the product 6-aminocaproic acid which was totally soluble in water. The product received more than 40 min was in homogenous phase. The water was removed by rotary evaporator and the solid phase was recovered along with PEG 400. The dehydration of 6-aminocaproic acid leads to the formation of caprolactum (**Scheme 1**). The solid phase composed of oligomers and caprolactam, The product separation was achieved by HPLC (Agilent Technologies,Santa Clara,CA,USA) with a C-18 Column. The presence of PEG 400 in liquid was confirmed through HPLC-ELSD analysis. Recovered solids were dried at 80 °C under vacuum to a constant weight. The solids were ground using a mortar and pestle into fine powder were used for analysis.

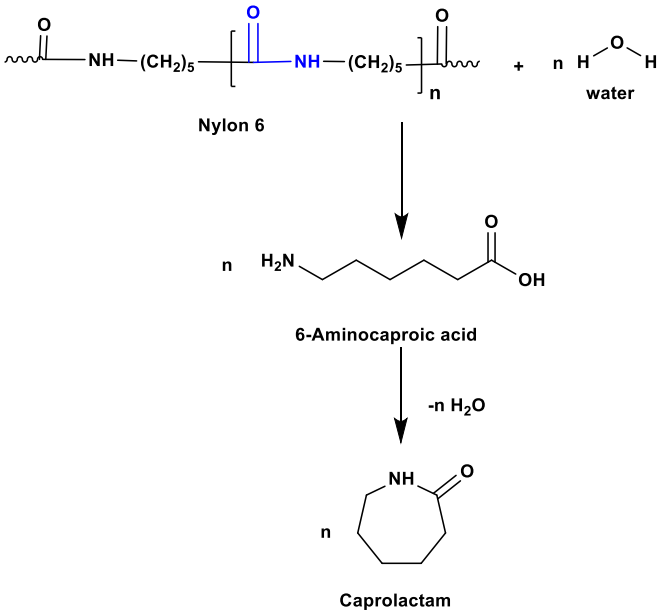

Scheme 3.1. Reaction scheme for nylon 6 hydrolysis: Two-step process: Part I- Depolymerization of nylon 6 to 6-aminocaproic acid (ACA), Part II- Cyclisation of to 6-ACA to caprolactam.

Concentration profile for caprolactam-(quantitative analysis based on HPLC)

$$\%\ conversion\ of\ nylon\ 6 = \frac{Initial\ mol - mol\ at\ time\ t}{inital\ mol\ of\ nylon}$$

$$\%\ yield\ of\ \ 6-\mathrm{ACA}\ = \frac{yield\ of\ 6-ACA\ \ at\ time\ t}{inital\ wt\ of\ nylon}$$

$$\%\ yield\ of\ olgiomer = \frac{yield\ of\ olgiomer\ at\ time\ t}{inital\ wt\ of\ nylon}$$

$$yield\ of\ olgiomer\ at\ time\ t = inital\ mass\ of\ nylon - mass\ at\ time\ t - mass\ of 6-APA\ at\ time\ t$$

Since the end product as a solid was caprolactam in the second stage, its yield was equal to that of 6-APA.

3.3. Results

Caprolactam was analyzed by various techniques (Scheme 1b).

3.3.1 Structural identification of product

The reaction mass containing 6-ACA dissolved in water and PEG 400, along with unreacted nylon 6 and oligomers, if any, was taken out and placed in a rotovac to distill off water. So the final product is caprolactam. The structural identification of the main product (solid phase) was performed using DSC, TGA, FTIR, NMR, GC-MS.

The TGA curves for reactant and product (without catalyst) at various reaction times are shown in **Fig. 3.1.** The weight loss of nearly 92% in the range of 390-400 °C at the start of reaction can be seen, which is caused by the thermal decomposition of nylon 6. Thermal decomposition at various reaction times occurs in different ranges with certain mass loss. The first temperature range 400-450 °C shows nearly 98% weight loss, for 0 min reaction time. For the second range of temperature of 120-190 °C for 60 min reaction time, the weight loss was observed in the range 99%, which is attributed to the thermal decomposition of caprolactam [59].

Figure 3.2 shows FTIR of standard caprolactam and nylon 6 reaction with PEG 400 at different reaction times, caprolactam shows a typical molecular vibration at 1734 (-C=O stretch, ester), 1238 C-O, 1043 (–O-(CH2)-O-), and 969 cm^{-1} C-O peaks. FTIR shows carbonyl peak for the all OH- stretch with increasing reaction time. These results when compared with standard caprolactam sample [87] confirms that product as caprolactam.

In NMR ^{13}C spectra, standard and recovered caprolactam with PEG 400 at different reaction times show **Fig. 3.3**, the signal at δ 129 ppm indicates aromatic protons of benzene ring,167(COOH), 134(aromatic C adjacent to ester). Also, reference spectra for commercial caprolactam are compared with the product recovered after 1 h reaction to find them to be

identical confirming the product is caprolactam [82]. NMR spectra also demonstrate the purity of product [88].

The MS spectrum of products in the liquid phase is depicted in **Fig. 3.5**, and corresponding compounds responsible for the main peaks is caprolactam. The findings unequivocally demonstrate that the primary product is epsilon-caprolactam. Furthermore, there are detectable quantities of 6-aminocaproic acid, dimer, trimer, tetramer, pentamer, and various oligomers of both epsilon-caprolactam and 6-aminocaproic acid, consistent with previous investigations of non-catalytic processes [13–15].

In **Fig. 3.6**, a typical HPLC spectrum is presented, revealing a dominant peak at approximately 7.8 min, akin to the standard ACA sample. This outcome confirms that epsilon-caprolactam is indeed the principal product of PA 6 degradation. The minor peaks observed in the liquid product spectrum, ranging from 5 to 6, likely correspond to other byproducts(i.e oligomer).

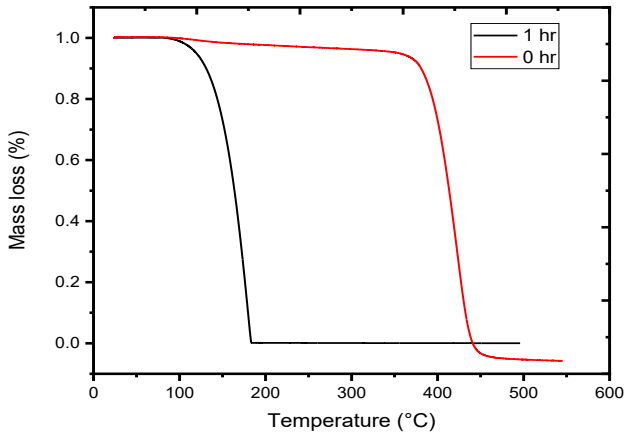

Figure 3.1. TGA plot variation of nylon 6 with PEG-400 treatment time.

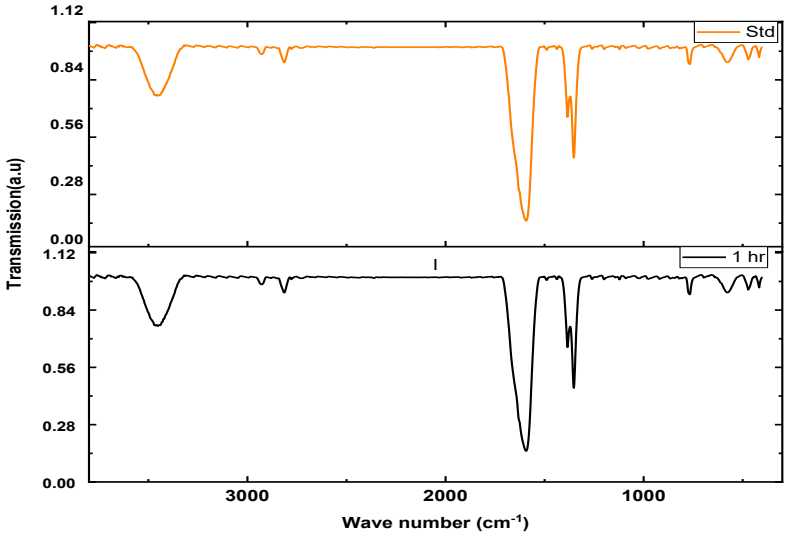

Figure 3.2. FTIR of standard caprolactam and nylon 6 with PEG-400 at various reaction time.

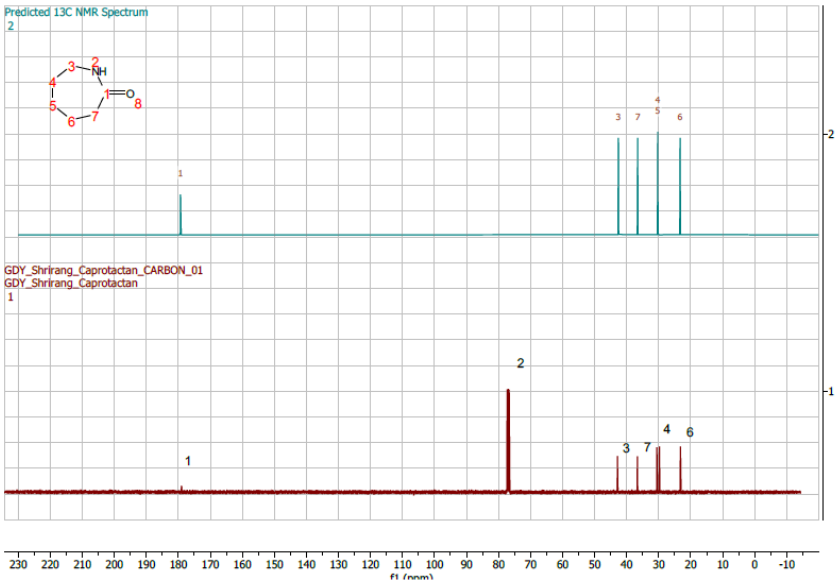

Figure 3.3. NMR^{13}C spectra of standard caprolactam and recovered caprolactam with from reaction.

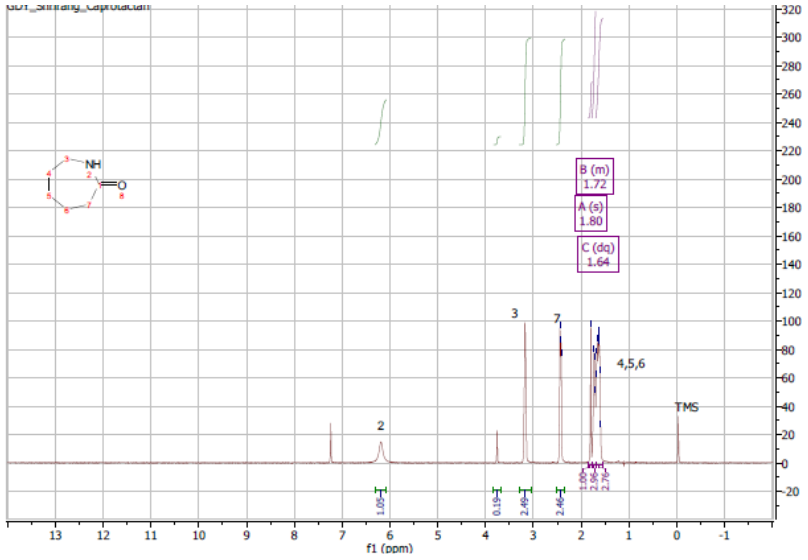

Figure 3.4. NMR ^{1}H spectra of recovered caprolactam from reaction.

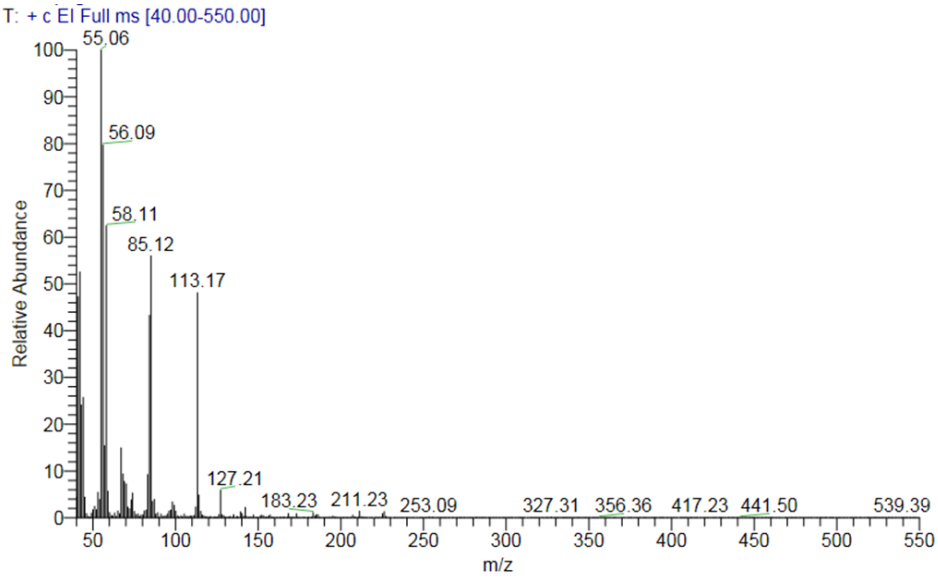

Figure 3.5. MS spectra of recovered caprolactam from reaction. (Reaction condition- Temperature: 240℃; Reaction time: 60 min; Catalyst concentration: 2.11× 10^{-6} mol/g nylon 6 cm^3; Speed of agiation: 650 rpm).

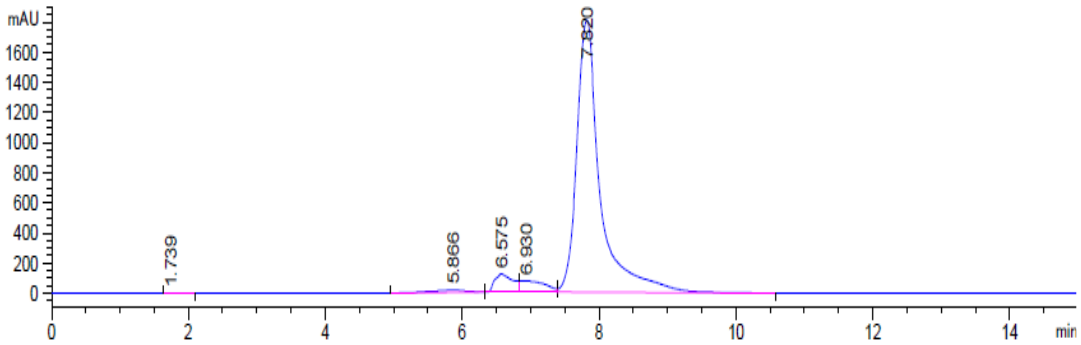

Figure 3.6. HPLC spectra of recovered caprolactam and oligomer from reaction. (Reaction condition- Temperature: 240℃; Reaction time: 60 min; Catalyst concentration: 2.11× 10^{-6} mol/g nylon 6 cm^3; Speed of agitation: 650 rpm).

3.3.2 Reaction mechanism

A new mechanism for the reaction is depicted as shown in **Scheme 2** , which describes the dissolution of nylon 6 into an interfacial mechanism.

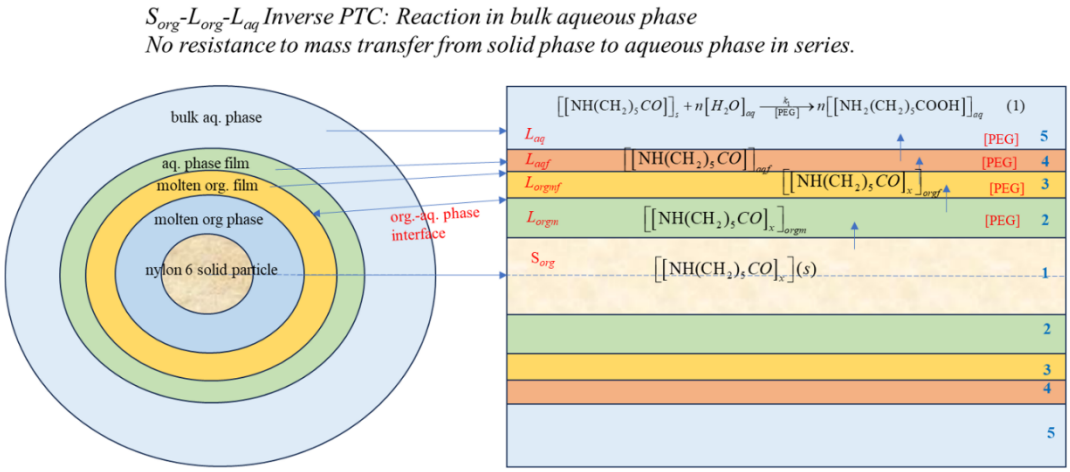

Scheme 3.2. Solid-liquid-liquid inverse PTC reaction of nylon 6 particles. There are two films on either side of the interface. The reaction occurs in the bulk aqueous phase and is not controlled by mass transfer resistance. The dissolve nylon 6 in bulk aqueous phase beyond the aqueous file is rate determining step (RDS).

Part I: Overall reaction under subcritical water phase in the autoclave to produce 6-APA:

$$\left[\left[\mathrm{NH(CH_2)_5CO}\right]\right]_s + n\left[H_2O\right]_{aq} \xrightarrow[[\mathrm{PEG}]]{k_1} n\left[\left[\mathrm{NH_2(CH_2)_5COOH}\right]\right]_{aq} \qquad (1)$$

Part II: Conversion of 6-APA by cyclization in rotovac by dehydration into caprolactum

$$n\left[\left[\mathrm{NH_2(CH_2)_5COOH}\right]\right]aq \xrightarrow[[\mathrm{PEG}]_i]{k_2} n\left[\left[(\mathrm{CH_2})_5\mathrm{CNOH}\right]\right]_s + \mathrm{nH_2O} \qquad (2)$$

Fine nylon 6 solid particles are dispersed in the liquid phase containing subcritcal water in significant excess and the phase transfer catalyst (PEG). When the temperature is raised to melt nylon, the solid particles are softened and converted into globules containing molten nylon (L*orgm*) as exterior and solid nylon (S_{org}) which is followed by the interface between organic and aqueous phases. According to the film theory of mass transfer, there is a thin film of molten phase (L_{orgmf}) next to the interface beyond which there is another thin film of aqueous phase (L_{aqf}) followed by bulk water phase (L_{aq}). So this is a S_{org}-L_{org}-L_{aq} PTC reaction; most of the PTC is in the bulk liquid phase is hydrated and forms a complex, but it is also distributed in aqueous phase film, the molten phase film next to the interface and some part in molten nylon shown as 2,3,4 and 5 in Scheme 2. PEG-water complex can react with nylon which is being transformed from the solid phase to the aqueous phase and finally in the bulk liquid phase (inverse PTC). Depending on the relative rate of mass transfer and chemical reaction the reaction can occur in the bulk aquous phase on in the film on aqueous side or organic side. Such cases have been known and mathematically handled by Yadav and is a case of inverse PTC [ref.]. Since the oligomers and monomer ACA are soluble in aqueous phase, experimental observation revealed that there was no presence of unreacted nylon 6 within 40 min; this indicates that nylon breaks down instantaneously into a mixture of oligomers. The following are the steps for nylon melting and transfer into the bulk aqueous phase.

$$\left[\left[\mathrm{NH(CH_2)_5}CO\right]_x\right](s) \overset{K_1}{\rightleftharpoons} \left[\left[\mathrm{NH(CH_2)_5}CO\right]_x\right]_{orgm}(l) \qquad (3)$$

$$K_1 = \frac{\left[\left[\mathrm{NH(CH_2)_5}CO\right]_x\right]_{orgm}}{\left[\left[\mathrm{NH(CH_2)_5}CO\right]_x\right]_s} \qquad (4)$$

Nylon (org-liq) distribution in thin organic film

$$\left[\left[\mathrm{NH(CH_2)_5}CO\right]_x\right]_{orgm} \overset{K_2}{\rightleftharpoons} \left[\left[\mathrm{NH(CH_2)_5}CO\right]_x\right]_{orgf} \quad (5)$$

$$K_2 = \frac{\left[\left[\mathrm{NH(CH_2)_5}CO\right]_x\right]_{orgf}}{\left[\left[\mathrm{NH(CH_2)_5}CO\right]_x\right]_{orgm}} \quad (6)$$

$$K_3 = \frac{\left[\left[\mathrm{NH(CH_2)_5}CO\right]_x\right]_{aqf}}{\left[\left[\mathrm{NH(CH_2)_5}CO\right]_x\right]_{orgf}} \quad (6)$$

$$K_4 = \frac{\left[\left[\mathrm{NH(CH_2)_5}CO\right]_x\right]_{aq}}{\left[\left[\mathrm{NH(CH_2)_5}CO\right]_x\right]_{aqf}} \quad (7)$$

The product of $K = K_1K_2K_3K_4 = \dfrac{\left[\left[\mathrm{NH(CH_2)_5}CO\right]_x\right]_{aq}}{\left[\left[\mathrm{NH(CH_2)_5}CO\right]_x\right]_s}$ (8)

Eq (8) gives the concentration of dissolved oligomers in aqueous phase in terms of solid nylon. In other words, there could be a concentration gradient, if the rate of reaction is faster in comparison with mass trasfer rate. When the rate of mass transfer is high, the reaction is slow and the aqueous phase will be saturated with dissolved nylon. PEG forms a complex with water by bonding as follows.

$$\left[\mathrm{PEG}\right]_{aq} + \left[\mathrm{H\text{-}OH}\right]_{aq} \overset{K_{PW}}{\rightleftharpoons} \left[\left[\mathrm{PEG\text{-}HOH}\right]\right]_{aq} \quad (9)$$

$$K_{PW} = \frac{\left[\left[\mathrm{PEG\text{-}HOH}\right]\right]_{aq}}{\left[\mathrm{PEG}\right]_{aq}\left[\mathrm{H\text{-}OH}\right]_{aq}} \quad (10)$$

The intermediate oligomers formation is given by .

$$\left[\left[\mathrm{NH(CH_2)_5CO}\right]_x\right]_{aq} + x[PEG - H_2O]_{aq} \overset{K_5}{\rightleftharpoons} \left[\left[\mathrm{NH_2(CH_2)_5COOH\text{-}}PEG\right]_x\right]_{aq} \quad (11)$$

$$K_5 = \frac{\left[\left[\mathrm{NH_2(CH_2)_5}COOH - PEG\right]_x\right]_{aq}}{\left[\left[\mathrm{NH(CH_2)_5}CO\right]_x\right]_{aq}[PEG - HOH]^x_{aq}} \quad (12)$$

The oligomer complex with PEG is broken since olihomers are highly soluble in water, particularly subscritical water to give ACA

$$\left[[\mathrm{NH_2(CH_2)_5COOH\text{-}}PEG]_x\right] \xrightarrow{k_r} x\left[\mathrm{NH_2(CH_2)_5COOH}\right] + x[PEG] \qquad (11)$$

The oligomers are then broken into ACA as per equ (11). PEG added initially is distributed in various complexes occurs as follows. Using eqns. 9 and 10,

$$\begin{aligned}[PEG]_0 &= \left[\left[PEG\text{-}HOH\right]\right]_{aq} + \left[[NH_2(CH_2)_5COOH\text{-}PEG]_x\right]_{aq} + [PEG]_{aq} \\ &= K_{PW}\left[PEG\right]_{aq}\left[HOH\right]_{aq} + K_5\left[\left[NH_2(CH_2)_5CO\right]_x\right]_{aq} K_{PW}^x \left[PEG\right]_{aq}^x \left[HOH\right]_{aq}^x + [PEG]_{aq} \\ &= \left[PEG\right]_{aq}[(K_{PW}\left[HOH\right]_{aq} + K_5\left[\left[NH_2(CH_2)_5CO\right]_x\right]_{aq} K_{PW}^x \left[PEG\right]_{aq}^{x-1}\left[HOH\right]_{aq}^x) + 1] \end{aligned} \qquad (12)$$

Thus, the concentration of free PEG in the aqueous phase is obtained from Eq. (12) as:

$$[PEG]_{aq} = \frac{[PEG]_0}{(K_{PW}\left[\mathrm{HOH}\right]_{aq} + K_5\left[\left[\mathrm{NH(CH_2)_5}CO\right]_x\right]_{aq} K_{PW}^x \left[\mathrm{PEG}\right]_{aq}^{x-1}\left[\mathrm{HOH}\right]_{aq}^x) + 1)} \qquad (13)$$

The above equation shows by considering the denominator that it can be represented as a fraction of the initial PEG added in the reaction mass. Let it be '*f*' which will be reasonably constant and will be in the range of 0-1. It will be constant for a substantial period of time but could increase as the reaction proceeds.

$$[PEG]_{aq} = f[PEG]_0 \qquad (14)$$

Thus, the rate of reaction of nylon oligomers dissolved in the aqueous phase is given by:

$$\begin{aligned}\frac{\left[[\mathrm{NH_2(CH_2)_5COOH\text{-}}PEG]_x\right]}{dt} &= k\left[[\mathrm{NH_2(CH_2)_5COOH\text{-}}PEG]_x\right] \\ &= krK_5\left[\left[\mathrm{NH(CH_2)_5CO}\right]_x\right]_{aq}[PEG - H_2O]_{aq}^x \\ &= krK_5\left[\left[\mathrm{NH(CH_2)_5CO}\right]_x\right]_{aq} K_{PW}^x [PEG]_{aq}^x [H_2O]_{aq}^x \\ &= krK_5K_{PW}^x [PEG]_{aq}^x [H_2O]_{aq}^x \left[\left[\mathrm{NH(CH_2)_5CO}\right]_x\right]_{aq} \\ &= krK_5K_{PW}^x K[H_2O]_{aq}^x [PEG]_{aq}^x \left[\left[\mathrm{NH(CH_2)_5}CO\right]_x\right]_s \\ &= k_{app}\ [PEG]_{aq}^x \left[\left[\mathrm{NH(CH_2)_5}CO\right]_x\right]_s \end{aligned}$$

Also, from stoichiometry, the rate formation of ACA is related by the following

$$-\frac{\left[[\mathrm{NH_2(CH_2)_5COOH\text{-}}PEG]_x\right]}{dt}=\frac{1}{x}\frac{d\left[\mathrm{NH_2(CH_2)_5COOH}\right]}{dt}=krK_5K_{PW}^{x}K[PEG]_{aq}^{x}[H_2O]^{x}\left[\left[\mathrm{NH(CH_2)_5}CO\right]_x\right]_s$$
$$=k_{app}\,[PEG]_{aq}^{x}\left[\left[\mathrm{NH(CH_2)_5}CO\right]_x\right]_s$$
$$=k_{app}\,f\,[PEG]_0^{x}\left[\left[\mathrm{NH(CH_2)_5}CO\right]_x\right]_s \qquad (15)$$

Typically, PTC reactions are first order in catalyst concentration, the above equation suggests that the order in PEG is more than one if oligomers are formed and broken into ACA.

Where $krK_5K_{PW}^{x}K[H_2O]^{x}=k_{app}$

A plot of equation 15 is shown in **Fig. 3.7** which shows concentration profile for nylon 6, oligomer and 6-Aminocaproic acid. The values of rate constant were calculated for different temperature as shown in **Fig. 3.8**. The experimental values at different reaction time of nylon 6 and 6-Aminocaproic acid calculated using peduofirst order kinetic model. For different reaction temperature, the rate constant values were determined and listed in **table 1**.

For a fixed concentration of catalyst, the reaction is a pseudo-first order reaction. In other words, the rate of hydrolysis of nylon 6 under subcritical reaction will be a pseudo-first order reaction. The material balance showed that the amount of caprolactam formed was equal to amount of ACA formed which is related to hydrolysis of dissolve nylon.

where,

$$n\left[\left[\mathrm{NH_2(CH_2)_5COOH}\right]\right]_i(l)\xrightarrow[[\mathrm{PEG}]_i]{k_2}n\left[(\mathrm{CH2})_5\mathrm{CNOH}\right](l)$$

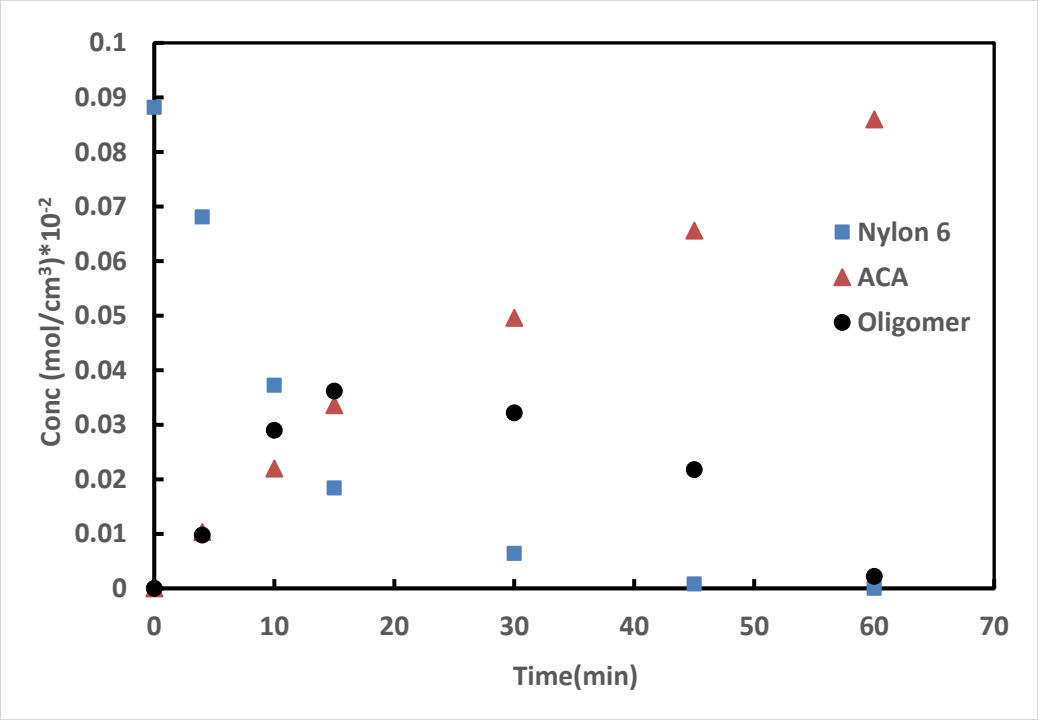

Figure 3.7. Concentration profile for nylon 6, 6-Aminocaproic acid (ACA) with respect to time with PEG 400 catalytic effect. (Reaction condition- Temperature: 240 °C; Catalyst concentration: 2.11× 10^{-6} mol/g nylon 6 cm^3; nylon 6 concentration: 8.088× 10^{-4} (mol/cm^3); Water: 100 cm^3; Speed of agitation: 650 rpm).

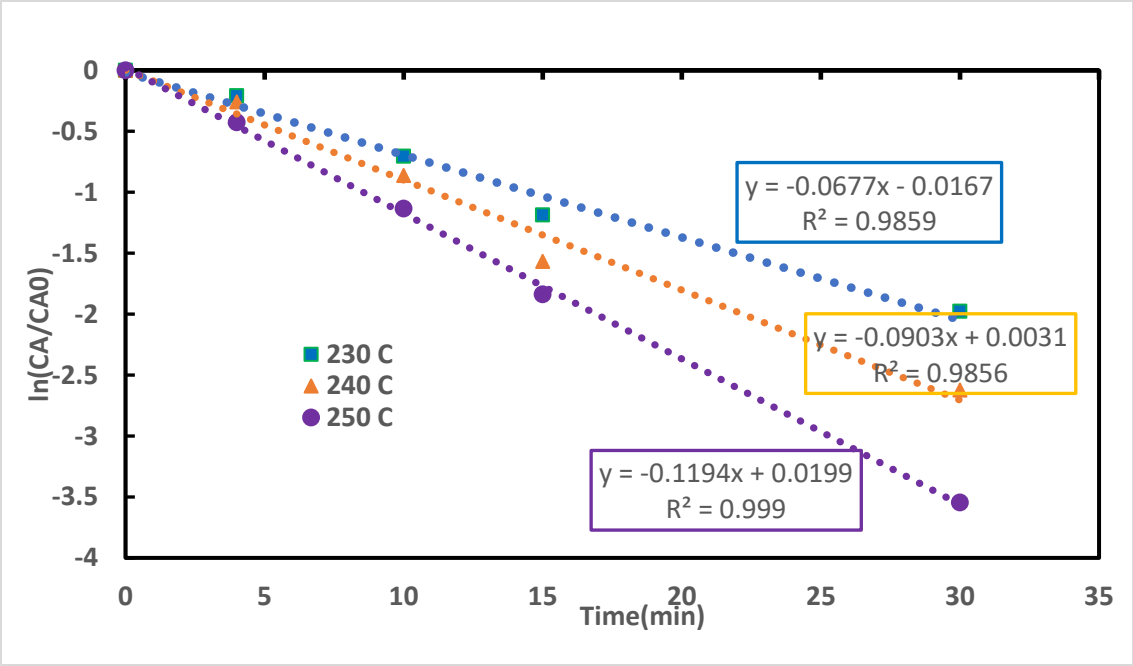

Figure 3.8. Fitting pseudo first order reaction model and calculate rate constant at different temperature. (Reaction condition- Catalyst concentration: 2.11× 10^{-6} mol/g nylon 6 cm^3; nylon 6 concentration: 8.088× 10^{-4} (mol/cm^3); Water: 100 cm^3; Speed of agitation: 650 rpm).

Table 3.1 Effect of Temperature on rate constant for PEG 400 catalysed hydrolysis to ACA

Temperature (°C)	k_1 (min^{-1})
230	0.025
240	0.032
250	0.038

3.3.3 Influence of reaction condition on hydrolysis reaction of Nylon 6

At the end of the reaction the reaction was contained aqueous solution of APA. The reaction mixture in the reactor vessel consisted of one phase for all reaction times studied. The reaction mass was subjected to evaporation using rotary evaporator leading formation of caprolactam. Further experiments were done to cyclize ACA and the formation of caprolactam was monitored. These experiments were done at atmospheric pressure.

3.3.3.1 Influence of Initial weight ratio

The hydrolysis reaction was investigated using the nylon 6 and water initial charge ratio range of 12-63 mol water/mol repeat unit nylon 6, **Fig. 3.9** depicts conversion of nylon to caprolactam as function of time with reaction condition of 230-250 °C and autogenous pressure (3.2 MPa) generated by water vapour. The initial weight ratio of 12 mol water/mol repeat unit nylon 6 gives 70% conversion within 45 min reaction time, however, afterward reach constant, only with 10% increase in conversion. On the other hand, for an initial weight ratio 31-63 mol water/mol repeat unit nylon 6 gives approximately 86-88% conversion for 45 min reaction time and reaches 100 % conversion within 60 min. Initial weight ratio 31-63 mol water/mol repeat unit nylon 6 gives complete depolymerization, other hands, less than mol water/mol repeat unit nylon 6 initial weight ratio reaction fails to provide complete depolymerization. Although water is an excess reactant for 12 mol water/mol repeat unit nylon 6, it does not create sufficient water vapor pressure. However, in the case of 31-63 mol water/mol repeat unit nylon 6 has the effect of vapour pressure which helps to break particle size of nylon [55] which in turn create larger surface area helps to form reactive polar intermediate. Also, particle size has major influence on heat and mass transfer, which governs the solubility of nylon in PEG 400.

3.3.3.2 Influence of reaction time

Since the experiments in the second stage were cyclization of ACA to caprolactam, it is taken as equivalent to ACA. The complete depolymerization is majorly governed by reaction time, as shown in **Fig. 3.7**. It can also seen from **fig. 3.8** to reach conversion up to 40 % requires 15-20 min reaction time.

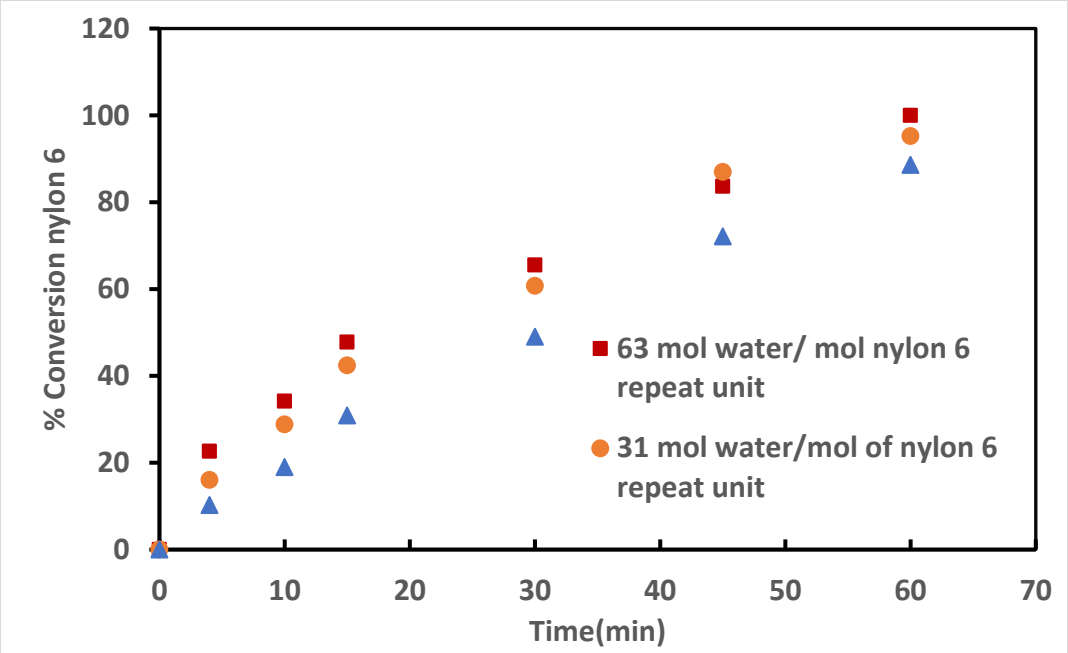

Figure 3.9. Conversion of nylon 6 with time for three different Initial charge ratio. (Reaction condition- Temperature: 240°C; Reaction time: 30 min; Catalyst concentration: 2.11×10^{-6} mol/g nylon 6 cm^3; Speed of agitation: 650 rpm).

3.3.3.3 Influence of catalyst concentration on hydrolysis

The influence of PEG 400 concentration on depolymerization is studied in autoclave in the temperature range 230-250 °C, with a reaction time 60 min, for initial reactor loading 63 mol water/mol repeat unit nylon 6 and with PEG 400. The effect of PEG 400 various concentration on scission of amide linkages to caprolactam shown in **Fig. 3.10.** Effect of catalyst concentration studied with control experiment carrying out reaction for same reaction time and initial reactor loading. The effect of catalyst concentration measured for four different concentrations used, shown in **figure 3.10**. It is observed that the initial rate of reaction was found to increase with increasing concentration of the catalyst. This nature is typical of PTC reactions[89].

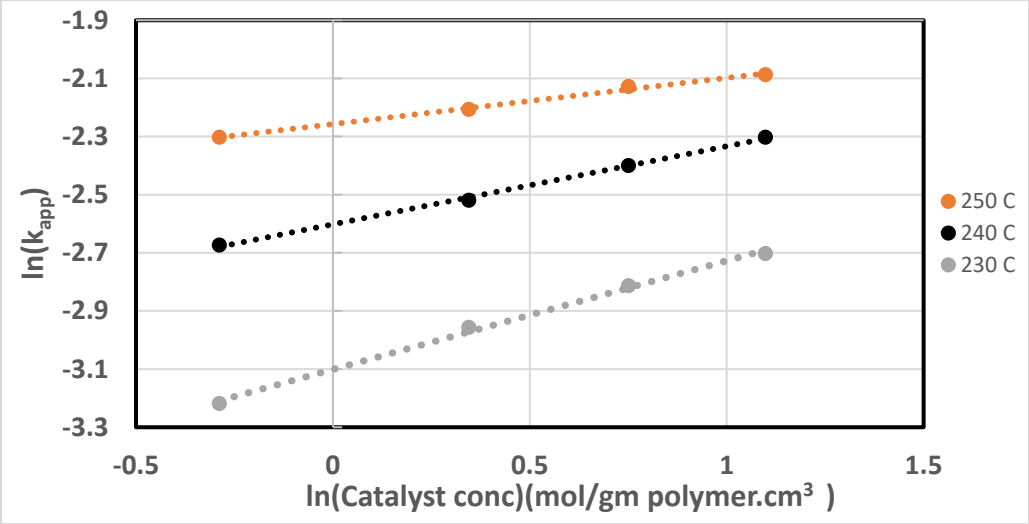

Figure 3.10. Effect of PEG 400 concentration on reaction rate constant at different temperature. (Reaction condition- Water: 100 cm^3; Speed of agitation: 650 rpm).

3.3.3.4 Influence of temperature on nylon hydrolysis

The rate constants for initial charge ratio 63 mol water/mol repeat unit nylon 6 were calculated at different temperatures (**Table 1)** The Arrhenius plot was made (**Fig. 3.11)** to get an apparent activation energy of 44.4 KJ/mol. The activation energy values can be compared with published literature (**Table 2**). Uncatalyzed melt phase hydrolysis is reported to have a activation energy as 55.7KJ/mol [67] whereas zinc acetate and zinc chloride catalysed hydrolysis with 47.8[68] and 64.9 KJ/mol [69] respectively. Thus, PEG 400 is the best catalyst in comparison with all previously used catalysts.

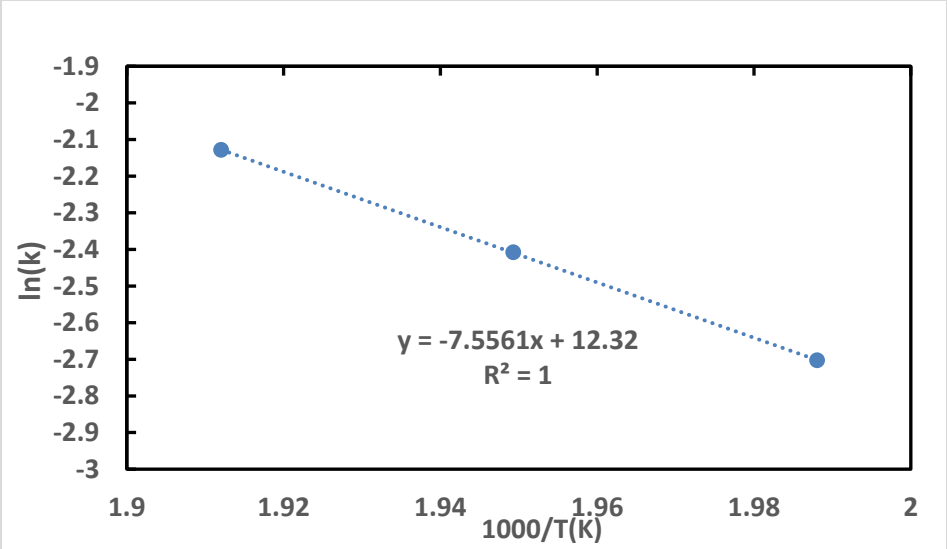

Figure 3.11. Arrhenius plot in presence PEG 400 catalytic depolymerisation. (Reaction condition- Catalyst concentration: 2.11×10^{-6} mol/g nylon 6 cm^3; Nylon concentration: 1.587×10^{-6} (mol/cm^3); Water: 100 cm^3; Speed of agitation: 650 rpm).

Table 3.2 Actitation energy for different catalyst

Catalyst	Activation energy (kJ/mol)	References
PEG400	44.4	Current study
Autocatalytic	205	[81]
Acid hydrolysis(H3PO4)	100	[81]
Base catalyst(NaOH/KOH mixture)	50	[81]
Uncatalysed	86.0	[89]
Phosphotungstic heteropoly acid (HPA)	77.0	[89]
Ionic liquid (1-butyl-3-methylimidazolium chloride)	102	[90]
Zeolite Hb-25	76	[88]
Hydrolysis catalyzed by Hb -25	73	[88]

3.4 Conclusion

PEG 400 was discovered as efficient phase transfer catalyst for hydrolysis of nylon 6. The S-L PTC hydrolysis reaction of nylon 6 was studied by using PEG 400 as the catalyst at melt phase. In fact, in melt phase, the so-called S-L PTC turns out to be S-L-L PTC reaction after melting of nylon. A new theory was developed to interpret dehydration of nylon 6 to 6-aminocproic acid (ACA) where the reaction takes place in subcrtical water phase. Addition of PEG 400 accelerate depolymerisation process by 45min reaction time in compared with super-critical and metal acetate depolymerisation. NMR showed excellent purity of monomer (caprolactam) without any purification or downstream processing of product when ACA was cyclized. Nylon depolymerization is series reaction with oligomers as intermediate which are converted to ACA which was converted in second reaction to caprolactam as final product. The experimental data found to be best fit for kinetic model predicted. The highest yield of caprolactam reached 96% in reaction time of 60 min. High temperature promoted secondary reaction which affected the yield of caprolactam. The depolymerisation of nylon using PEG 400 could be seen as an eco-friendly process for recycling of nylon and reuse of monomer.

Chapter 4

Synthesis of biobased high molecular weight polyester

4.1 Introduction

Starting from the 1950s, plastics manufacturing has exhibited a growth rate surpassing that of all other material categories. Furthermore, the anticipated expansion of petrochemicals, encompassing plastics, is foreseen to be responsible for 50% of the world's oil consumption by the year 2050[91]. Roughly 77% of plastics manufactured worldwide are comprised of polymers featuring carbon-carbon backbone[92]. The molecular composition grants these materials high durability against environmental degradation, allowing them to endure for decades or more, unless incinerated. The major application driving plastic demand is packaging (constituting 44.8% of all polymers used), even though its usage lifespan is notably brief before turning into waste. Projected on the current trajectory, plastic production, utilization, and waste practices could result in the accumulation of about 12 billion metric tons of plastic waste worldwide by 2050. Plastic pollution impacts land, freshwater, and ocean ecosystems. In 2010, approximately 31.9 million metric tons of poorly managed plastic waste contaminated coastal areas, with a significant portion entering the ocean. This issue is especially pronounced in areas with limited waste management infrastructure, including growing economies. Even regions with advanced waste systems, like the United States, contribute to ocean-bound plastic waste through improper disposal. Additionally, exporting recyclable materials to inadequately equipped regions leads to substantial plastic leakage into the environment (estimated at 0.15–0.99 million metric tons in 2016)[93]. Plastic waste is prevalent across various environments, from marine and aquatic settings to terrestrial areas like agricultural soils and even the atmosphere. This widespread contamination has raised concerns among the public regarding its impact on wildlife and human health. As a response, governments at different

levels have implemented bans or charges on plastic products like bags and food containers. Additionally, international policy forums such as the G7, G20, and organizations like UNEP and APEC have proposed action plans to combat marine litter, underscoring the urgency for policymaker attention[94]. Global organizations have put forth suggestions for addressing plastic pollution. These include proposals to curtail deliberate use of microplastics (endorsed by ECHA for the European Commission), restrict the international trade of plastic waste (under the UN Basel Convention Annex II), and even prohibit specific single-use plastic items (European Parliament Resolution P8 TA (2019)0305). Additional efforts emphasize enhancing waste management systems, like the Alliance to End Plastic Waste, mainly consisting of chemical and consumer brand companies. Single-use plastics, like packaging, possess essential benefits such as pathogen protection and food safety enhancement, making complete elimination impractical. Yet, it's crucial to manage plastic waste from important uses to minimize environmental buildup while preserving material value. Current efforts have concentrated on managing common polymers within existing waste systems rather than redesigning materials for easy recycling or developing new end-of-life strategies[95]. The urgent need for improved waste management, especially where formal systems are absent, offers an opportunity for collaboration among polymer scientists, product designers, and environmental engineers. This collaboration can lead to the creation of materials and products that, if effectively collected and processed, not only prevent environmental pollution but also maintain their value and potential for future applications[96]. This trend underscores a considerable demand for developing and enhancing biodegradable plastics that possess biodegradability and align with anticipated material property requirements[97].

The current section is focused on preparing biobased and biodegradable/compostable polyester. In the context of packaging, it's crucial for the polymer to have a substantial molecular weight

(63000-83000 gm/mol), which aids in processing and achieving the desired mechanical properties. The primary objective of this section is to investigate the production of biobased and biodegradable polyesters with high molecular weight. A synthetic approach to polymerization has been formulated to generate compostable polymers with elevated molecular weight. The resultant polymer is assessed using intrinsic viscosity, acid number, and molecular weight and subsequently compared against a commercially available variant. Furthermore, the kinetics of the transesterification and esterification reactions have been examined.

4.2 Chemistry and synthesis

4.2.1 General structure of PET

The general structure of polyester can be written as follows in **fig. 4.1** .

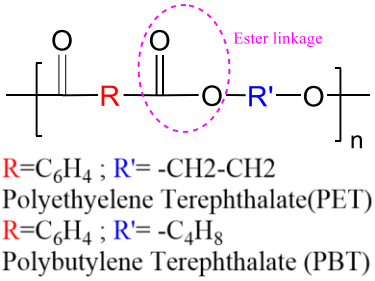

Figure 4.1. General structure of polyester.

The end groups R and R' of polyester can be hydroxy, carboxy, or methoxy. It will depend upon the method of preparation. The stoichiometric amount of acid and diol used in practice decides what will be the end group. In case of excess diol preparation end group will be hydroxy[98].

4.2.2 General structure of co-polyesters

The general structure of co-polyester can be written as follows **fig. 4.2**[99].

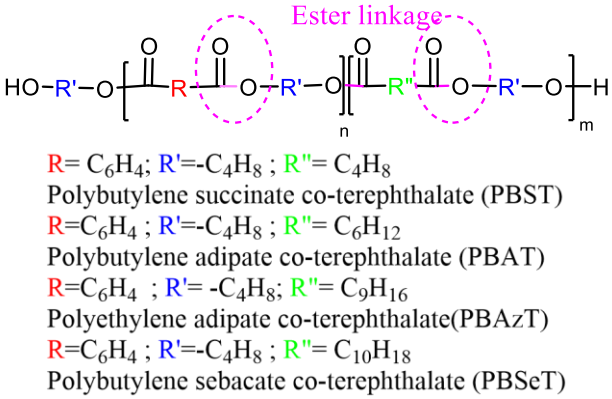

Figure 4.2. General structure of co-polyester of butanediol.

The groups R, R' and R'' of polyester can be from acid and diol. In the case of PBAT synthesis, R will be terephthalic unit, R' will be butanediol unit and R'' will be from adipic acid unit. The stoichiometric amount of acid or diol used in preparation decides what will be the end groups. In case of excess diol preparation, the end group will be hydroxy.

4.3 Analytical Methods

4.3.1 Intrinsic Viscosity

Viscosity depends on molecular weight distribution; correlations have been made between dilute solution viscosity and molecular weight. The ASTM D2857-16: "Standard Practice for Dilute Solution Viscosity of Polymers and Intrinsic Viscosity of Polymer and Biopolymers Measured by Microchip" has been referenced for the following viscosity procedure and molecular weight determination procedure. **Procedure:** For all trials, a constant-volume viscometer was used inside a fume hood operating at 27°C. The primary viscometer used was Canon 0C-D290. Four trial concentrations were made for one polymer sample by adding the required sample weight (mg) to a vial of 15 ml chloroform. The trial concentration in the vial was poured through a funnel into the viscometer. The sample was plunged into the viscometer with a syringe. The solution's passage

through the marked region of the viscometer was timed to obtain an efflux time. The process was repeated three times for each sample concentration and pure solvent sample. The average of the sample efflux times was used in viscosity calculations.

Relative Viscosity (Viscosity Ratio) was calculated by dividing the average sample efflux time, t, by the average solvent efflux time, t_s, in units of seconds. Due to negligible differences in densities and kinetic energy factors used within the viscosity calculation of the pure solvent, η_s, and trial concentrations, η, the unitless ratio of the viscosities simplifies to this formula:

$$\eta_{rel} = \frac{t}{t_0} \qquad (1)$$

Inherent Viscosity (Logarithmic Viscosity Number) was calculated by taking the natural logarithm of the relative viscosity and dividing it by the sample concentration, c, with units of g/cm^3. Inherent viscosity has units of ml/g.

$$\eta_{inh} = \frac{\ln(\eta_{rel})}{C} \qquad (2)$$

Reduced viscosity was calculated by subtracting one (1) from the relative viscosity and dividing by the sample concentration. Reduced viscosity has units of ml/g.

$$\eta_{red} = \frac{(\eta_{rel} - 1)}{C} = \frac{(\eta_{spec})}{C} \qquad (3)$$

Polymer Intrinsic Viscosity (Limiting Viscosity Number), $\eta_{Intrinsic}$, was determined graphically. Inherent and Reduced Viscosity values were plotted for the huggins and Kreamer equation. However, Huggins' constant depends on the hydrodynamic interactions among polymer chains in solution and may change with incorporating another polymer in the backbone. Hence, for better estimation of the IV, solution viscosities of the polyester samples were measured at different

concentrations for each sample and the IV was obtained by extrapolating the $\eta sp/c$ vs c plot to infinite dilution or zero concentration. **Fig. 4.3** below is an example of the graphical determination of Intrinsic viscosity obtained from ASTM D2857-16.

Huggin's equation

$$\eta_{red} = \frac{(\eta_{rel} - 1)}{C} = \frac{\eta_{spec}}{C} = [\eta] + K_h [\eta]^2 C \quad (4)$$

Kraemer equation

$$\frac{\ln(\eta_{rel})}{C} = [\eta] - K_k [\eta]^2 C \quad (5)$$

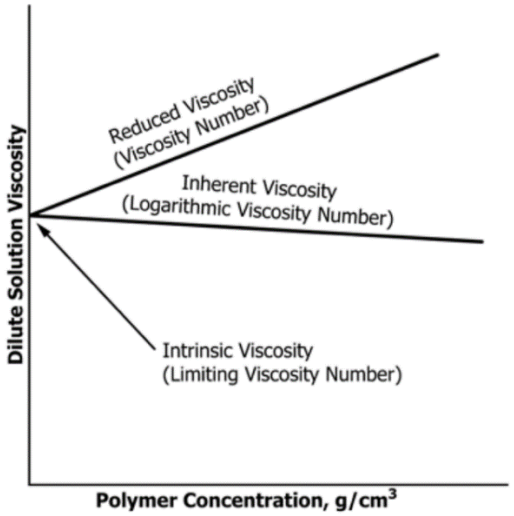

Figure 4.3. Typical plot for polymer concentration versus dilute solution viscosity.

The Intrinsic Viscosity value was converted to dl/g and used within a rearranged equation of the Mark-Houwink-Sakurada equation to obtain the average molecular weight of polymer chains in units of :

$$[\eta] = K[M]^{\alpha} \quad (6)$$

$$Molecular\ weight = \frac{\log(\eta_{Intrinsic}) - \log(K)}{a} \quad (7)$$

Parameters "K" and "a" depend on solvent polymer interactions, temperature, and coil size of the sample polymer. Value for used "a" was 0.59 , and K was 0.00075 dl/g for all trial samples[100]. A more detailed discussion of the Mark-Houwink-Sakurada parameters can be found in the literature.

4.3.2 Acid value method

Measuring acidic constituents of polymer is done to monitor acid functional group, quality control method and gives insight into polymer formation. This measurement was done with the following procedure, which was created with the guidance of the ASTM D7409 – 15, the Standard Test Method for Acid Number of Petroleum Products by Potentiometric Titration, and the ASTM D664 – 18, the Standard Test Method for Carboxyl End Group Content of Polyethylene Terephthalate (PET) Yarns**.** Acid numbers obtained from this method indicate acid functional groups in the polymer sample, which gives insight into the reaction progress. **Procedure:** For one trial sample, around two (2) grams of the polymer were weighed and put into an 125 ml erlenmeyer flask. About 50 ml of dichloromethane (DCM) solvent was added to the flask to dissolve the polymer. The titration was repeated for 2-3 replicates for each polymer sample. Once the polymer sample was dissolved into the DCM, a stir bar and 2-4 drops of color indicator (1% bromophenol in methanol) were added to the flask. The flask was placed on a mixing plate under the manual titration burette filled with a known potassium hydroxide (KOH) concentration in methanol. Bromophenol blue as a color indicator shows a yellow color at a pH of 3.0 and a blue color at a pH of 4.6. Titration was finished when the polymer solution reached a violet (blue-purple) endpoint, and the volume of the KOH solution was recorded for later calculations to determine the trial acid number of the sample.

Solutions of 0.05 N and 0.003 N KOH in methanol were used, depending on the acid group present

in the sample. Higher acid groups required higher KOH concentration to mitigate polymer precipitation from the DCM-methanol solution. Conversely, the 0.05 N solution would often be too concentrated and would result in the color indicator reaching the end point with only 1-2 drops of titrant dispensed into the flask. Acid value determination was done using the following equation (obtained from ASTM D7409 − 15):

$$\text{Acid value}\left(\text{AV}\right) = \left[\frac{M_{KOH} \times \text{Vol}_{\text{KOH}}(\text{ml}) \times 1000}{\text{w(g)}}\right] \quad (8)$$

V_{KOH} is the volume of KOH titrant used for the sample trial (ml), M is the molarity of the KOH in methanol solution (mol/L), and w is the weight of the polymer sample in units of grams. The resulting acid value has units of mmol/kg.

The samples were collected at different reaction times. It was used to measure acid numbers by the ASTM method. The total carboxyl end group conversion for the esterification kinetics study of PBAT was monitored by titration using ASTM D7409. The extent of the reaction was calculated by determining the acid value (AV) of the samples at an initial time and desired time. The total carboxyl end group conversions were calculated by following the equation.

4.3.3 TGA and DSC

The thermal degradation properties were evaluated using a thermogravimetric analyzer, TGA Q50 (TA Instruments, USA), by heating the sample from room temperature to 550 °C at a rate of 10 °C/min under a nitrogen atmosphere. The samples' thermal properties were obtained using a differential scanning calorimeter, DSC Q20 (TA Instruments, USA). The samples were first heated up to 250 °C starting at room temperature at 10 °C/min under a nitrogen atmosphere to erase any thermal history associated with processing. The glass transition temperature was obtained by cooling up to -55 °C at 10 °C/min and heated again up to 250 with rate of 250 °C starting at room

temperature at a rate of 10 °C/min under a nitrogen atmosphere.

4.3.4 ^{13}C. and ^{1}H NMR

^{13} C. and^{1} H analysis of the samples were performed by dissolving the sample in a deuterated chloroform (CDCl3) and DMSO-d-6 solvent. The spectra were then recorded on a 500 MHz Varian Unity Plus NMR spectrometer (California, USA) at room temperature.

4.3.5 Gel permeation chromatography

The molecular weight distributions of the synthesized polymer were assessed through employment of gel permeation chromatography (GPC). A Waters GPC (Massachusetts, USA) equipped with a Waters 1515 isocratic HPLC pump, a Waters 717 autosampler, Waters Styragel columns, and a Waters 2414 refractive index detector were used for the study. The mobile phase adopted was tetrahydrofuran (THF), flowing at a rate of 1 mL/min. Both the detector and columns were consistently maintained at a temperature of 35°C during the experimental runs. To prepare the samples, they were dissolved in tetrahydrofuran (THF) at a concentration of 2 mg/mL, while being kept at room temperature. The resulting solution was then subjected to filtration using a PTFE syringe filter, after which it was transferred to vials. These vials containing the filtered solution were subsequently positioned on the autosampler plate. Each sample underwent a runtime of 50 minutes during the analysis. To ensure the reliability of the data, every sample was subjected to triplicate runs. For the determination of molecular weights, calibration standards of polystyrene were employed as reference materials.

4.3.6 Molecular weight and degree of polymerization and extent of reaction

The number-average degree of polymerization of the reaction mixture, denoted as X_n and described by Ghosh (1990) and Odian (1991), is determined by dividing the initial total number of monomer molecules, denoted as N_0, by the total number of molecules present at time 't,'

represented as N [101]. This relationship can be expressed as follows:

$$X_n = \frac{N_0}{N} \tag{9}$$

It is easy to see that for hydroxy acids and for stoichiometric mixtures of diol and diacid, there is an average of one carboxyl per molecule at any state of reaction

$$p = \frac{N_0 - N}{N} \tag{10}$$

Where N_0 is the initial (at t=0) concentration of hydroxyl or carboxyl groups and N_t is the concentration at some time t.

Two approaches may be used to calculate X_n after different stages of reactions[101].

1. Approach- I

When the monomer present in the mixture is in nonstoichiometric amount degree of polymerization for extent of reaction *p* can be written as follows:

$$X_n = \frac{1+r}{1+r-2rp} \tag{11}$$

Where r is stoichiometric ratio such that $r = N_{A0}/ N_{B0}$, the ratio *r* is always defined such that it has a value equal to or less than unity, but never greater than unity, i.e., the groups present in excess are denoted as B groups.

2. Approach- II

When reaction mixture will have monomer with different functional group. The f_{avg} represents the average number of useful equivalents of functional groups of all kinds per molecule present initially in the reaction mixture.

$$f_{avg} = \frac{\sum N_i f_i}{\sum N_i} \tag{12}$$

where N_i is the number of moles of species i with f_i number of functional groups. Note that f_{avg} represents the average number of functional groups per molecule in the reaction mixture. Equation holds strictly when functional groups of opposite kinds are present in equal concentrations,i.e., for stoichiometric mixtures.

$$f_{avg} = \frac{2N_{A0}}{\sum N_{io}} \qquad (13)$$

In nonstoichiometric mixtures, the excess reactant does not enter the polymerization (in the absence of side reactions) and so it should not be considered for calculating f_{avg} . Let us consider a polymerization system in which $N_{A0} < N_{B0}$, where N_{A0} and N_{B0} are number of equivalents of initial functional groups of types A and B, respectively, present initially. In this case, the number of B equivalents that can react cannot exceed N_{A0} , and therefore[102]. Let

$$p = \frac{2(N_0 - N)}{N_0 f_{avg}} \qquad (14)$$

Where,

N_0 = total number (mol) of monomers (of all types) present initially.

N = total number (mol) of molecules (monomers plus polymers of all sizes) when the reaction has proceeded to an extent p.

$N_0 - N$ = number of linkages formed at the extent of reaction p.

(This follows from the fact that every time a new linkage is formed the reaction mixture will contain one less molecule.) From equation 14 and 9 the degree of polymerization can be written as in terms of average functionality as follows:

$$X_n = \frac{N_0}{\left[\frac{2N_0 - N_0 pf_{avg}}{2}\right]}$$

$$X_n = \frac{2N_0}{\left[2N_0 - N_0 pf_{avg}\right]}$$

$$X_n = \frac{2}{\left[2 - pf_{avg}\right]} \quad (15)$$

4.4 Materials and methods

4.4.1 Material

DMT (99% pure), 1,4 butanediol (99% pure), sebacic acid (98% pure) and azelaic acid (88% pure) were purchased from sigma Aldrich, USA. Titanium butoxide was obtained from VWR, USA.

4.4.2 Experimental method

A stainless-steel reactor (Parr instrument company, IL, USA), with internal diam.101.6 mm, volume 2500 ml, standard 4-blade pitch turbine impeller, equipped with proper agitation, heating arrangements, and controllers, was used for all hydrolysis experiments. The reactor was preheated to 80- 90 °C, and the reactants were added. The reaction temperature was set per the stage mentioned in the experimental methodology. The titanium butoxide catalyst was mixed with BD and added to the molten DMT reactor. The amount of catalyst, based on the DMT content in the reactor, was used without further purification. Upon addition of catalyst solution, methanol vapor evolved from the reactor almost immediately. The methanol vapor was condensed and collected in a bubbler, and the rate of methanol evolution was used to estimate the conversion of methyl ester groups of the DMT. The reaction was carried out under an argon atmosphere to avoid oxidation reactions. PET and co-polyesters were prepared using the same reactor setup but with different experimental methodologies.

4.4.3 Experimental methodology-polyester of butanediol

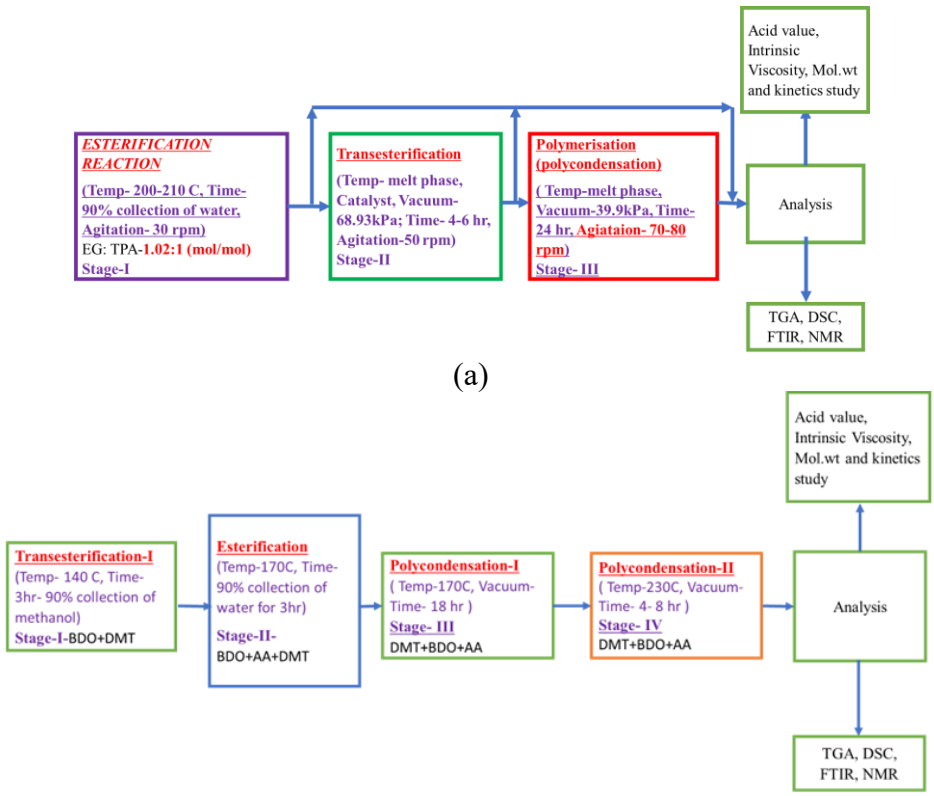

Figure 4.4. Synthesis methodology for (a) PET and (b) co-polyesters of butanediol.

4.4.4 Polyethylene terephthalate (PET)

Poly (ethylene terephthalate) (PET) is widely used as a commodity as well as an engineering product for various applications. It's mainly used as raw material for making products like fibers, packaging articles and film. PET is one of the fastest growing markets and will continue this trend in the future enhanced by world economic growth and continuous development of new application fields[103]. Polyethylene terephthalate (PET) is polymer formed by step-growth polycondensation from ethylene glycol and dimethyl terephthalate (DMT). High molecular weight PET production by polymerization of ethylene glycol and dimethyl terephthalate or terephthalic acid is essential[104]. This study used EG to prepare PET from DMT in the presence of titanium butoxide as a catalyst. The result showed that high molecular weight PET was produced using 3 stage

polymerization technique.

4.4.4.1 Synthesis of PET

4.4.4.1.1 Monomer purification

Acetone, Dimethyl terephthalate - 99 % purified (moisture free), titanium butoxide-IV, and Ethylene Glycol were procured from Sigma Aldrich, USA. Dry ice was purchased from the MSU chemistry store in East Lansing. Ethylene glycol was further purified for removal of water and other contaminant by cubic size molecular sieve. The pore size of the molecular sieve was 4 A. The equilibrium water capacity was 24 % wt. Ethylene glycol and molecular sieve were used in a ratio of 2:1 (v/w). It was kept inside the oven for 8-12 hr at 60 °C. Ethylene was separated from sieves and used for the polymerization reaction.

4.4.4.1.2 Reaction chemistry and synthesis procedure

The experiments were conducted as mentioned in **section 5.4.2**. PET was synthesized as methodology described in **section 5.4.4** and **Fig. 4.4(a)**. The reactions involved in each stage are as follows:

4.4.4.1.2.1 Stage-I (trans-esterification reaction)

Transesterification exhibits reversibility, making effective removal of generated methanol crucial for achieving a substantial yield of BHET. The process of BHET formation is envisioned as a two-step progression. Initially, p-methoxycarbonyl-2-hydroxyethyl benzoate is formed, reacting with another ethylene glycol molecule to produce BHET(as shown in **Scheme 4.1)**. A key question arises in the kinetic analysis of transesterification: whether there is a distinction between the rate constants of the two steps. Researchers like Tomita and Ida have examined this matter. Based on their experimentation with model compounds, they concluded that such a difference is negligible[105]. Thus, from the collected evidence, it's reasonable to assume that the rate constants

for both steps are quite similar. Consequently, the formation of BHET can be understood as a straightforward interaction between a methyl ester group and a hydroxyl group within ethylene glycol. Challa presented the argument that both rate constants are essentially indistinguishable[106]. The transesterification of dimethyl terephthalate (DMT) with ethylene glycol (EG) may be represented by the following equation where methanol and bis (hydroxyethyl) terephthalate (BHET) are formed as equation (1).

The reactor was Preheated above 90 ℃. Both monomers were taken in the ratio- EG: DMT- 1.02:1 (mol/mol) and added in the preheated reactor. After adding both reactants to the reactor, the reactor was closed. The reactor was purged with argon gas at around 551 kPa pressure. After the removal of air and purge of argon, the temperature of the reactor was set at 130-150 ℃. Once the temperature reached the desired set point - the stirrer was started at a minimum of 30 rpm. Methanol was Collected from a transesterification reaction. The esterification reaction is considered complete when methanol collection reaches- 95 % of the theoretical amount of methanol. The time required for the collection of water is typically 3-4hr. The reactor heater and stirrer were switched off, and after cooling, untightened the screw and took out some reaction samples from the reactor for analysis. DSC, TGA, FTIR, IV, Mol wt.

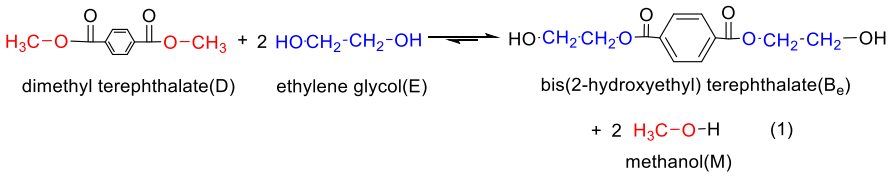

Scheme 4.1. Transesterification reaction between DMT and the ethylene glycol (Reaction conditions: Temp: 130-150°C; Time: 90% collection of methanol; Speed of agitation: 30 rpm).

4.4.4.1.2.2 Stage-II (polycondensation-I)

The second stage primary reaction can be transesterification and polycondensation, as shown

below (2) and (3). In this stage, polymer chains are formed. The reaction temperature was slightly above the melt temperature. It was determined using DSC. The reactor was again purged with argon gas, as mentioned above. Once the reactor reached the set temperature, the stirrer was started. The vacuum was applied in this stage (6.6 kPa). The reaction was run for 4-6hr. Samples were collected at different times for analysis DSC- TGA- IV-FTIR. Chain extension takes places at polycondensation-I stage where oligomer react with themselves and release ethylene glycol.

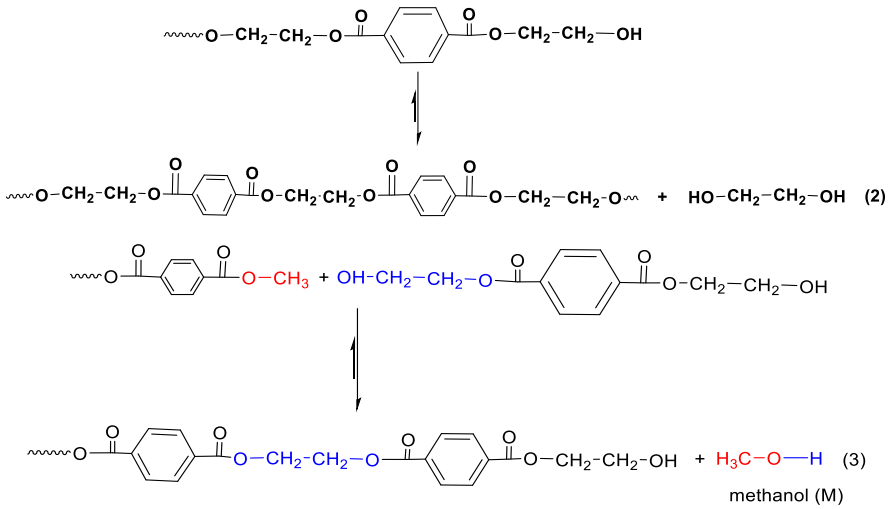

Scheme 4.2. Polycondensation reaction of PET oligomer and trans esterification of oligomer terminated with methoxy group. (Reaction conditions- Temperature: melt phase; Vacuum: 66.66 kPa; Time- 4-6 hr; Speed of agitation:50 rpm).

4.4.4.1.2.3 Stage-III (polycondensation-II)

The reaction temperature was set just below the melt phase of the reaction mixture. The reactor was purged with argon gas, as mentioned above. The vacuum applied at this stage was 33.99 kPa. The reaction samples were collected at different time intervals and analyzed for IV and molecular weight. The significance of the third stage is to avoid degradation and side reactions during polycondensation[104]. It was conducted slightly below the melt phase of the reaction mixture (Temp- 240-270 C, Vacuum- 3.99 kPa, time- 24 hr, Rpm- 50-60).

4.4.5 Polybutylene adipate co-terephthalate (PBAT)

Synthetic polyesters, such as polyethylene terephthalate (PET) and poly(butylene adipate-co-terephthalate) (PBAT), rank among the most widely used plastics in our daily lives due to their advantageous properties: low cost, lightweight, and durability. The annual aliphatic-aromatic co-polyester production is projected to exceed 360 million tons in 2023. PBAT, also recognized as Ecoflex® (BASF, Germany), is a copolymer comprising flexible (butylene adipate) and rigid (butylene terephthalate) segments with varying degrees of polymerization. PBAT finds widespread applications in food packaging, agriculture, textiles, and other industries. In agriculture, PBAT-made mulch films enhance soil conditions and crop production. In contrast to polymers linked by carbon-carbon bonds, PBAT was proved as compostable biopolymer due to the higher susceptibility of polyesters to enzymatic degradation caused by ester linkages[107].

Table 4.1 Literature- PBAT synthesis

Method	Temperature (°C)	Pressure (Vaccum)	Molecular weight(g/mol) (Number average)	Reference
TA (33.2 g, 0.20 mol), AA (7.3 g, 0.05 mol), BDO (45.06 g, 0.50 mol),	220	2 kPa	20000	[108]
Raw materials (succinic acid, adipic acid, and 1,4-butanediol) molar ratio of the succinic acid to the adipic acid being 0.6:0.4, 1,4-butanediol to a total mole number of the two carboxylic acids being 1.3:1.0.	1st- 190 2nd- 240	1.99 kPa	112000	Method for synthesizing poly (butylene succinate-co-butylene adipate) US9469724B2 [109]
Mole ration of AA:TPA:BDO- 1:1:2.2	1st- 190 2nd- 230	2.66kPa	50000	[110]
Mole ration of 1,4 BDO: AA: TPA: - 2.3:1:1 Molar ratio of diol to acid- 1.2	1st- 230 2nd-260	na	50000-6000	[111]
Mole ratio of Diol : Acid- 1.07 Molar ratio of TPA: AA- 0.888	1st- 230 2nd-260	na	IV- 0.8- 0.9 (dl/gm)	[100]

4.4.5.1 Monomer

1,4 Butanediol- Sigma Aldrich, USA supplied DMT. It was 99 % pure. Titanium tetra butoxide (TBT) was purchased from Merck Co. (Sigma Aldrich, USA) as a catalyst for the synthesis. **DMT-** Sigma Aldrich, USA, supplied DMT. **Adipic acid** was purchased from Sigma Aldrich, USA.

4.4.5.2 PBAT structure

PBAT structure has two segment butylene terephthalate (BT) and butylene adipate (BA), each unit contributes unique physical and chemical properties for polymer[110].

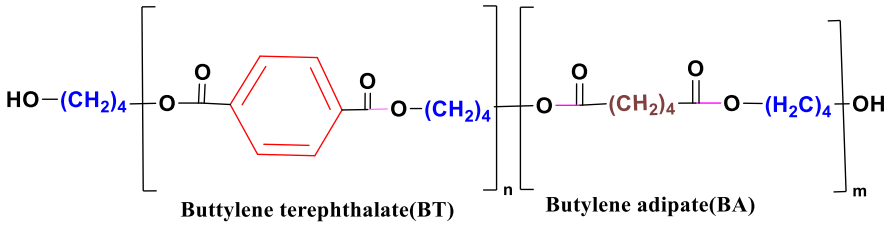

Scheme 4.3. PBAT repeat unit structure.

Table 4.2 Properties of repeat unit segment

Butylene terephthalate (BT)	**Butylene adipate (BA)**
Hard segment	Soft segment
High Crystalline	Low crystalline
High melt strength	Low melt strength
Slow biodegradation	Fast biodegradation
Increase heat resistance	Lower heat resistance

4.4.5.3 Steps for PBAT Synthesis

The synthesis used two melting stages with varying vacuum levels (**Figure 4.1**). It was conducted by dosing calculated amounts of materials based on 1 mole of dicarboxylic acid. Detailed mass balance calculations are available in Appendix (**Fig. A4.1**).

4.4.5.3.1 Stage-I (transesterification)

At the transesterification stage, the following main reactions occur in the presence of metal acetate catalyst. By assuming equal reactivities of dimethyl terephthalate methyl group, it reacts with alcohol of butanediol which releases methanol and forms BHBT.

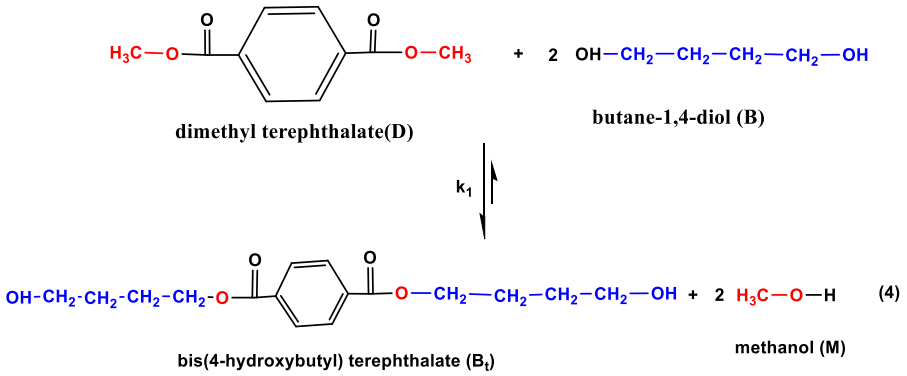

Scheme 4.4. Transesterification reaction between DMT and 1,4 butanediol (Reaction conditions- Temperature:130-140 °C; Time: 90% collection of methanol; Speed of agitation- 30 rpm).

4.4.5.3.2 Stage-II (esterification)

The first stage of esterification butanediol was 100% excess. However, in second stage when adipic acid was added which makes diol/acid ratio 0.94. Such that 1,4 butanediol become slight excess. There are two probable reactions (Scheme **4.5)** of adipic acid either with 1,4 butanediol or BHBT. NMR of samples collected after collection 95 % water reveals that there is mostly formation of BHBA (bishydroxybutyl adipate). It is assumed that both functional groups have equal reactivities.

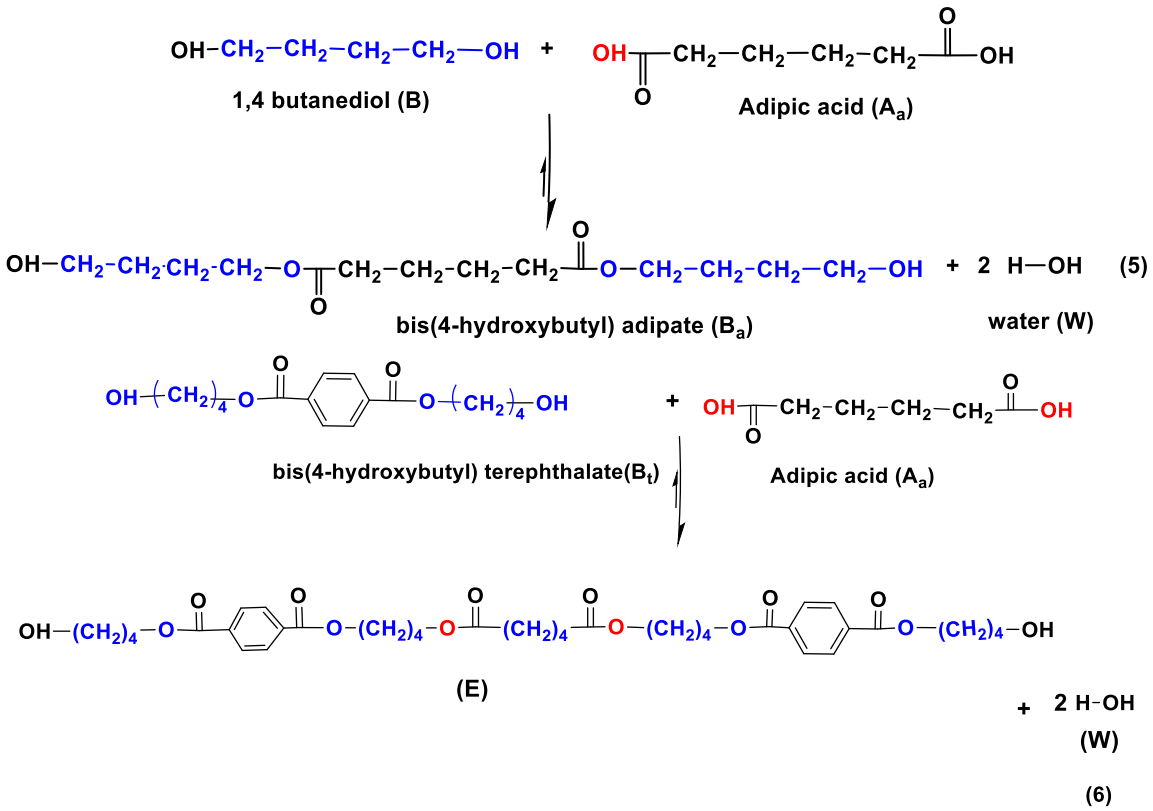

Scheme 4.5. Esterification reaction between adipic acid and 1,4 butanediol (Reaction conditions: Temperature: 170-180°C; Time- 90% collection of water; Speed of agitation: 50 rpm).

4.4.5.3.3 Stage-III (polycondensation-I)

In this stage, the temperature and vacuum were moderately increased. The significance of this step lies in the elevation of low molecular weight PBAT oligomer concentration. This is accomplished through an acyl acid catalytic mechanism in which the end group of dimer and oligomer attacks the ester linkage, leading to the removal of 1,4 butanediol **(Scheme 4.6).**. As discussed in the earlier section, the esterification stage brings about a significant degree of polycondensation, resulting in the creation of oligomers composed of 4 to 8 repeating units. The reaction can be expressed as follows:

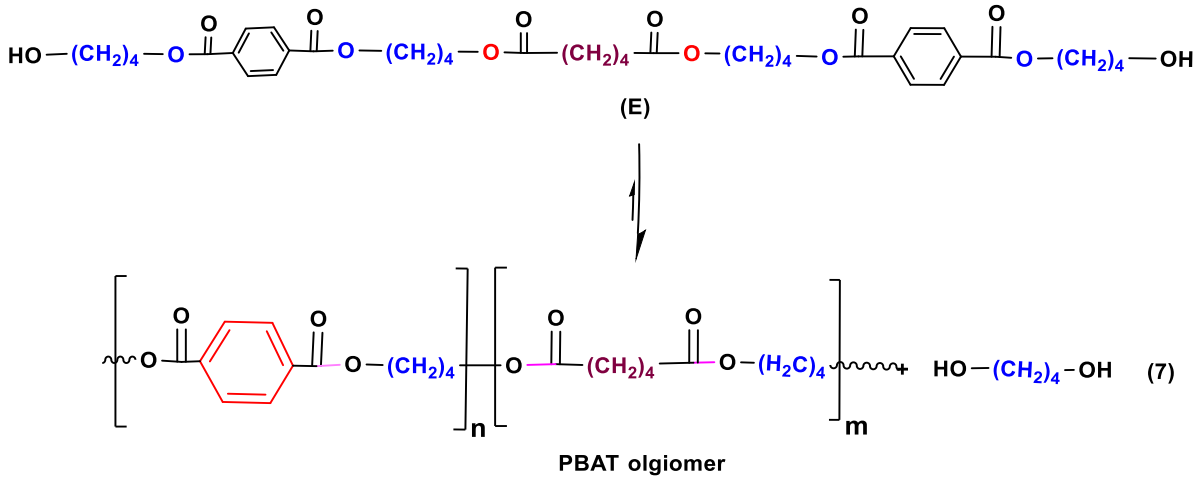

Scheme 4.6. Polycondensation of PBAT oligomer (Reaction conditions: Temperature: 170-180°C; Vacuum:66.66 kPa; Time:18hr; Speed of agitation: 50 rpm).

4.4.5.3.4 Stage-IV (polycondensation- II (melt)

As the esterification reaction progresses, the concentration of carboxyl acid end groups decreases. Consequently, titanium butoxide catalysts play a significant role in achieving higher molecular weights in the polycondensation reaction. With the advancement of the reaction, the melt viscosity increases, and the removal of butanediol and side products from the mixture becomes crucial. Therefore, this step was carried out at a high vacuum and elevated temperature. The high vacuum aids in eliminating mass transfer barriers during polycondensation step-II.

During this phase, both temperature and vacuum conditions are heightened, facilitating the interaction of PBAT oligomers to form high molecular weight PBAT. There's also a potential for the formation of THF through the dehydration of 1,4 butanediol(**Scheme 4.7)**. Moreover, the catalyst degradation can impact the final product's color. The reaction during this stage can be depicted as follows:

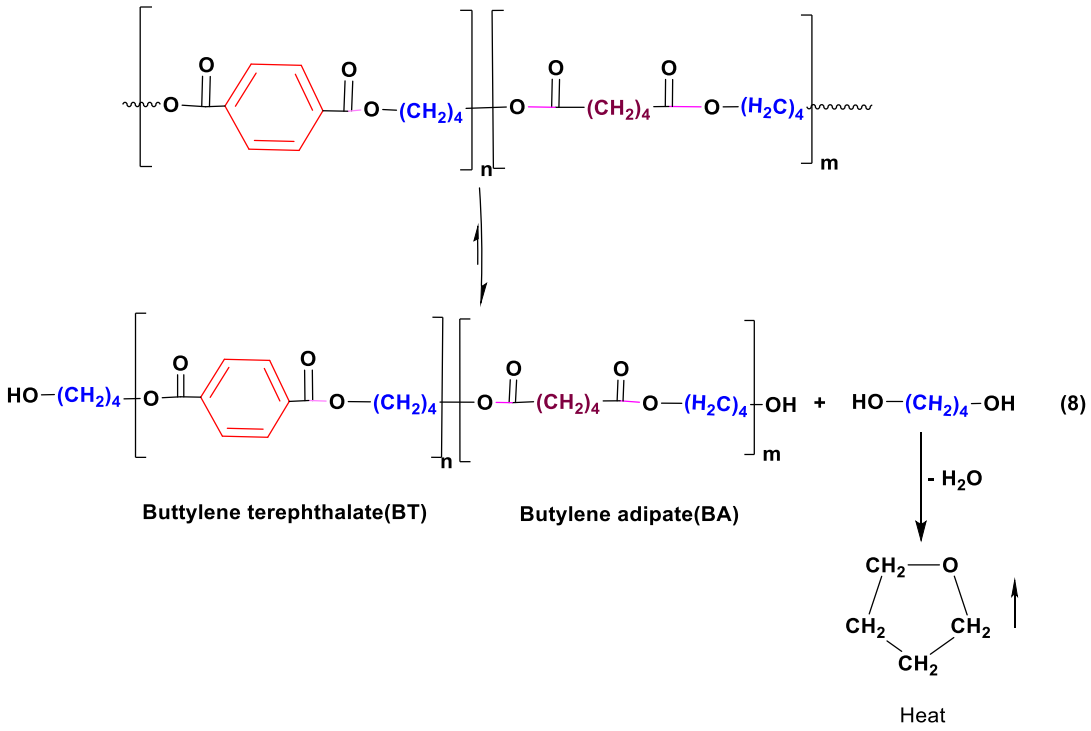

Scheme 4.7. Polycondensation of PBAT oligomer (Reaction conditions: Temperature: 170-180°C; Vacuum:3.99 kPa; Time:18hr; Speed of agitation: 50 rpm).

4.4.6 Synthesis of PBSeT and PBAzT

Polybutylene sebacate co-terephthalate (PBSeT) and Polybutylene azelate co-terephthalate (PBAzT) were prepared by similar methodology as shown in **Fig. 4.4 (b).** The adipic acid was replaced by sebacic acid and azelaic acid. In polycondensation stage-II step the reaction time for PBSeT and PBAzT was 6 and 8 hr respectively.

4.5 Results and discussion

4.5.1 Intrinsic viscosity

The D228 ASTM method was utilized to gauge the intrinsic viscosity of reaction samples[112]. The solvents of choice, both at room temperature, were chloroform and dichloromethane. The physical significance of intrinsic viscosity lies in its correlation with the polymer molecular weight. The molecular weight is in direct proportion to the polymer's intrinsic viscosity. The overlap concentration indicates the point where polymer chains cease their random movement

within the solvent. The polymerization process unfolded across three stages: trans-esterification, esterification, and polycondensation-I, followed by polycondensation-II. The output from the trans-esterification phase served as the input for the esterification reaction, and subsequently, the product of the esterification reaction was used as input for the polycondensation stage. Samples were collected at various stages, and the intrinsic viscosity of each collected sample was determined (as shown in **table 4.2**)using the Huggins and Kraemer equations[113].

$$\eta_{rel} = \frac{t}{t_0} \qquad (16)$$

$$\eta_{inh} = \frac{\ln(\eta_{rel})}{C} \qquad (17)$$

$$\eta_{red} = \frac{(\eta_{rel} - 1)}{C} = \frac{(\eta_{spec})}{C} \qquad (18)$$

Huggin's equation

$$\eta_{red} = \frac{(\eta_{rel} - 1)}{C} = \frac{\eta_{spec}}{C} = [\eta] + K_h [\eta]^2 C \qquad (19)$$

Kraemer equation

$$\frac{\ln(\eta_{rel})}{C} = [\eta] - K_k [\eta]^2 C \qquad (20)$$

K_h is the Huggins coefficient, K_k is the Kraemer coefficient, and η_{rel} is the relative viscosity. Both plots of $\eta sp/c$ versus c and ln $(\eta_{rel})/c$ versus c give two straight lines with an identical intercept at c = 0, and the intercept corresponds to the intrinsic viscosity [η]. Its unit is the reciprocal of the unit of concentration (g dl^{-1}).

Table 4.2 Intrinsic viscosity (dl/g) for various stages

Polymer	Step-I(3hr)	Step-II(6hr)	Step-III (24hr)	Step-IV(3hr@230 C)
PET	0.02	NA	0.32	0.46
PBAT	0.01	0.16	0.37	0.65
PBSeT	0.018	0.096	0.24	0.61
PBAzT	0.014	0.09	0.20	0.48
PNST	0.016	0.03	0.06	0.11

4.4.2 Molecular weight (viscosity avg.)

Furthermore, the IV calculated values were used to determine the molecular weight using the Mark–Houwink method, the intrinsic viscosity value used for each sample corresponds to the average between the values obtained by method ASTM D2857. Parameters "K" and "a" depend on solvent polymer interactions, temperature, and coil size of the sample polymer[114]. Value of "a" range from 0.58 to 0.60 depending on polymer flexibility, and K was 0.00075 dl/g for all trial samples. **Table 4.3** shows increase in molecular weight reaction progresses to higher stage.

$$[\eta] = K[M]^{\alpha}$$

$$[\eta] = 4.68\times10^{-4}\left(M_v\right)^{0.60} \qquad (21)$$

Table 4.3 Molecular weights (viscosity avg.) for each step

Polymer	Step-I (3 h)	Step-II (6h)	Step-III (18h)	Step-IV (3h @230)
PET	NA	NA	NA	34000
PBAT	450	5700	18000	78000
PBSeT	300	3728	22000	70867
PBAzT	360	6312	16000	68903
PNST	560	2500	10500	42000

4.5.2 TGA and DSC

After each stage, the samples were collected and conducted thermogravimetric analysis on them. The data listed in **tables 4.4-4.6** has been compiled using the corresponding graphs in **Figures A4.4-A4.12**. **Table 4.3** illustrates the degradation temperature range for various polymers with

differing lengths of aliphatic carbon chains. Notably, polymers synthesized with aliphatic acid carbon chain lengths of C9 (PBSeT) and C10 (PBAzT) exhibited higher degradation temperatures (a difference of 50°C) compared to C6 (PBAT). The degradation temperature range for C9 and C10 closely resembled that of C0 (PET).

DSC analysis was done using heating and cooling cycle with a heating rate of 10°C/min. **Table 4.3** provides information on the glass transition and melting temperatures for a variety of polymers with differing aliphatic acid carbon chain lengths. **Figure A4.5** illustrates the results obtained through thermal analysis using DSC, showcasing the glass transition temperature (-32°C), crystallization temperature (76°C), and melting temperature (120°C) for various polymers. Interestingly, as depicted in **Fig. A4.6**, the sample from the transesterification stage exhibits distinct and dual melting peaks (i.e PBT oligomers). After stage II (esterification) and stage III (polycondensation-I), only a single melting peak is observed. However, in step IV (polycondensation-II), the sample demonstrates increased crystallinity and a melting peak similar to the characteristics observed in a commercial PBAT sample (**Fig. A4.5**). In **table 4.4 and 4.5** values are derived from melting and crystallization enthalpy **(Fig. A4.5-4.7)** for polymer varying for aliphatic acid carbon chain in polyester backbone. It has been observed that PBSeT and PBAzT exhibit polymorphism. However, detailed study of polymorphism is out of scope of this work.

Table 4.4 Thermal properties of samples collected after stage IV (polycondensation-II)

Polymer	Tm (°C)	Tg (°C)	Degradation temp range (°C)
PET	240	72	400-450
PBAT	118	-33	300-400
PBSeT	110	48	400-450
PBAzT	112	-	400-450
PNST	NA	25	400-450

Table 4.5 Melting enthalpy of samples collected after IV (polycondensation-II) stage for varying aliphatic carbon chain length (second heating cycle)

Aliphatic acid carbon content	Polymer	ΔH_1(J/g)	T_{m1}(°C)	ΔH_2(J/g)	T_{m2}(°C)
C0	PET	0	243.0	-	-
C6	PBAT	16.82	121.0	-	-
C9	PBAzT	17.35	21.0	7.73	83
C10	PBSeT	11.68	34.0	9.6	98

Table 4.6 Melt crystallization enthalpy of samples collected after IV (final) stage for varying aliphatic acid content (cooling cycle)

Aliphatic acid carbon content	Polymer	ΔH_1(J/g)	T_{m1}(°C)	ΔH_2(J/g)	T_{m2}(°C)
C0	PET	0	243	-	-
C6	PBAT	19.62	66.70	-	-
C9	PBAzT	12.0	35.98	5.37	10.41
C10	PBSeT	8.27	33.60	2.37	14.63

4.5.3 NMR

We used ^{1}H NMR to investigate the molecular structures of PBATs. **Figure 4.5** shows that the aromatic proton peak appeared at a chemical shift of 8.1 ppm. The peaks between 4.1 and 4.6 ppm corresponded to the −CH2− groups within the BDO segment, which were connected to the ester group (CH2-O-CO−). If BDO's ends were associated with DMT, the −CH2− protons were found at 4.38 and 4.21 ppm, referred as B-T-B. Integration of NMR peaks yielded a total of 28-30 protons, consistent with the theoretically calculated values for the PBAT repeat unit, as indicated

in **scheme 4.3**. The ^{1}H spectrum of the prepared PBAT in **Figure 4.5** resembles that of a commercial-grade PBAT (Kingfa resin).

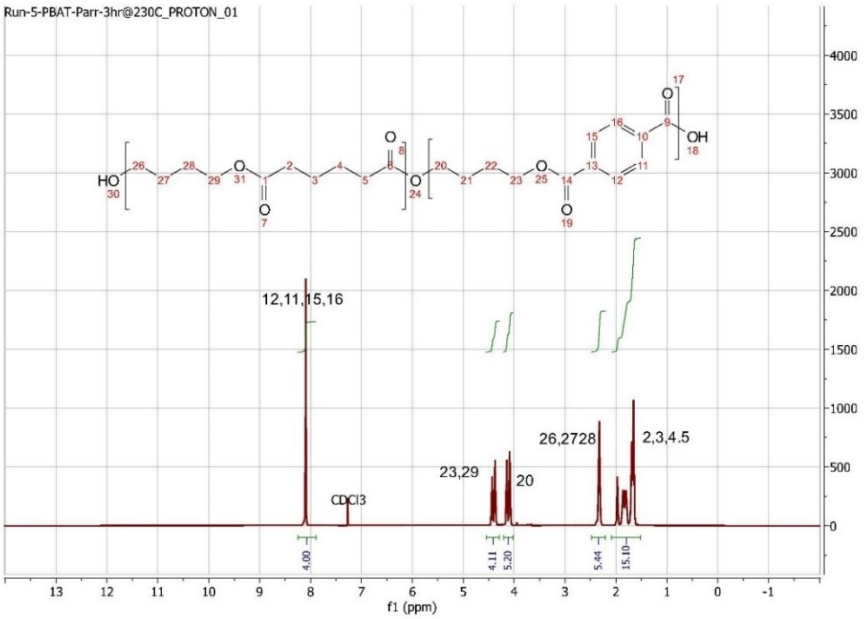

Figure 4.5. ^{1}H NMR of PBAT sample after stage-IV (polycondensation-II).

4.5.4 Acid value

The esterification study of PBAT involved monitoring the complete conversion of carboxyl end groups, which was assessed through titration using the ASTM D7409 method[115]. In this analysis, 1.0 g of the sample was dissolved in 5 mL of DCM (dichloromethane). The resulting solution was titrated with 0.1 M potassium hydroxide (KOH), using bromo phenol blue as an indicator. By determining the acid value (AV)(**table 4.7**) of the samples both at the initial time and the desired time, the total conversion of carboxyl end groups was calculated using the provided equations.

$$\text{Acid value}(\text{AV}) = \left[\frac{\text{N}_{NaOH} \times \text{Vol}_{\text{NaOH}}(\text{ml}) \times \text{MW}_{NaOH}}{\text{Sample weight(g)}} \right] \qquad (22)$$

Table 4.7 acid value of sample collected at various stages

Polymer	Step-I (mmol/kg)	Step-II (mmol/kg)	Step-III (mmol/kg)	Step-IV (mmol/kg)
PET	NA	NA	NA	10.0
PBAT	22.5	35	25	6.7
PBSeT	22.5	43	15.1	2.1
PBAzT	22.5	40	12.0	8.15
PNST	22.5	120	80	57.11

4.5.5 Gel permeation chromatography (GPC)

Polystyrene calibration data was used to detrmine relation between log(Mi) and retention time (**Fig A4.2**). The calibration equation was empolyed to correlate retention time of sample with molecular weight (i.e log(Mi)). The polydispersity for all samples were calculated from Mn and Mw. The PBAT sample showed (**table 4.8**) high average molecular weight compared to PBSeT and PBAzT. Sebacic acid and azelaic acid purity were 96 and 88 %. Low purity of acid monomer might be a reason for having higher polydispersity. For PBSeT and PBAzT polycondensation-II stage the reaction time was higher than PBAT. The reaction time required to achieve the desired viscosity might affect polydispersity.

Table 4.8 Molecular weight of polyesters using different method

	Mn(GPC number avg.)	Mv (Viscosity avg. -ASTM IV method)	Mw (GPC -weight avg.)	PDI
PBAT	21001.24	71852.3	73805.84	3.51
PBSeT	14885.40	70867.5	72277.54	4.85
PBAzT	18981.84	68903.5	76716.58	4.04

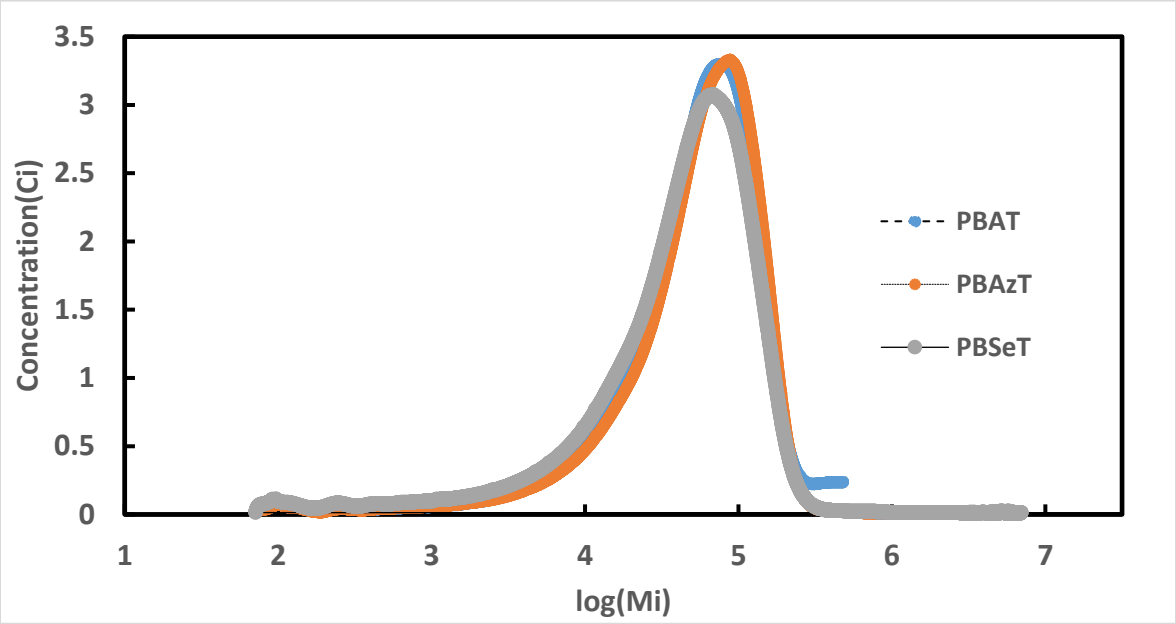

Figure 4.6. GPC analysis for various polyester.

4.5.6 Degree of polymerization and extent of reaction

The stoichiometric imbalance was taken by using slight excess of butanediol for all trials. The acid group was limiting functional group. The acid value for sample collected at each stage was determined and used to calculate the extent of reaction. **Fig. A4.1** shows the degree of polymerization for each stage. The extent of reaction was employed to calculate the degree of polymerization using equation 14[101].

4.6 Kinetics

4.6.1 Step- I- 1,4 BDO and DMT

Transesterification exhibits reversibility, making effective removal of generated methanol crucial for achieving a substantial yield of BHBT (Bis-4-hydroxybutyl terephthalate). The transesterification of dimethyl terephthalate (DMT) with 1,4 butanediol (BDO) may be represented by the following equation where methanol and bis (hydroxybutyl) terephthalate (BHBT) are formed:

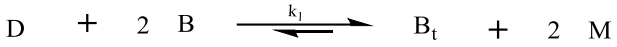

Where D (dimethyl terephthalate), B (1,4 butanediol), B_t (bis-4-hydroxybutyl terephthalate), M(methanol).

In this context, the reverse reactions have been omitted under the assumption that the removal of methanol from the reaction mixture is effective[116]. Additionally, any side reactions and oligomerization processes are disregarded. Also, it is assumed that the volume correction factor is negligible for the reaction system. Consequently, the rate expressions for both reactions are formulated as follows:

$$+\frac{1}{2}\frac{d[M]}{dt} = -\frac{d[D]}{dt} = k_1[D][B][Catalyst] \qquad (23)$$

$$k' = 2k_1[B][Catalyst] \qquad (24)$$

$$+\frac{d[M]}{dt} = k'[D]$$

$$[D] = [D]_0 - [M]$$

$$+\frac{d[M]}{dt} = k'\left[[D]_0 - [M]\right]$$

$$\int_{[M]_0}^{[M]_t} + \frac{d[M]}{\left[[D]_0 - [M]\right]} = \int_0^t k'dt$$

Intergrating with limit from 0 to t

$$-\ln\left[D\right]_0 - [M]\Big]_{[M]_0}^{[M]_t} = k't$$

$$-\ln\left(\frac{[D]_0 - [M]}{[D]_0}\right) = k't \qquad (25)$$

Methanol was collected at different reaction times, as shown in **Figure 4.7**. The graph was plotted using Equation 25, as depicted in **Figure 4.8**. The apparent rate constant for the transesterification of DMT using methanol was determined to be 0.00118 min^{-1}. Model values were calculated and compared with experimental data. **Figure 4.9** demonstrates a good fit for themodel at lower conversion.

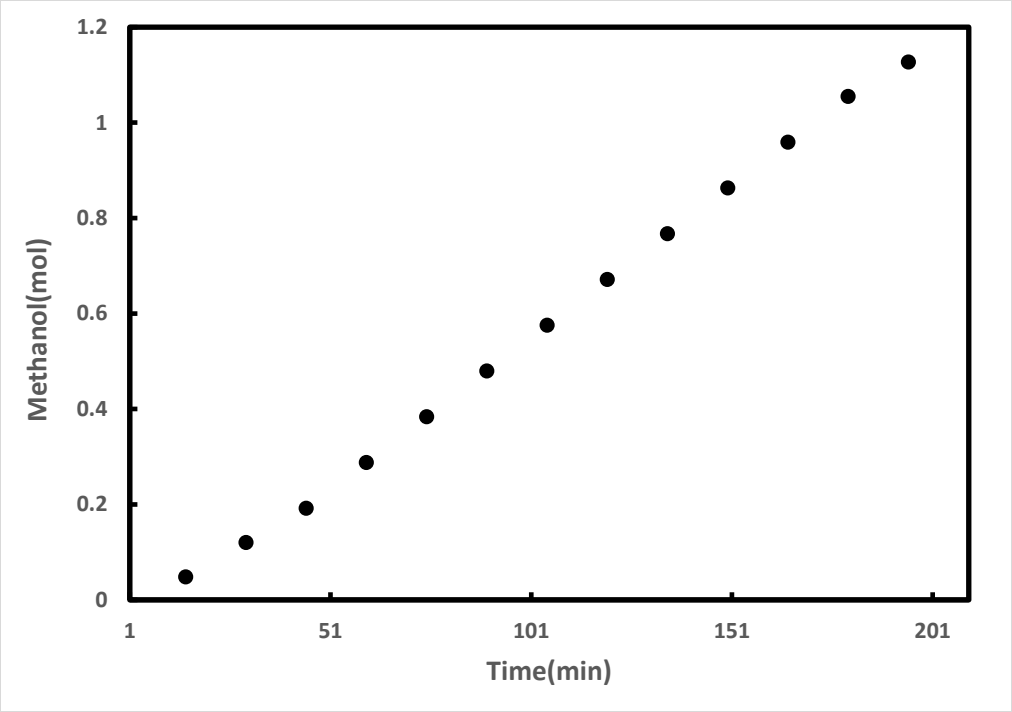

Figure 4.7. Concentration of methanol produced during Step-I with time. (Reaction condition- Temperature: 130℃; Pressure: 101kPa; Time: 3hr).

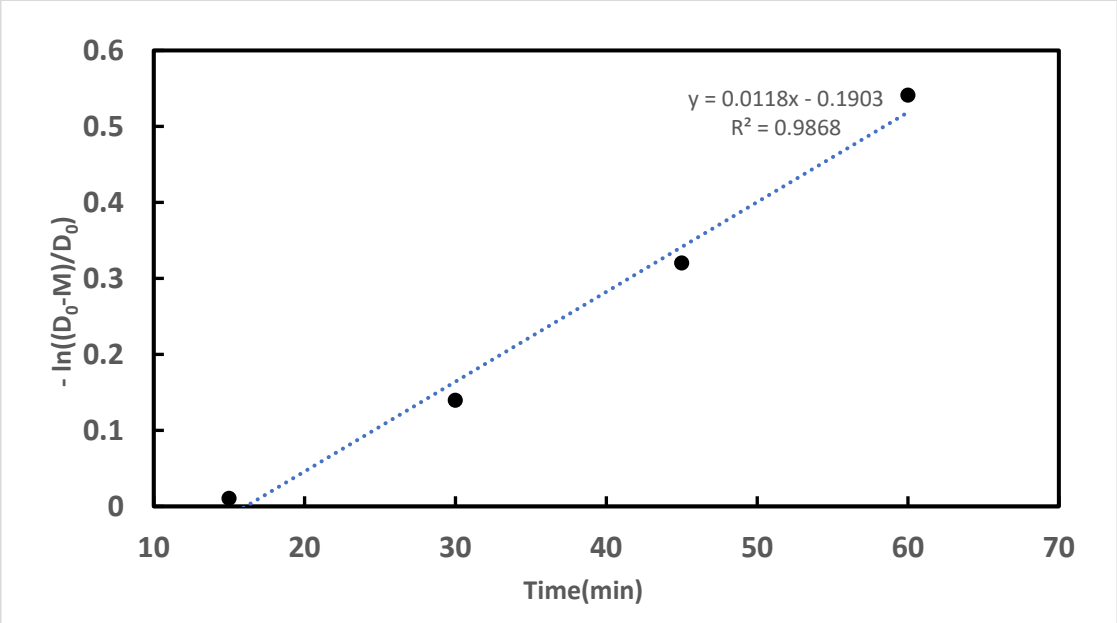

Figure 4.8. Kinetic model fitting for methanol produced in Step-I. (Reaction condition- Temperature: 130°C; Pressure: 101kPa; Time: 3hr).

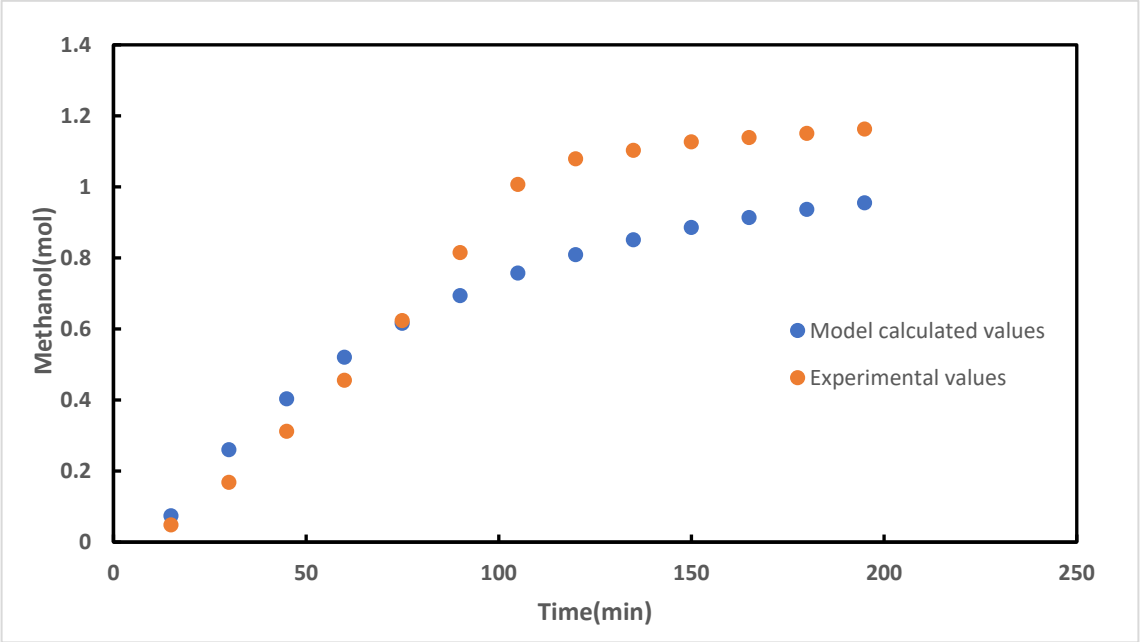

Figure 4.9. Kinetic model comparison with experimental values. (Reaction condition- Temperature: 130°C; Pressure: 101kPa; Time: 3hr).

4.6.2 Step-II- Oligomer with diol end cap +butanediol and adipic acid

Esterification exhibits reversibility, making effective removal of generated water important for achieving a substantial yield of BHAT (Bis-4-hydroxyadipate terephthalate). The transesterification of dimethyl terephthalate (DMT) with ethylene glycol (EG) may be represented by the following equation where methanol and bis (hydroxyadipate) terephthalate (BHAT) are formed with assumption of change in reaction mass volume due to methanol was negligible and rate of formation of BHAT is one step.

$$A_a + 2\,B \underset{}{\overset{k_1}{\rightleftharpoons}} B_a + 2\,W$$

$$+\frac{1}{2}\frac{d[W]}{dt} = -\frac{d[A_a]}{dt} = k_1[A_a][B][Catalyst] \qquad (26)$$

$$+\frac{d[W]}{dt} = k_1[A_a][B][Catalyst]$$

$$k' = 2k_1[B][Catalyst]$$

$$+\frac{d[M]}{dt} = k'[A_a] \qquad (27)$$

$$[A_a] = [A_a]_0 - [W]$$

Substituting in equation 27

$$+\frac{d[W]}{dt} = k' \; [A_a]_0 - [W]$$

$$\int_{[W]_0}^{[W]_t} + \frac{d[W]}{[A_a]_0 - [W]} = \int_0^t k' dt$$

Integrating with limit from 0 to t

$$\left[-\ln\left[[A_a]_0 - [W]\right]\right]_{[W]_0}^{[W]_t} = k't$$

$$\ln\frac{[A_a]_0 - [W]}{[A_a]_0} = -k't \qquad (28)$$

Methanol was collected at different reaction times, as shown in **Fig. 4.10**. The graph was plotted using equation 28, as depicted in **Fig. 4.11**. The apparent rate constant for the transesterification

of DMT using methanol was determined to be 0.0112 min^{-1}. Model values were calculated and compared with experimental data. **Figure 4.12** demonstrates a good fit for the model at lower conversion.

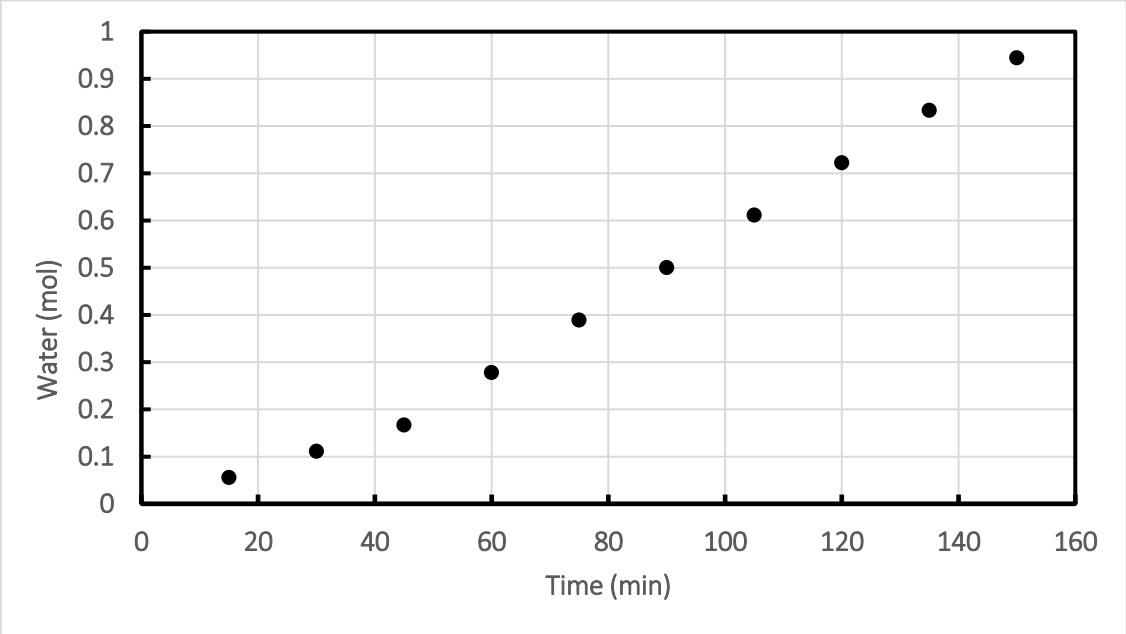

Figure 4.10. Concentration of methanol produced during Step-I with time. (Reaction condition- Temperature: 130°C; Pressure: 101kPa; Time: 3hr).

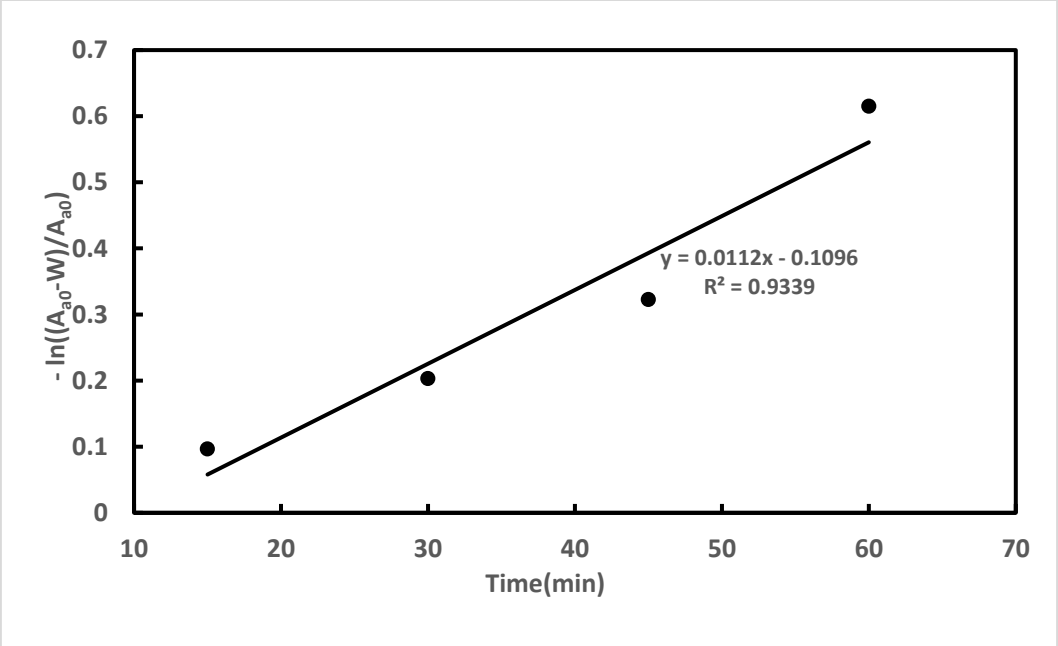

Figure 4.11. Kinetic model fitting for water produced in Step-II (Reaction condition- Temperature: 170°C; Pressure: 101kPa; Time: 3hr).

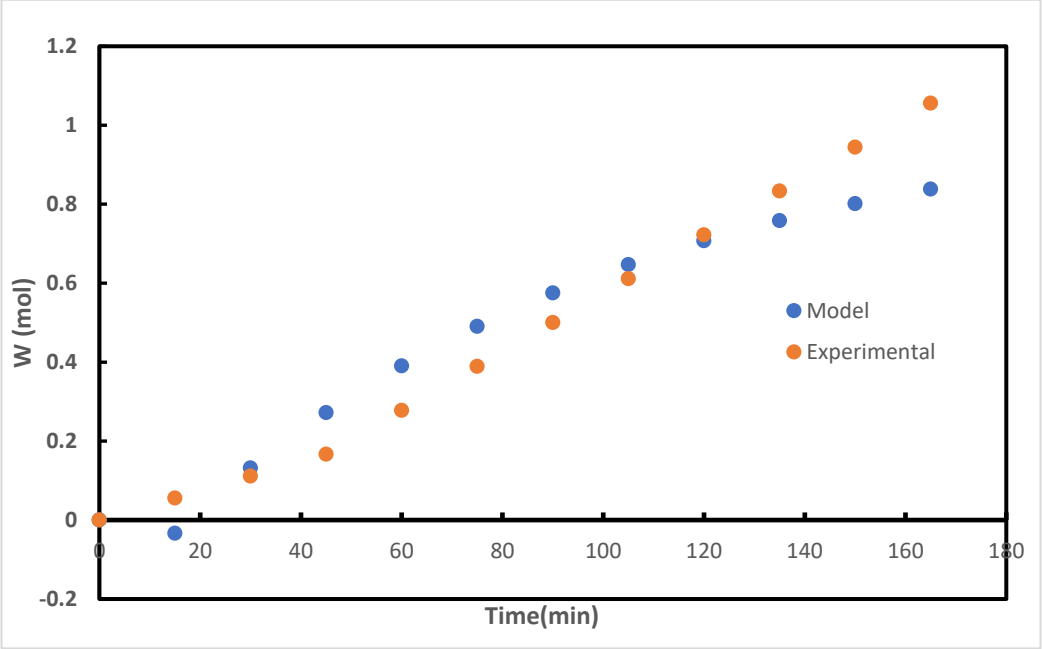

Figure 4.12. Comparison of kinetic model with experimental values. (Reaction condition- Temperature: 130°C; Pressure: 101kPa ; Time: 3hr).

4.7 Conclusion

Polymerization reaction methodology was developed using transesterification, esterification, and polycondensation mechanisms. The Reaction conditions for different steps have been optimized for high molecular-weight polyester. The molecular weight of polyesters of butanediol with varying aliphatic acid content was prepared and found to be in the range of 60000–80000. In PBAT synthesis methodology, adipic acid was replaced by azelaic acid and sebacic acid to synthesize polybutylene azelate co-terephthalate and polybutylene sebacate co-terephthalate. The molecular weight and intrinsic viscosity of PBSeT and PBAzT is slightly lower than PBAT. However, the methodology was found to be effective in synthesizing high molecular polyester. Titanium butoxide was observed to be an effective catalyst for the synthesis of high molecular weight polymer.

Chapter 5

Composting of food waste and polyester bags

5.1 Introduction

Food waste (FW) contributes almost (45%) of total municipal solid waste generated in Europe (IPCC, 2006). This number shoots up approximately 55% in developing nations (Troschinetz and Mihelcic, 2009). Most of this waste generated either end up in landfills or sent for incineration. Until recently environmentalists have begun raising serious concerns as mismanagement of food waste has emerged as one of the major causes for greenhouse gas emission. In order to make food waste management more sustainable, developed countries have formed new legislation that involves valorization of food waste. Valorization, defined as upcycling of waste products has been applied on food waste via composting and anaerobic digestion methods. The methods proposed are based on biological degradation of the food waste and occur either aerobic or anaerobic conditions, respectively. The two processes discussed have potential to handle the FW in an efficient and environmentally friendly ways. Diverting municipal solid waste organic material from landfills to composting or anaerobic digestion has many environmental benefits. Among them, reduction in landfill emissions of greenhouse gases (GHGs) and improvement of soil properties through compost application have been highlighted (Bernstad et al., 2016). Briefly, the production of high-quality compost requires that the process must be properly controlled and managed. One of the major issues that arises while handling FW for composting face challenges from the contamination of plastic waste. The origin of plastic contamination is generally attributed to food packaging and containers that comes together in food waste streams collected for processing at compost and anaerobic digestion facilities. The plastic contamination present in food waste streams has not been well established in the scientific literature. Recently analyzed food

waste collected from grocery stores found approximately 300k pieces of microplastics/kilogram of food waste in the United States.

In the early 1990s, composting emerged as a widely embraced approach for managing organic waste. In his work "The Practical Handbook of Compost Engineering" published in 1993, Haug (p.1) presented the following comprehensive definition of composting: "Composting refers to the biological decomposition and stabilization of organic materials. This occurs under controlled conditions that facilitate the generation of thermophilic temperatures due to biologically induced heat production. The ultimate outcome of this process is a stable end product that is devoid of pathogens and plant seeds, rendering it suitable for beneficial land application.[117]" Another perspective on composting comes from Diaz et al. (2007, p. 26), who define it as follows: "Composting is a biodegradation process involving a blend of substrates. It takes place within a microbial community comprising diverse populations, all in aerobic conditions and within a solid substrate." Golueke (1977, p. 2), focusing on its waste management aspect, defines composting as: "Composting serves as a method of solid waste management whereby the organic fraction of solid waste undergoes biological decomposition under controlled conditions. This transformation brings it to a state where it can be managed, stored, or applied to land surfaces without causing adverse environmental impacts." The Bureau de Normalisation du Québec (BNQ) echoes Haug's emphasis on temperature in their definition of composting, stating: "Composting is a managed process of bio-oxidation applied to a heterogeneous organic substrate. It encompasses a thermophilic phase and results in a solid, fully mature product." While various authors and institutions have proposed diverse definitions of composting, these definitions collectively highlight several fundamental characteristics inherent to composting, as outlined in the literature.

1. Decomposition of organic substrates

2. It is a controlled process
3. The process operates under thermophilic conditions (greater than 50°C)
4. Aerobic decomposition
5. Results in a stable end product

The breakdown of organic substrates in the composting process is orchestrated by a diverse array of aerobic microorganisms, encompassing bacteria, fungi, and actinomycetes. The composition and prevalence of these microorganisms within the compost are contingent upon the nature of the substrate being composted and the specific stage of the composting procedure. Various microbial communities assume dominance at different phases throughout composting. Throughout the composting process, microorganisms harness oxygen (O2) to transform organic matter into the final product, compost. This metabolic transformation generates byproducts such as carbon dioxide (CO2), water, nitrate (NO -), sulfate (SO 2-), and heat. This intricate relationship is mathematically represented in the equation as elucidated by Chiumenti et al. in 2005.

$$\text{organic matter} + O2 \longrightarrow CO2 + H2O + NO + (SO4)$$

The composting process can be divided into four distinct stages, each characterized by its own temperature range, duration, and dominant microbial community. These four composting stages are detailed below, although it's important to recognize that they are not entirely separate and often overlap.

Stage 1: Mesophilic Phase (25-40°C) The mesophilic phase, which operates within a moderate temperature range, marks the initial phase of composting. During this stage, primary decomposers such as bacteria, fungi, and actinomycetes target and break down the easily degradable compounds found in the biomass, which include sugars and proteins. Their biological activity initiates a temperature increase within the compost (Diaz et al., 2007).

Stage 2: Thermophilic Phase (35-65°C) The temperature elevation initiated by the mesophilic organisms in Stage 1 inhibits their growth and renders them inactive. The thermophilic phase, characterized by higher temperatures, takes over in Stage 2. Decomposition rates continue to accelerate until the compost reaches a temperature of approximately 65°C. Beyond 55°C, fungal growth is suppressed, making bacteria and actinomycetes the dominant microorganisms actively contributing to the compost's decomposition (Diaz et al., 2007).

Stage 3: Cooling Phases As the easily degradable substrate becomes depleted, microbial activity declines, resulting in a gradual decrease in compost temperature. During this phase, both bacterial and fungal classes shift their focus toward breaking down more resilient compounds like cellulose (Diaz et al., 2007).

Stage 4: Maturation Phase In the maturation phase, the compost's quality starts to decline as non-degradable compounds become prevalent (Diaz et al., 2007). To be considered mature and stable according to the Guidelines for Compost Quality published by the Canadian Council of Ministers of the Environment (CCME, 2005), compost must meet one of the following three criteria at the time of sale and distribution: (1) The respiration rate is less than or equal to 400 milligrams of O2 per kilogram of volatile solids per hour; (2) the CO2 evolution rate is less than or equal to 4 milligrams of carbon in the form of CO2 per gram of organic matter per day; or (3) the compost's temperature rise above ambient temperatures is less than 8°C.

5.1.1 Influential factors in the composting process

The composting process is subject to the influence of several key process parameters. Below, we provide descriptions of these essential factors.

5.1.1.1 Substrate composition

The compost substrate, comprising the organic material destined for decomposition, can be

characterized by its nutrient availability (Golueke, 1977). The presence, concentration, and relative abundance of nutrients in the compost substrate significantly impact the efficiency of the composting process and the quality of the final product. The crucial macronutrients required by the microorganisms involved in composting include carbon (C), nitrogen (N), phosphorus (P), and potassium (K) (Diaz et al., 2007; Golueke, 1977). Among these nutrients, the carbon-to-nitrogen ratio (C:N) stands out as a paramount parameter. Microorganisms engaged in composting necessitate approximately 25 times more carbon than nitrogen. Therefore, when formulating a composting blend, it is essential to maintain a C:N ratio ranging from 25 to 30 (on a mass basis) to facilitate rapid composting (Cundiff & Mankin, 2003). Striking the right balance in the C:N ratio is critical because an excessive amount of carbon (a high C:N ratio) can decelerate the composting process, while an excess of nitrogen (a low C:N ratio) can elevate ammonia (NH3) and nitrous oxide (N2O) emissions from the compost, potentially leading to odor issues (Cundiff & Mankin, 2003). Although other nutrient ratios (e.g., N:P) exist, they are typically less of a concern in composting waste materials because they are usually present in sufficient quantities, and their concentrations do not impose limitations (Golueke, 1977).

5.1.1.2 Temperature

Compost temperature as an indicator of process progress. The temperature of the compost serves as a commonly employed gauge to assess the progression and condition of the composting process, primarily due to its ease of monitoring (Block, 1999; Keener et al., 2000; Ressetti et al., 1999). The elevation in compost temperature results from the thermal energy liberated by microorganisms involved in the decomposition of organic matter within the compost. In compost, thermophilic bacteria have the capacity to drive temperatures up to 60-70°C. Nevertheless, these heightened temperatures eventually curb bacterial growth, thereby limiting further temperature increases. In

exceptional instances where extreme thermophiles, such as hyper-thermophilic bacteria, are part of the compost's microbial community, temperatures exceeding 80°C can be achieved, as exemplified by the industrial composting pioneered by the Sanyu Company in Japan (Oshima et al., 2007). Oshima et al. (2007) posit that the expansive size of the compost bed facilitates the development of exceedingly high temperatures, thereby favoring the proliferation of hyper-thermophilic bacterial communities. Diaz et al. (2007) underscore that one of the three objectives in converting organic matter into compost is to reduce the presence of agents that pose a pathogenic risk to humans, animals, and plants, bringing them to levels that no longer constitute a health hazard. It is during the thermophilic phase that the most crucial work in eliminating pathogenic organisms takes place, as noted by Diaz et al. (2007). The Canadian Council of Ministers of the Environment prescribes that compost must be maintained at a temperature of 55°C or higher for a duration of three days in the case of in-reactor and aerated static pile composting systems (as described in section 1.2.4.3) and for at least 15 days in the context of windrow composting piles. These measures are designed to mitigate potential health concerns associated with pathogenic organisms commonly found in compost substrates (Statistics Canada, 2005).

5.1.1.3 Moisture Content

Water serves as the medium for facilitating chemical reactions, the transportation of nutrients, and the movement of microorganisms within the compost substrate (Cundiff & Mankin, 2003). The ideal moisture content in compost is influenced by the physical properties of both the compost substrate and the bulking agent employed. However, for optimal decomposition in compost, a moisture content of 60% has been deemed effective (Campbell et al., 1990). Excessive water in the compost substrate compresses the available air spaces between compost particles, hindering air movement through the compost matrix and thereby diminishing the supply of oxygen (O2) to

aerobic microorganisms. Biological activity becomes minimal when moisture content falls below 12%, although in practical terms, it is advisable to maintain a moisture content of no less than 40-50% (Golueke, 1977).

5.1.1.4 Oxygen Concentration

Composting is characterized by the decomposition of organic substrates under aerobic conditions, necessitating a continuous supply of O2 to maintain these conditions. According to Cundiff and Mankin (2003), microbial growth necessitates a minimum O2 concentration of 5%, which is one-fourth the O2 concentration present in the ambient air. The advantages of aerobic decomposition over anaerobic processes encompass fewer objectionable odors, elevated temperatures leading to the destruction of pathogenic organisms, and a more rapid decomposition rate (Golueke, 1977).

5.1.1.5 Aeration Rate

The role of aeration in composting is to uphold an adequate O2 concentration and moderate temperature. Aeration ensures the consistent renewal of O2 in the air surrounding compost substrate particles, thereby reducing the occurrence of anaerobic respiration pockets. As the composting process advances and the physical structure of the compost evolves (e.g., compaction), the aeration can be adjusted accordingly. Among all the parameters discussed, temperature, O2 concentration, and aeration have been identified as the most pivotal factors influencing the composting of organic waste materials (Campbell et al., 1990).

5.1.1.6 Composting Systems

There are two general classifications for the wide variety of composting systems:

(1) non-reactor systems, where composting takes place outside of a reactor, also referred to as "windrows". (2) Reactor systems, where the composting occurs within a closed reactor. These systems are also referred to as "in-vessel" systems.

1) Non-reactor Systems

Non-reactor systems can be further divided into two groups, (1) passive aeration where the compost pile is torn down and reconstructed in order to provide aeration to the compost; and (2) active aeration where the compost pile is not disturbed and aeration is provided by forcing air through the compost pile. **Figure 5.1(a)** shows an illustration of a basic non-reactor composting system with the ventilation system positioned at the base of the pile. Aeration in a active compost pile can be achieved through updraft aeration, where ambient air is forced through the compost pile, or by creating negative pressure in the compost pile through a downdraft aeration scheme. When forced aeration is not used the industrial compost tuner is used to agitate a compost windrow to provide aeration. Due to the inexpensive equipment required and limited materials handling, windrow composting systems are inexpensive compared to reactor systems (Diaz et al., 2007).

2) In-reactor Systems

In-reactor composting systems, often referred to as "bioreactors," derive their name from the active composting phase that takes place within a designated reactor. During this phase, the substrate resides in the reactor for a period ranging from 7 to 15 days before transitioning to a curing phase within a windrow. **Figure 5.1(b)** illustrates a vertical in-vessel composting system, where compost material is introduced at the top of the reactor and the finished compost is extracted from the bottom. A fan situated at the reactor's base facilitates aeration. In-reactor systems typically employ

forced aeration and mechanized turning mechanisms, which increase both the construction and operational costs compared to windrow composting (Diaz et al., 2007). The primary objective of compost technology, whether in-vessel or windrow composting, is to uphold the optimal process parameters influencing composting, thereby yielding a high-quality final product in the shortest possible timeframe. **Table A5.1** shows review of commercial scale such systems.

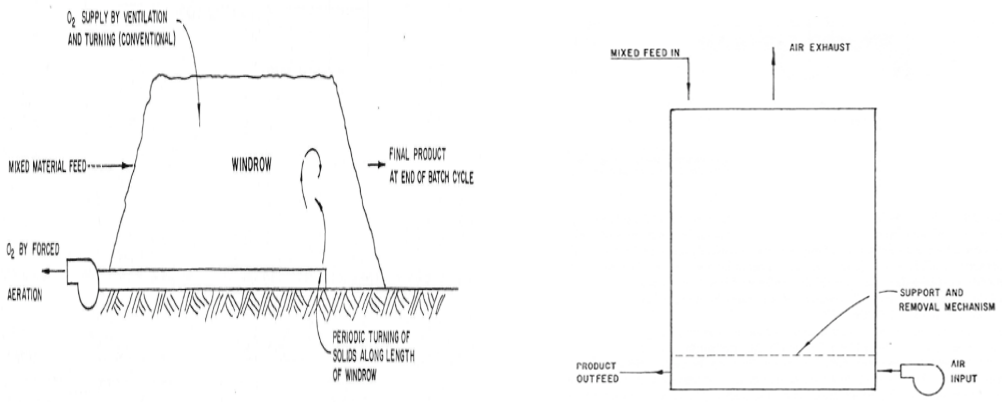

(a) **(b)**

Figure 5.1. Composting system (a) Windrow Vertical flow (b) packed bed reactor (Haug, 1993).

This study will demonstrate a reduction in volume of food waste by 70-80 %. In addition, after collection of food waste it requires to pick up in particular time, otherwise it generates smell and attract flies, maggots etc. The proposed method will help to reduce the collection urgency and frequency. Besides, food waste packed with compostable plastic will be able to manage in this process. Compostable plastic can be processed with food waste. This study will show the biodegradation of compostable plastics (i.e. gloves, trash bags, cutlery etc.). The goal of process control for compost reactor systems is to study and optimize the environmental conditions for the microorganisms within the compost to provide maximum degradation rates of substrates. This study will deal with onsite treatment of food waste and compostable bags.

5.2 Materials and methods

5.2.1 Material

Food waste was received from Brody Dining Hall East Lansing, MSU. It was collected in a compostable 64-gallon bin liner and added in the compost bioreactor. The bin liner was obtained from Natur-tech, MN, USA. A Solvita test kit was obtained for respiration analysis from Solvita.

5.2.1.1 Feed composition for experiment

The feed added in the reactor as composition is listed in the **table 5.1.** Kitchen waste contains more than 70 percent water, to retain moisture **(Fig. 5.2)** compost and brown paper were added. The reactor maintained more than 40 percent moisture all the time.

Table 5.1 Compost bioreactor feed composition

Sr.no	Factors	Percent (%)
1	Kitchen waste	83.33
2	Coffee ground	8.7
3	Brown paper	2.1
4	Compost (from MSU composting facility)	4.0(of total dry mass)
5	Innoculum	12-15 liter for 6 days run
6	Compostable bags (per/10kg food waste)	1-2

Figure 5.2. Compost bioreactor with input (food waste) and output product (soil amendment**).**

5.2.2 Method

The Harp Renewables Digester processes organic waste within a closed, non-pressurized stainless-steel chamber. Loading the compost bioreactor is accomplished manually by introducing the material through the entrance door (as shown in **Fig.5.3**). The digested material is conveyed to the output compartment within the same chamber, where it accumulates and is ultimately discharged using an output Auger. The released material is collected in a suitable container chosen by the client. Essentially, the material undergoes digestion within the Input section of the Chamber. Subsequently, this dried material traverses a baffle wall within the Chamber, leading it into the Output section of the Chamber. There, the material undergoes further conditioning before proceeding into the output Auger, where it is then expelled from the Digester.

5.2.2.1 Mixer operation

The Mixer, located within the digester's internal chamber, runs on a constant timed cycle.

1. Runs forward for a 30sec
2. Pauses for 60 sec
3. Runs forward for a 30
4. Pauses for 60 sec
5. Runs reverse for 120 sec
6. Pauses for 60 sec
7. Repeats cycle

However, mixture is pushed out of chamber only auger is activated. When the digester is ready for discharging digested waste, the mixer will run forward to push material to the output auger. The auger will run forward to discharge the material.

5.2.2.2 Fan operation

The Fan operated on a constant timed cycle.

1. Fan ON for 30 sec

2. Fan OFF for 120 sec

5.2.2.3 Heat pad operation

The digester uses heat pads that operate independently based on a hysteresis principle, which means that changes in the heat pad's temperature lead to a lag in the temperature of the material being digested. When the core temperature reaches its target, the heat pads are turned off, and they switch back on when the core temperature drops below the set level. The digester is well-insulated, allowing it to retain thermal energy even when the heat pads are off, which helps save on energy costs. The core temperature, used as a reference by the HMI (Human Machine Interface), also follows a hysteresis approach, aiming for a specific temperature and fluctuating within certain leniency set points, which are determined by Harp Renewables.

5.2.2.4 Output auger operation

The Output Auger runs when the Main Mixer runs forward, and the auger will discharge the digestate continuously or run at a set time of the day for a set runtime

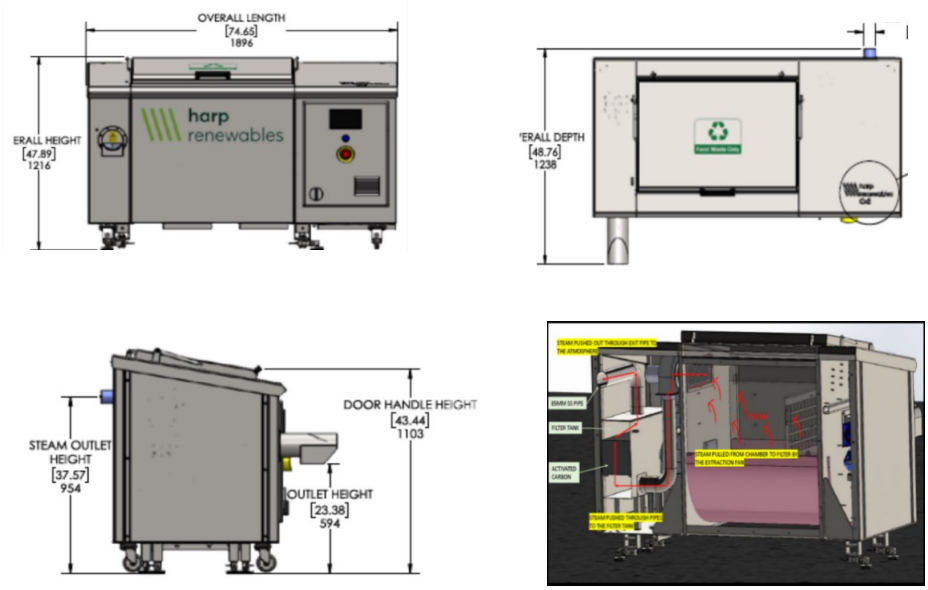

Figure 5.3. Compost reactor a) front view b) top view c) side view d) air flow direction in side chamber.

5.2.3 Analytical methods

Laboratory analyses included moisture content measurements, total organic carbon (TOC), temperature, and phytotoxicity. About 0.5 kg of the compost was collected from 15 different places in the mixture and manually blended. The temperature was taken every day at four different places.

5.2.3.1 The moisture content

The moisture content (MC) of the sample was evaluated by drying it for 24 h at 105 ◦C in an incubator (Binder). Equation (1) was used to determine the moisture content percentage. Bio stability was analyzed using respiration ASTM method and solvita test.

5.2.3.2 Respiration study

Compost stability, the extent to which the biodegradable portion of solid waste diminishes during composting, has long been of interest to composting facility operators and users. Understanding the rate of stabilization and the stability of the resulting compost allows for process optimization and comparisons between different systems. Stability also impacts microbial activity in compost, which, in turn, affects the potential for generating odors from the final product. Additionally, stability plays a role in preventing the regrowth of pathogens in compost and can influence phytotoxicity, which is the suppression of plant diseases caused by compost. Evaluations of composting systems that neglect to consider stability as a factor may fail to identify systems that cannot meet necessary process parameters and are at risk of failure.

The stabilty of samples collected from digester tested by measuring evolved CO2 (also visual observation- fungal growth). 12 Jar composting set was set up used for respiration analysis. Respiration set up was validated using cellulose as positive control. The **D5338 –15** ASTM methodology was followed to set respiration study. Active aeration was used for bioreactor to maintain oxygen more than 6%. Moisture content was maintained more than 50% and vermiculite was added to maintain the porosity in the bioreactor. **Procedure:** Compost was prepared as follows: It was sieved to achieve the particle size less than 10mm size. Vermiculite was added to create porosity in the vessel in proportion of about 1:4 of dry weight of compost. Saturated vermiculite pr was prepared with deionized water 1:4 mass/volume (water). To maintain 50% RH, saturated vermiculite added to compost should be 1:4 ratio (dry wt. compost). The moisture of mixture was maintained above 50%, such that there is no formation of the clumps by excessive moisture.

5.3 Reactor and composting process

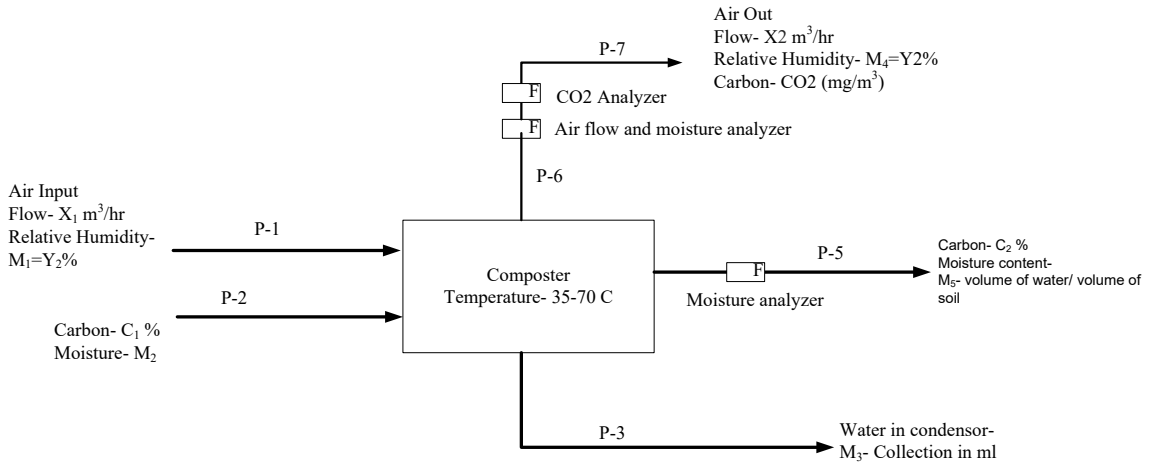

Figure 5.4. Compost reactor material balance for moisture, carbon and total mass.

Basis- 1 hr operation

Carbon balance:

Mass of carbon in Feed(P-2) = Mass of carbon in P-5 + Mass of carbon in stream P-7

Mass of carbon in Feed(P-2) = P-2(kg)*C_1

Mass of carbon in stream P-7= (mol of CO2/44) kg/m3 * X_2(m3/hr)

Mass of carbon in P-5 = P-5(kg)*C_2

$\frac{dm_c}{dt}$= P-2*C_1 - (mol of CO2/44) * X_2 + P-5*C_2 …… (1)

For steady state process the accumulation is zero then equation (1) becomes

P-2*C_1 = (mol of CO2/44) * X_2 + P-5*C_2

Moisture balance

Moisture in Feed stream+ Moisture in air input =

moisture in output air + moisture in product+ water in condenser

$\frac{dm_w}{dt}$= P-2*M_2 + P-1 * M_1 - P-7*M_4 + P-5*M_5 +P-3*M_3 …… (2)

For steady state equation 2 can be written as follows:

$P\text{-}2*M_2 + P\text{-}1 * M_1 = P\text{-}7*M_4 + P\text{-}5*M_5 + P\text{-}3*M_3$

5.4 Result and discussion

Three runs were conducted at different temperatures. The results are shown in **Fig.5.5-5.7**. Water was added every 20-24 hr to maintain the moisture of the reactor by more than 40%. Samples were taken every time interval to measure the moisture content. The reactor feed composition was the same for all runs. However, the reaction time was not the same, and the reaction was stopped when the dry mass lost more than 25 %. **Figure 5.6** shows the percent loss of dry mass at different temperatures. The percent loss of dry mass is calculated by dry mass loss divided by initial dry mass. The disappearance of compostable bags was observed by visual inspection. Everyday pictures were taken to observe the degradation of bags. **Figure A5.2** shows no presence of bags after 7-10th days.

5.4.1 Mass balances on compost bioreactor

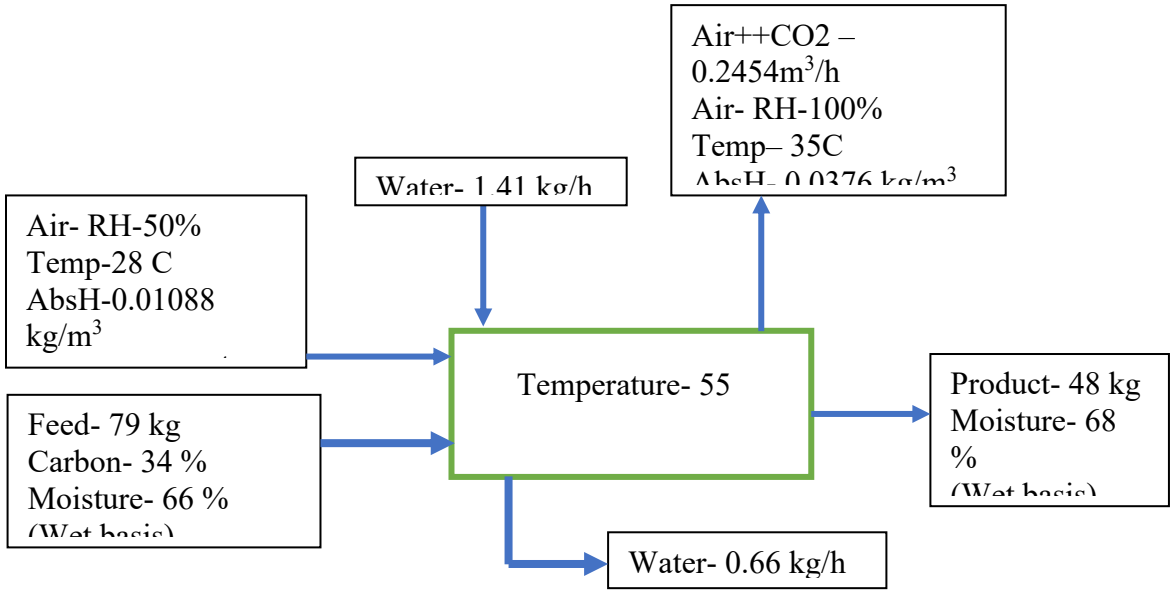

Figure 5.5. Compost reactor material balance for moisture, carbon and total mass.

5.4.2. Moisture

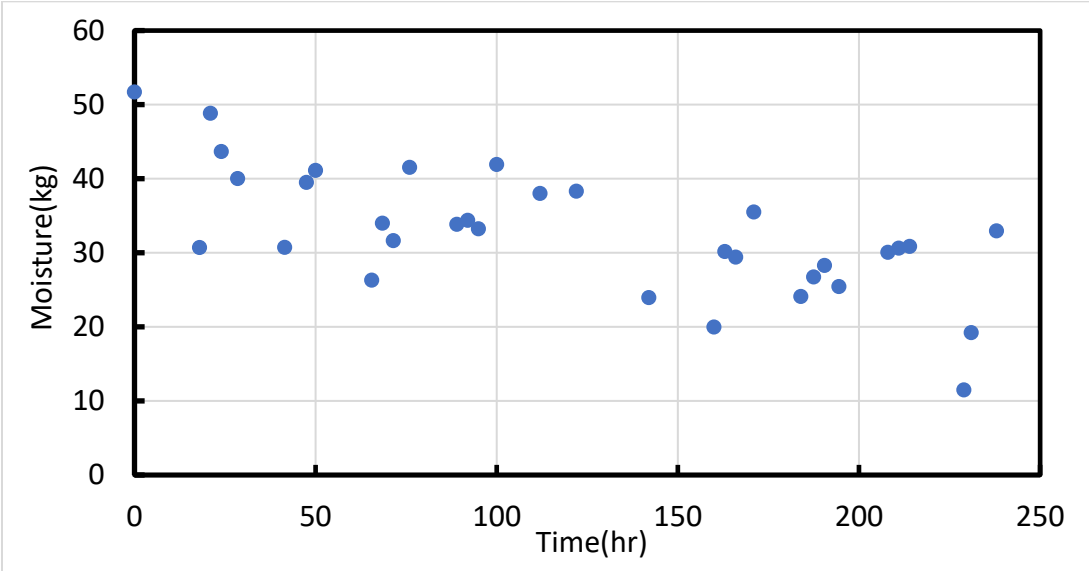

Figure 5.6. Change in moisture with time for Compost bioreactor.

5.4.3 Temperature

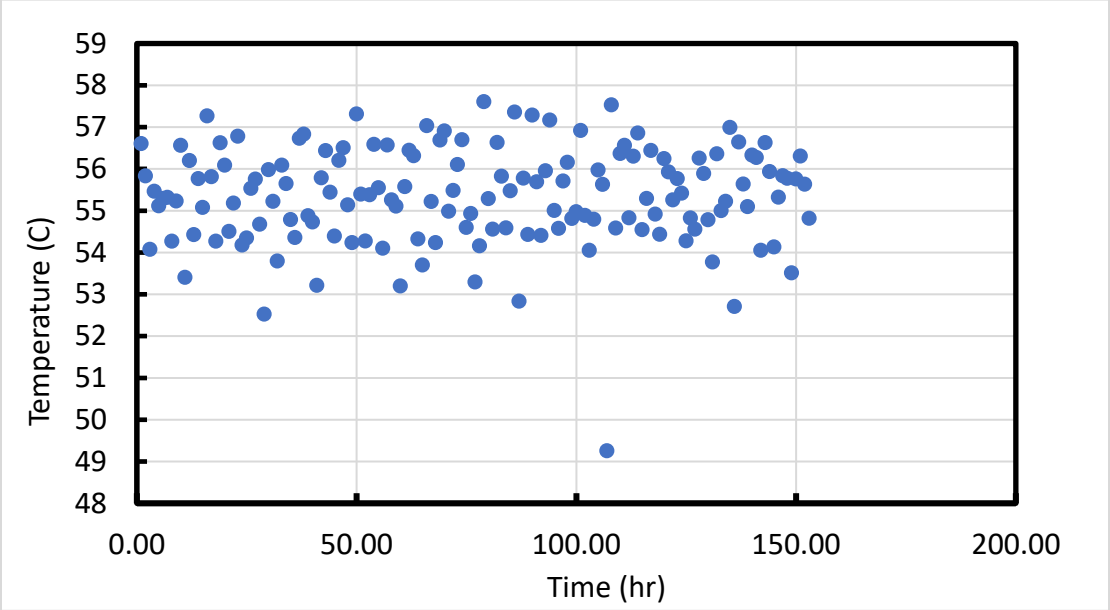

Figure 5.7. Variation in temperature with time for compost bioreactor.

5.4.4. Total mass

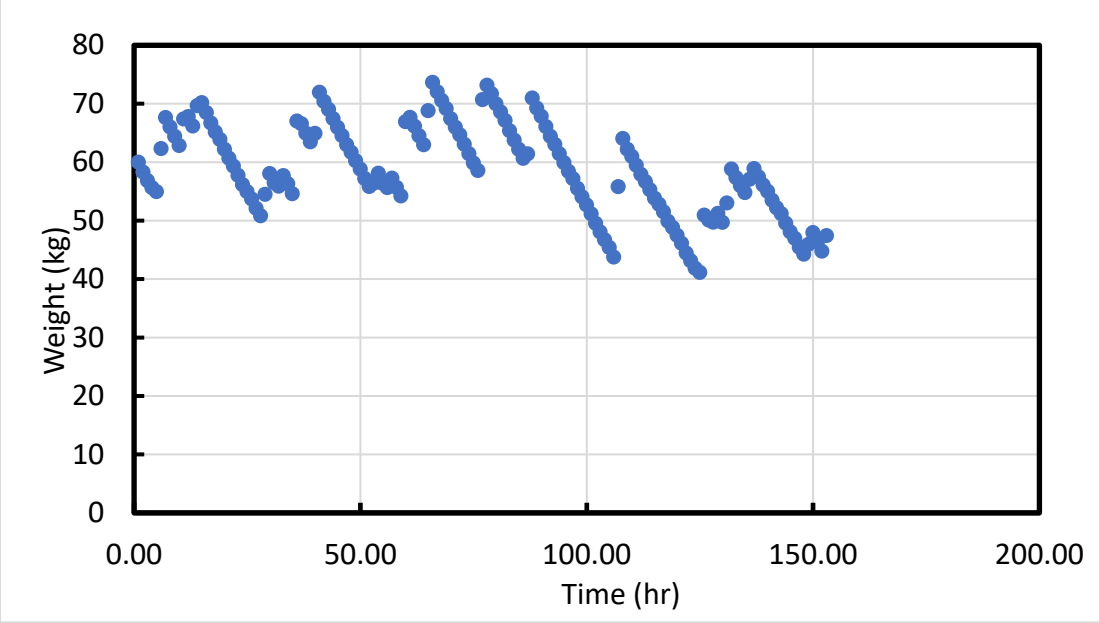

Figure 5.8. Change in total mass with time for Compost bioreactor.

5.4.5 Dry mass

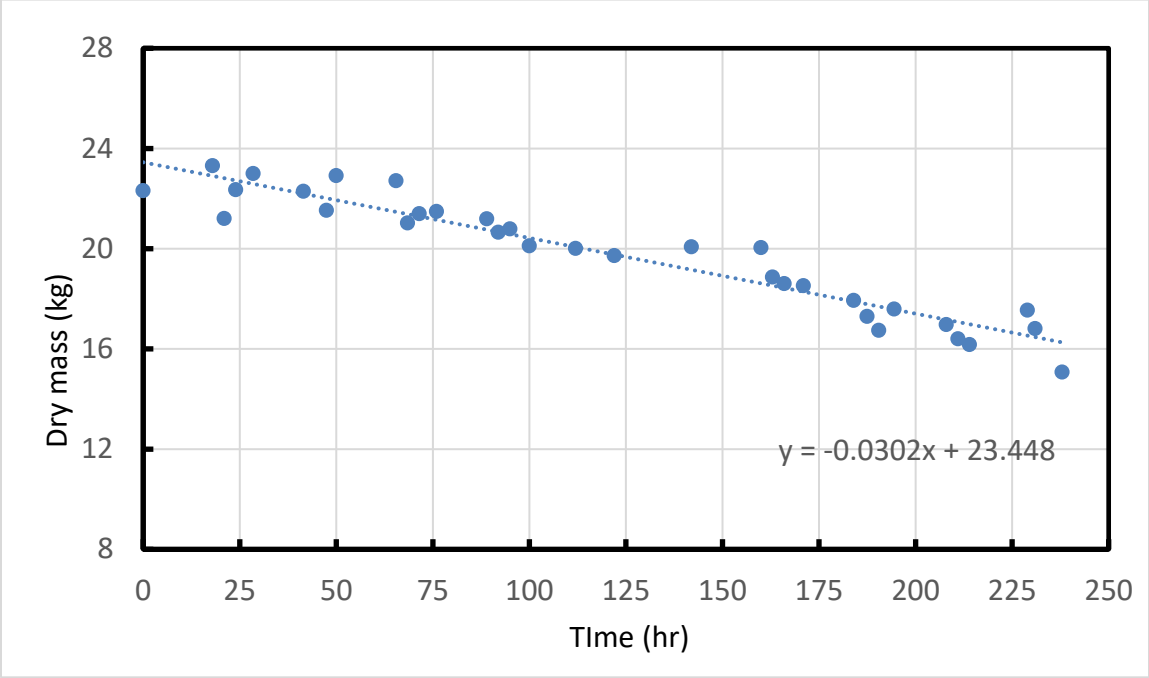

Figure 5.9. Change in dry mass with time for Compost bioreactor.

5.4.6 Respiration study

5.4.6.1 Solvita Test

Manure compost maturity tests were conducted using the Solvita® kit from WoodsEnd® Research Laboratory, Inc. The test followed the protocol outlined in the Solvita® kit manual provided by the manufacturer. This kit simultaneously measures carbon dioxide (CO2) evolution and ammonia (NH3) emission. The moisture content of all the samples fell within the optimal range (50-55%, w/w) for microbial activity. The samples were allowed to stabilize at 25°C in partially closed plastic bags before being loaded into Solvita® jars up to a specified fill line. Gel-paddles for Solvita® CO2 and NH3 tests were inserted into the compost without touching the gels after opening the packs. The sample jars were securely closed after this step. During this process, the gel portion of the paddle did not come into contact with the samples, and the positioning of the paddles allowed for easy observation of gel color changes. To determine Solvita® CO2 and NH3

kit values, the observed gel color change after a 4-hour incubation at 25°C was compared to the color charts provided with the kit. As showed in **Fig 5.10**, the gel color change was used to assess Solvita® kit CO2 values on a scale of 1-8 and NH3 values on a scale of 1-5. These two values were then combined to calculate the Solvita® maturity index, represented on a scale of 1-8, which indicates the maturity level of the compost samples. As shown in **table 5.2** final product from compost bioreactor showed good stability.

Table 5.2 Bioreactor content and theoretical CO2 calculation for each sample

Sample	Color	CO2(%)	Color	NH3 mg	Compost Maturity index (Solvita instruction sheet - From table 1)
Hammond farm	7.35	0.14	5	0.05	7
Final product from compost bioreactor	8.03	0.08	5	0.05	7.8

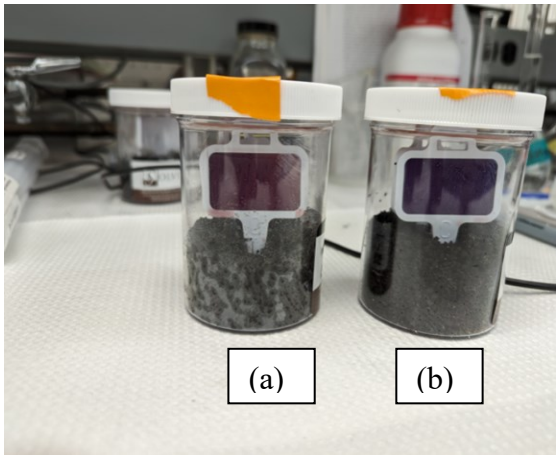

Figure 5.10. Images of solvita test probe after 4 hr (a) Hammond farm compost ;(b) final product from compost bioreactor.

5.4.6.2 D5338 –15 ASTM

The stability of samples collected from digester by measuring evolved CO2 (also visual observation- fungal growth). 12 Jar composting set was set up used for respiration analysis. The **D5338 –15** ASTM methodology was followed to set respiration study. Active aeration was used for bioreactor to maintain oxygen more than 6%. Moisture content was maintained more than 50% and vermiculite was added to maintain the porosity in the bioreactor. **Table 5.3** gives the amount of sample and vermiculite added in the sytem. **Figure 5.11** validates the respiration system the biodegradation of cellulose and starch as positive control. **Figure 5.12-13** demonstrates that Hammond farm compost as a benchmark to compare the rate of CO2 production with the product from the compost bioreactor. Respiration set up was validated using cellulose as source of carbon and studied the carbon balance **(**as shown in **table 5.4)**.

Table 5.3 Bioreactor content and theoretical CO2 calculation for each sample

Sample name	%C	**Compost n gm (moisture %)**	**Vermiculite in gm (moisture%)**	**Weight of dry mass added in bioreactor (w)(g)**	**Theoretical CO2(g) =(%C)*(44/12)*(w)**	**Theoretical CO2 (mmoles)**
Run 14	34	350 (45%)	50(80%)	157	195.7267	4448.33
1HC	20	350 (45%)	50(80%)	165	121.0000	2750
2HC	20	350 (45%)	50(80%)	165	121.0000	2750
1 HC + Cellulose	43.3	350 (45%)	50(80%)	8	12.7013	288.67
2 HC+ Cellulose	43.3	350 (45%)	50(80%)	8	12.7013	288.67
1 HC + Starch	49	350 (45%)	50(80%)	8	14.3733	326.67
2 HC+ Starch	49	350 (45%)	50(80%)	8	14.3733	326.67

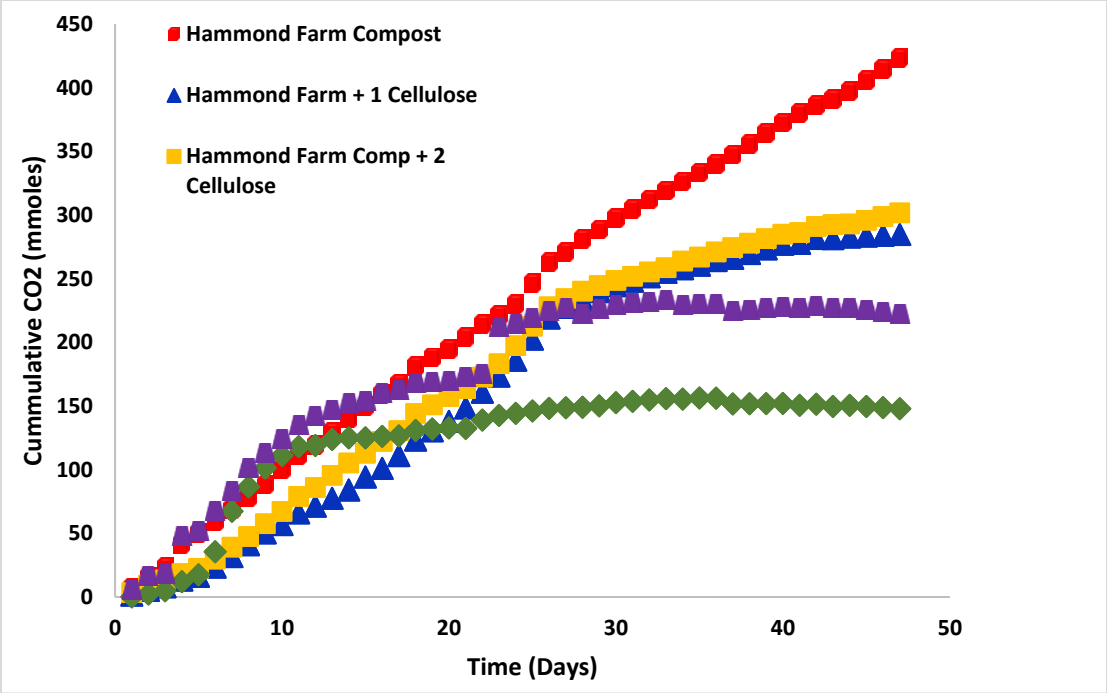

Figure 5.11. Percent biodegradation for cellulose and starch samples.

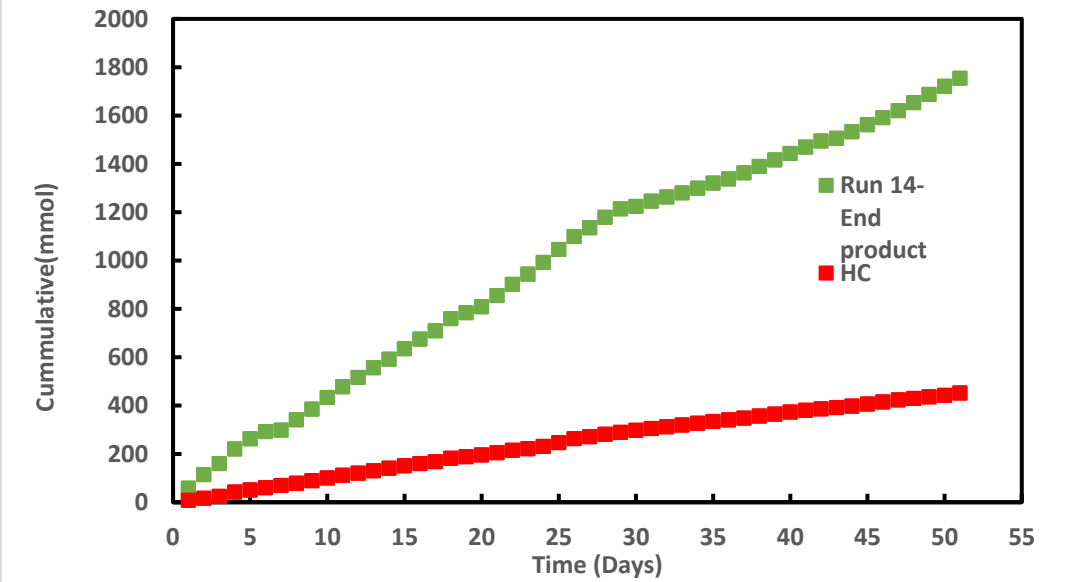

Figure 5.12. Evolved cumulative CO2 (mmol) with time for Hammond farm compost and final product from compost bioreactor.

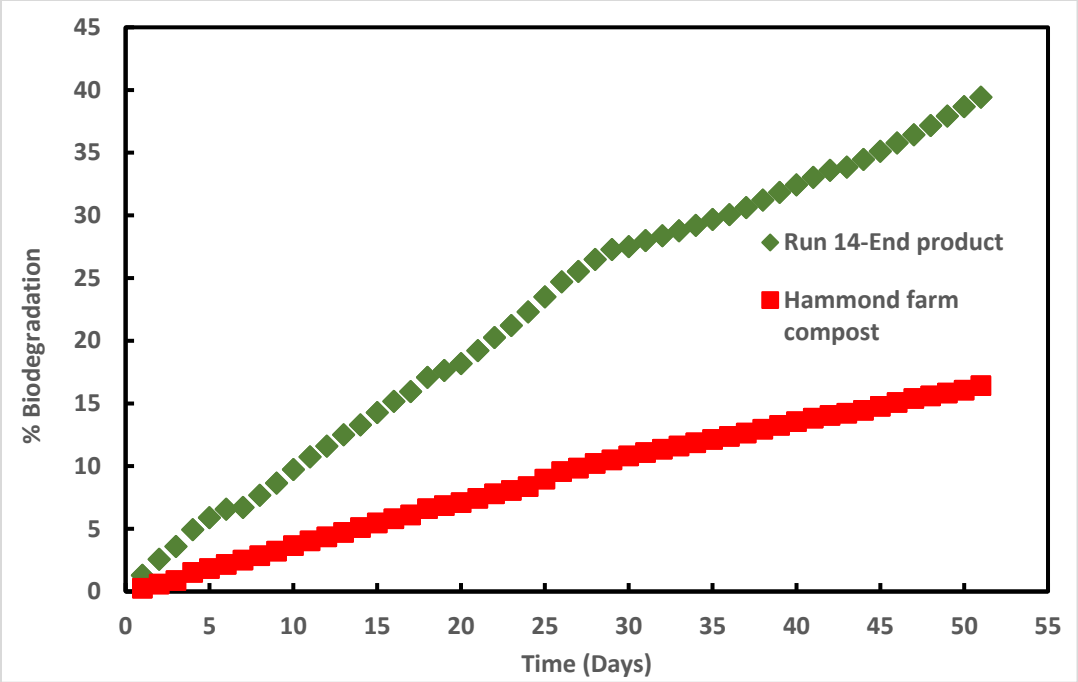

Figure 5.13. Percent biodegradation for Hammond farm compost and final product from compost bioreactor.

Table 5.4 Carbon balance for samples

Samples	Carbon Input (mmol)	Evolved CO2 (mmol)	Carbon balance (mmol)
Run 14- end product. (consist of Hammond farm compost+ wastewater inoculum+ cellulose- **400gm+1.5 lit+10 gm)**	4448	1754	Carbon remaining = 4448-1754=2694
Hammond farm	2750	451	Carbon remaining = 2750-451=2299
Hammond farm+ Cellulose (Balance only for cellulose)	288	313	Carbon remaining = 288-313*=-*19
Hammond farm+ Starch (balance only for cellulose)	326	222	=326-222=124

5.5 Conclusion

This study demonstrated a 70-80% reduction in the volume of food waste. Additionally, food waste was collected in compostable bags and added to a compost bioreactor system. A feed composition for the bioreactor was developed to yield a stable soil amendment product from the reactor. It was observed that there was negligible presence of compostable bags present in the product. The optimum operating temperature was found to be 55°C. The fan on-off cycle played a major role in maintaining the moisture level in the compost bioreactor. It is essential to maintain the moisture level above 45-50% but below 70% to yield a stable soil amendment product. The maturity of the product was tested using respiration of CO2 and compared with commercial grade compost. The respiration test showed that product is less stable than commercial standard sample and product can be use after curing.

Chapter 6

Summary and future work

Polymers are essential in everyday life because they are a broad and friendly application. Thus, the mass production of polymers has increased over the last few decades. United States (EPA) report from 1960 to 2015 mentioned that the waste developed percentage has risen to 8 % [2]. The plastic industry has diverse applications in various industries like packaging, automotive, agriculture, etc., which is approximately 41.5 million tons of total plastic consummation[118]. There are various challenges available for recycling waste plastic to new plastic or value-added materials. Plastic's diverse application and the product is a significant issue with polymer waste management. Because the collection and segregation become complex altogether for polymer waste [4], as in the case of metal, wood, and glass waste does not have such complex challenges[5]. The recycling of metal is easy because of uniformity in waste, due to which the recycling percentage is high for metal. The principal activity in polymer recycling is the separation of MSW (Municipal solid waste) to PSW (polymer separated waste)[6]. These are divided into two groups-polymer with carbon backbone (i.e., addition polymer-PP.PE, PS) and polymer with heteroatom in the backbone (i.e., condensation polymer-PET, Nylon, PU)[7]. Polymeric waste can be recycled by four main methods such as *primary recycling, mechanical recycling (secondary), chemical recycling (Tertiary), and energy recovery (quaternary)*[8]. Depolymerization is tertiary recycling technique and an axiomatic approach to green sustainability. Among these approaches, solvolysis is an ideal, sustainable, green method for processing polymer waste [9][10]. The Mechanism involves breaking a polymer chain with the help of a solvent. It is called solvolysis, such as methanolysis, hydrolysis, glycolysis, and aminolysis [11]. Although the chemical recycling process has the potential of a zero-emission recycling technique, many challenges have to be

resolved before establishment on a practical scale. These problems can be divided into three categories: 1) Economical and 2) Technical, and 3) chemistry involved. In this work to plastic waste like PET and Nylon selected for study, solvolysis technique was used to convert waste into monomer.

In Chapter 2, hydrolytic depolymerisation of polyethylene terephthalate (PET) waste was studied using high pressure autoclave reactor at 240 ºC (molten state) and autogenous pressure using excess of water in the presence of phase transfer catalyst polyethylene glycol (PEG 400) and the product profile was traced at various time intervals. In comparison with zinc acetate (used before), PEG 400 was the best catalyst. Concentration profiles were developed for PET, oligomer and terephthalic acid (TPA) using HPLC. The effect of the initial molar ratio of 22-110 mol of water/mol PET on depolymerization conversion was studied using HPLC and end group analysis. Initial molar ratio of 55-110 mol of water/mol PET gave 99 percent conversion in 30 min at 240 ^{o}C. A complete conversion of ester linkages to acid group and the desired product (TPA) was studied. based on ester linkage, 100 % conversion was observed in 10-12 min reaction time. At 30 min additional time, it gave 95% yield of TPA. Molar concentration of PEG 400 of 2.0×10^{-5} mol/cm^3 was sufficient to give the maximum conversion in breaking of ester linkages. The yield and purity of TPA was found to be 90 and 99.1 %, respectively. A new mechanism of solid (polymer)-liquid(melt)-liquid (water) phase transfer catalysis (PTC) for hydrolysis was proposed and validated. A pseudo-first order rate equation was fitted depolymerisation with a rate constant of 1.4 min^{-1} at 240 ^{o}C and apparent activation energy of 34.4 KJ/mol. The rate of hydrolysis is very fast and complete depolymerization takes place within 30 min. This is an excellent example of circular economy and cleaner production from waste plastic. Future work in this work could be conducted reaction on continuous scale.

In chapter 3, A similar approach was used for depolymerization of nylon 6 into 6-aminocaproic acid (ACA) in the first stage using PEG as the phase transfer catalyst and the aquous phase containing ACA and PEG was subjected to dehydration and cyclization to caprolactam in the second stage. Hydrolytic depolymerization method was applied to nylon 6 by using pure water as depolymerization agent, reacting under subcritical water 230-250 °C and autogenous pressure, the reaction time was 60 min. The highest yield of ACA and hence caprolactam was 90-95% in less than 60 min. The research realized the valorization of waste nylon 6 and separation of the water-soluble catalyst. Application of catalyst gives monomer ACA and then caprolactam which is a completely pure form that results in a simple process, reduction in time, reaction steps, and total reaction cost. PEG 400 was discovered as efficient phase transfer catalyst for hydrolysis of nylon 6. The S-L PTC hydrolysis reaction of nylon 6 was studied by using PEG 400 as the catalyst at melt phase. In fact, in melt phase, the so-called S-L PTC turns out to be S-L-L PTC reaction after melting of nylon. A new theory was developed to interpret dehydration of nylon 6 to 6-aminocproic acid (ACA) where the reaction takes place in subcrtical water phase. Addition of PEG 400 accelerate depolymerisation process by 45min reaction time in compared with super-critical and metal acetate depolymerisation. NMR showed excellent purity of monomer (caprolactam) without any purification or downstream processing of product when ACA was cyclized. Nylon depolymerization is series reaction with oligomers as intermediate which are converted to ACA which was converted in second reaction to caprolactam as final product. The experimental data found to be best fit for kinetic model predicted. The highest yield of caprolactam reached 96% in reaction time of 60 min. plastic.

In terms of future work, this work serves as a primary guide for the commercial scale-up of each technology developed. In terms of a fundamental understanding of solvolysis using phase transfer

catalyst. This work offers novelty in two key areas – first, in developing a hydrolysis process and second, in a phase transfer catalytic model for depolymerization reaction. These concepts have never been directly addressed in existing literature, thus filling the gap in the previous studies.

The next part of the thesis deals with polymerization and designing biodegradable and compostable polyester and develops an end-of-life strategy. There is the challenge of separating plastic waste (i.e, PET or Nylon) from organic waste as well as non-biodegradability. Segregation of plastic waste from organic waste is a difficult task. Our next approach was to prepare biobased and biodegradable/compostable polyester to prepare compostable bags. Biodegradability was achieved by decreasing aromatic content in PET by adding aliphatic diacid.

Also, the polymer must have a high molecular weight for processing conditions. So, this study contributed in developing polymerization methodology to prepare high molecular weight biobased and biodegradable polyester.

The polymerization synthesis methodology was developed to synthesize high molecular-weight polymers. High molecular weight (60-80 kg/mol) polybutylene adipate co-terephthalate (PBAT), polybutylene sebacate co-terephthalate (PBSeT), and polybutylene azelate co-terephthalate (PBAzT) were synthesized using a developed methodology. The polymers obtained were characterized by intrinsic viscosity, acid number, and molecular weight and compared with a commercial polymer. The intrinsic viscosity of the synthesized polymer was found to be in the range of 0.6-0.8 dl/gm. The estimated acid value was about of 7-12 mmol KOH/gm sample. All reactions were conducted in a scale of 0.2 to 5 kg. Future work would be solving discoloration issues.

In the next step, the food waste and compostable bags were mixed with a composition of brown and green. The reactor feed composition was maintained the same for all experiments. Various

runs were conducted at different temperatures. The temperature was optimized to 55 °C, at which all further investigations were conducted. The percent loss of dry mass was calculated by the ASTM-D2974 method. It was observed that. dry mass loss increases with reaction time. It was observed that all bags disintegrated within 8-10 days and disappeared from the mixture. In the future, a similar experiment can be done in semi-batch mode and study the disintegration of bags as well as the stability of the product.

Overall, this work contributes to circular economy concepts and sustainable technology development. Study of depolymerization using solvolysis, and repolymerization for redesigning polymer for end of life i will help solve the menace issues by plastic waste.

BIBLIOGRAPHY

[1] S. Sabde, G.D. Yadav, R. Narayan, Conversion of waste into wealth in chemical recycling of polymers: Hydrolytic depolymerization of polyethylene terephthalate into terephthalic acid and ethylene glycol using phase transfer catalysis, J. Clean. Prod. 420 (2023) 138312. https://doi.org/10.1016/j.jclepro.2023.138312.

[2] EEA, Waste Generation, Eurostat. (2015) 8–12. https://doi.org/10.1016/j.msea.2011.02.040.

[3] U, A European strategy for plastics, (n.d.). http://europa.eu/rapid/press-release_MEMO-18-6_en.htm.

[4] PlasticsEurope Market Research Group (PEMRG) / Consultic Marketing & Industrieberatung GmbH, Plastics – the Facts 2017, Assoc. Plast. Manuf. (2017) 16. https://doi.org/10.1016/j.marpolbul.2013.01.015.

[5] S. Corn, C. Wong, A Study of Plastic Recycling Supply Chain 2010 A Study of Plastic Recycling Supply Chain, 2010. http://www.ciltuk.org.uk/portals/0/documents/pd/seedcornwong.pdf.

[6] A.R. Rahimi, J.M. Garciá, Chemical recycling of waste plastics for new materials production, Nat. Rev. Chem. 1 (2017) 1–11. https://doi.org/10.1038/s41570-017-0046.

[7] Plastics – the Facts 2014 / 2015 An analysis of European plastics production , demand and waste data, Plast. Eur. (2015) 1–34. https://doi.org/10.1016/j.marpolbul.2013.01.015.

[8] V. Sinha, M.R. Patel, J. V. Patel, Pet waste management by chemical recycling: A review, J. Polym. Environ. 18 (2010) 8–25. https://doi.org/10.1007/s10924-008-0106-7.

[9] D. Paszun, T. Spychaj, Chemical Recycling of Poly(ethylene terephthalate), Ind. Eng. Chem. Res. 36 (1997) 1373–1383. https://doi.org/10.1021/ie960563c.

[10] W. Kaminsky, B. Schlesselmann, C. Simon, Olefins from polyolefins and mixed plastics by pyrolysis, J. Anal. Appl. Pyrolysis. 32 (1995) 19–27.

[11] M. Goto, Chemical recycling of plastics using sub- and supercritical fluids, J. Supercrit. Fluids. 47 (2009) 500–507. https://doi.org/10.1016/j.supflu.2008.10.011.

[12] Grand view research, Plastic Market Size, Share & Trends Analysis Report By Product By Application, By End Use, And Segment Forecasts, 2022 - 2030, 2023. https://www.grandviewresearch.com/industry-analysis/global-plastics-market/toc.

[13] S. Cornago, D. Rovelli, C. Brondi, M. Crippa, B. Morico, A. Ballarino, G. Dotelli, Stochastic consequential Life Cycle Assessment of technology substitution in the case of a novel PET chemical recycling technology, J. Clean. Prod. 311 (2021) 127406. https://doi.org/10.1016/j.jclepro.2021.127406.

[14] C. Ingrao, A. Lo Giudice, C. Tricase, R. Rana, C. Mbohwa, V. Siracusa, Recycled-PET fibre based panels for building thermal insulation: Environmental impact and

improvement potential assessment for a greener production, Sci. Total Environ. 493 (2014) 914–929. https://doi.org/10.1016/j.scitotenv.2014.06.022.

[15] A.B. Raheem, Z.Z. Noor, A. Hassan, M.K. Abd Hamid, S.A. Samsudin, A.H. Sabeen, Current developments in chemical recycling of post-consumer polyethylene terephthalate wastes for new materials production: A review, J. Clean. Prod. 225 (2019) 1052–1064. https://doi.org/10.1016/j.jclepro.2019.04.019.

[16] L.M. Heidbreder, I. Bablok, S. Drews, C. Menzel, Tackling the plastic problem: A review on perceptions, behaviors, and interventions, Sci. Total Environ. 668 (2019) 1077–1093. https://doi.org/https://doi.org/10.1016/j.scitotenv.2019.02.437.

[17] M. Cordier, T. Uehara, How much innovation is needed to protect the ocean from plastic contamination?, Sci. Total Environ. 670 (2019) 789–799. https://doi.org/https://doi.org/10.1016/j.scitotenv.2019.03.258.

[18] R.-J. Müller, H. Schrader, J. Profe, K. Dresler, W.-D. Deckwer, Enzymatic Degradation of Poly(ethylene terephthalate): Rapid Hydrolyse using a Hydrolase from T. fusca, Macromol. Rapid Commun. 26 (2005) 1400–1405. https://doi.org/https://doi.org/10.1002/marc.200500410.

[19] R. Wei, T. Oeser, J. Schmidt, R. Meier, M. Barth, J. Then, W. Zimmermann, Engineered bacterial polyester hydrolases efficiently degrade polyethylene terephthalate due to relieved product inhibition., Biotechnol. Bioeng. 113 (2016) 1658–1665. https://doi.org/10.1002/bit.25941.

[20] V. Tournier, C.M. Topham, A. Gilles, B. David, C. Folgoas, E. Moya-Leclair, E. Kamionka, M.-L. Desrousseaux, H. Texier, S. Gavalda, M. Cot, E. Guémard, M. Dalibey, J. Nomme, G. Cioci, S. Barbe, M. Chateau, I. André, S. Duquesne, A. Marty, An engineered PET depolymerase to break down and recycle plastic bottles, Nature. 580 (2020) 216–219. https://doi.org/10.1038/s41586-020-2149-4.

[21] R. Brackmann, C. de Oliveira Veloso, A.M. de Castro, M.A.P. Langone, Enzymatic post-consumer poly(ethylene terephthalate) (PET) depolymerization using commercial enzymes, 3 Biotech. 13 (2023) 135. https://doi.org/10.1007/s13205-023-03555-6.

[22] S. King, K.E.S. Locock, A circular economy framework for plastics: A semi-systematic review, J. Clean. Prod. 364 (2022) 132503. https://doi.org/10.1016/j.jclepro.2022.132503.

[23] J. Scheirs, Polymer recycling : science, technology, and applications, Wiley, Chichester; New York, 1998.

[24] L.M. Rios, C. Moore, P.R. Jones, Persistent organic pollutants carried by synthetic polymers in the ocean environment, Mar. Pollut. Bull. 54 (2007) 1230–1237.

[25] M. Artetxe, G. Lopez, M. Amutio, G. Elordi, J. Bilbao, M. Olazar, Light olefins from HDPE cracking in a two-step thermal and catalytic process, Chem. Eng. J. 207–208 (2012) 27–34. https://doi.org/10.1016/j.cej.2012.06.105.

[26] N. Lee, K.Y.A. Lin, J. Lee, Carbon dioxide-mediated thermochemical conversion of banner waste using cobalt oxide catalyst as a strategy for plastic waste treatment, Environ. Res. 213 (2022) 113560. https://doi.org/10.1016/j.envres.2022.113560.

[27] Manali Dhawan, VALORIZATION OF BIOMASS USING NOVEL CATALYTIC AND ELECTROCATALYTIC PROCESSES, 2021. http://journal.unilak.ac.id/index.php/JIEB/article/view/3845%0Ahttp://dspace.uc.ac.id/handle/123456789/1288.

[28] C. Park, K.Y.A. Lin, E.E. Kwon, J. Lee, Y.K. Park, Energy recovery from banner waste through catalytic pyrolysis over cobalt oxide: Effects of catalyst configuration, Int. J. Energy Res. 46 (2022) 19051–19063. https://doi.org/10.1002/er.8531.

[29] C. Park, H. Lee, N. Lee, B. Ahn, J. Lee, Upcycling of abandoned banner via thermocatalytic process over a MnFeCoNiCu high-entropy alloy catalyst, J. Hazard. Mater. 440 (2022) 129825. https://doi.org/10.1016/j.jhazmat.2022.129825.

[30] S. Kim, Y.T. Kim, L.S. Oh, H.J. Kim, J. Lee, Marine waste upcycling—recovery of nylon monomers from fishing net waste using seashell waste-derived catalysts in a CO2-mediated thermocatalytic process, J. Mater. Chem. A. 10 (2022) 20024–20034. https://doi.org/10.1039/d2ta02060b.

[31] Q. Liu, R. Li, T. Fang, Investigating and modeling PET methanolysis under supercritical conditions by response surface methodology approach, Chem. Eng. J. 270 (2015) 535–541. https://doi.org/10.1016/j.cej.2015.02.039.

[32] G. Güçlü, T. Yalçinyuva, S. Özgümüş, M. Orbay, Hydrolysis of waste polyethylene terephthalate and characterization of products by differential scanning calorimetry, Thermochim. Acta. 404 (2003) 193–205. https://doi.org/10.1016/S0040-6031(03)00160-6.

[33] S. Wang, C. Wang, H. Wang, X. Chen, S. Wang, Sodium titanium tris(glycolate) as a catalyst for the chemical recycling of poly(ethylene terephthalate) via glycolysis and repolycondensation, Polym. Degrad. Stab. 114 (2015) 105–114. https://doi.org/10.1016/j.polymdegradstab.2015.02.006.

[34] M.E. Tawfik, S.B. Eskander, Chemical recycling of poly(ethylene terephthalate) waste using ethanolamine. Sorting of the end products, Polym. Degrad. Stab. 95 (2010) 187–194. https://doi.org/10.1016/j.polymdegradstab.2009.11.026.

[35] Y. Liu, M. Wang, Z. Pan, Catalytic depolymerization of polyethylene terephthalate in hot compressed water, J. Supercrit. Fluids. 62 (2012) 226–231. https://doi.org/10.1016/j.supflu.2011.11.001.

[36] M. Sajdak, R. Muzyka, Use of plastic waste as a fuel in the co-pyrolysis of biomass. Part I: The effect of the addition of plastic waste on the process and products, J. Anal. Appl. Pyrolysis. 107 (2014) 267–275. https://doi.org/10.1016/j.jaap.2014.03.011.

[37] H. Wang, Z. Li, Y. Liu, X. Zhang, S. Zhang, Degradation of poly(ethylene terephthalate) using ionic liquids, Green Chem. 11 (2009) 1568. https://doi.org/10.1039/b906831g.

[38] G.M. de Carvalho, E.C. Muniz, A.F. Rubira, Hydrolysis of post-consume poly(ethylene terephthalate) with sulfuric acid and product characterization by WAXD, 13C NMR and DSC, Polym. Degrad. Stab. 91 (2006) 1326–1332. https://doi.org/10.1016/j.polymdegradstab.2005.08.005.

[39] R. López-Fonseca, M.P. González-Marcos, J.R. González-Velasco, J.I. Gutiérrez-Ortiz, A kinetic study of the depolymerisation of poly(ethylene terephthalate): By phase transfer catalysed alkaline hydrolysis, J. Chem. Technol. Biotechnol. 84 (2009) 92–99. https://doi.org/10.1002/jctb.2011.

[40] V. Sharma, P. Parashar, P. Srivastava, S. Kumar, D.D. Agarwal, N. Richharia, Recycling of waste PET-bottles using dimethyl sulfoxide and hydrotalcite catalyst, J. Appl. Polym. Sci. 129 (2013) 1513–1519. https://doi.org/10.1002/app.38829.

[41] R. Breinbauer, Organic Reactions in Water: Principles, Strategies and Applications, Synthesis (Stuttg). 2007 (2007) 3094.

[42] G.D. Yadav, B.G. Motirale, Microwave-irradiated synthesis of nitrophen using PEG 400 as phase transfer catalyst and solvent, Org. Process Res. Dev. 13 (2009) 341–348.

[43] L. Zhang, J. Gao, J. Zou, F. Yi, Hydrolysis of poly (ethylene terephthalate) waste bottles in the presence of dual functional phase transfer catalysts, J. Appl. Polym. Sci. 130 (2013) 2790–2795.

[44] E. De Lima Borges, P. Carvalho Nobre, M.S. Da Silva, R.G. Jacob, E.J. Lenardão, G. Perin, PEG-400 as a recyclable solvent in the synthesis of β-arylthio-α,β-unsaturated esters, ketone and aldehyde under base and catalyst-free conditions, J. Environ. Chem. Eng. 4 (2016) 2004–2007. https://doi.org/10.1016/j.jece.2016.03.027.

[45] M. Imran, D.H. Kim, W.A. Al-Masry, A. Mahmood, A. Hassan, S. Haider, S.M. Ramay, Manganese-, cobalt-, and zinc-based mixed-oxide spinels as novel catalysts for the chemical recycling of poly(ethylene terephthalate) via glycolysis, Polym. Degrad. Stab. 98 (2013) 904–915. https://doi.org/10.1016/j.polymdegradstab.2013.01.007.

[46] A.M. Al-Sabagh, F.Z. Yehia, A.M.F. Eissa, M.E. Moustafa, G. Eshaq, A.M. Rabie, A.E. Elmetwally, Cu- and Zn-acetate-containing ionic liquids as catalysts for the glycolysis of poly(ethylene terephthalate), Polym. Degrad. Stab. 110 (2014) 364–377. https://doi.org/10.1016/j.polymdegradstab.2014.10.005.

[47] A.M. Al-Sabagh, F.Z. Yehia, A.M.M.F. Eissa, M.E. Moustafa, G. Eshaq, A.R.M. Rabie, A.E. Elmetwally, Glycolysis of poly(ethylene terephthalate) catalyzed by the Lewis base ionic liquid [Bmim][OAc], Ind. Eng. Chem. Res. 53 (2014) 18443–18451. https://doi.org/10.1021/ie503677w.

[48] R. Tincu, A. Slabu, C. Stavarache, M.M. Duldner, E. Bartha, F. Teodorescu, Metal-containing Ionic Liquids as Catalyst in PET Glycolysis, Mater. Plast. 59 (2022) 143–151. https://doi.org/10.37358/MP.22.3.5612.

[49] T. Yalçinyuva, M.R. Kamal, R.A. Lai-Fook, S. Özgümüs, Hydrolytic Depolymerization of

Polyethylene Terephthalate by Reactive Extrusion, Int. Polym. Process. 15 (2022) 137–146. https://doi.org/10.1515/ipp-2000-0005.

[50] G.P. Karayannidis, A.P. Chatziavgoustis, D.S. Achilias, Poly (ethylene terephthalate) recycling and recovery of pure terephthalic acid by alkaline hydrolysis, Adv. Polym. Technol. 21 (2002) 250–259. https://doi.org/10.1002/1439-2054(20011001)286:10<640::AID-MAME640>3.0.CO;2-1.

[51] O. Sato, K. Arai, M. Shirai, Hydrolysis of poly(ethylene terephthalate) and poly(ethylene 2,6-naphthalene dicarboxylate) using water at high temperature: Effect of proton on low ethylene glycol yield, Catal. Today. 111 (2006) 297–301. https://doi.org/10.1016/j.cattod.2005.10.040.

[52] R. López-Fonseca, J.R. González-Velasco, J.I. Gutiérrez-Ortiz, A shrinking core model for the alkaline hydrolysis of PET assisted by tributylhexadecylphosphonium bromide, Chem. Eng. J. 146 (2009) 287–294. https://doi.org/https://doi.org/10.1016/j.cej.2008.09.039.

[53] R. López-Fonseca, I. Duque-Ingunza, B. de Rivas, L. Flores-Giraldo, J.I. Gutiérrez-Ortiz, Kinetics of catalytic glycolysis of PET wastes with sodium carbonate, Chem. Eng. J. 168 (2011) 312–320. https://doi.org/https://doi.org/10.1016/j.cej.2011.01.031.

[54] R.C. Golike, S.W. Lasoski, Kinetics of Hydrolysis of Polyethylene Terephthalate Films, J. Phys. Chem. 64 (1960) 895–898. https://doi.org/10.1021/j100836a018.

[55] H.I. Khalaf, O.A. Hasan, Effect of quaternary ammonium salt as a phase transfer catalyst for the microwave depolymerization of polyethylene terephthalate waste bottles, Chem. Eng. J. 192 (2012) 45–48. https://doi.org/10.1016/j.cej.2012.03.081.

[56] J.R. Campanelli, M.R. Kamal, D.G. Cooper, A Kinetic Study of the Hydrolytic Degradation of Poly(Ethylene Terephthalate) at High Temperatures, J. Appl. Polym. Sci. 48 (1993) 443–451.

[57] C. a. Lucchesi, W.T. Lewis, Latent heat of sublimation of terephthalic acid from differential thermal analysis data, J. Chem. Eng. Data. 13 (1968) 389–391. https://doi.org/10.1021/je60038a026.

[58] F. Bi, J. Shao, Z. Xi, L. Zhao, D. Liu, Synthesis and characterization of copolymers of poly(m-xylylene adipamide) and poly(ethylene terephthalate) oligomers by melt copolycondensation, Chinese J. Chem. Eng. 24 (2016) 1290–1297. https://doi.org/10.1016/j.cjche.2016.04.003.

[59] X. Zhou, X. Lu, Q. Wang, M. Zhu, Z. Li, Effective catalysis of poly (ethylene terephthalate)(PET) degradation by metallic acetate ionic liquids, Pure Appl. Chem. 84 (2012) 789–801.

[60] A.B. Elmas Kimyonok, M. Ulutürk, Determination of the Thermal Decomposition Products of Terephthalic Acid by Using Curie-Point Pyrolyzer, J. Energ. Mater. 34 (2016) 113–122.

[61] S.D. Mancini, J.A.S. Schwartzman, A.R. Nogueira, D.A. Kagohara, M. Zanin, Additional steps in mechanical recyling of PET, J. Clean. Prod. 18 (2010) 92–100. https://doi.org/10.1016/j.jclepro.2009.09.004.

[62] F. Chen, G. Wang, W. Li, F. Yang, Glycolysis of poly(ethylene terephthalate) over Mg-Al mixed oxides catalysts derived from hydrotalcites, Ind. Eng. Chem. Res. 52 (2013) 565–571. https://doi.org/10.1021/ie302091j.

[63] G. Montaudo, R.P. Lattimer, Mass spectrometry of polymers, CRC Press, 2001.

[64] G.D. Yadav, Engineering Aspect of Ionic, (2021).

[65] G.D. Yadav, Insight into green phase transfer catalysis, Top. Catal. 29 (2004) 145–161. https://doi.org/10.1023/b:toca.0000029797.93561.cd.

[66] J.R. Campanelli, D.G. Cooper, M.R. Kamal, Catalyzed hydrolysis of polyethylene terephthalate melts, J. Appl. Polym. Sci. 53 (1994) 985–991. https://doi.org/10.1002/app.1994.070530801.

[67] J.R. Campanelli, M.R. Kamal, D.G. Cooper, A kinetic study of the hydrolytic degradation of polyethylene terephthalate at high temperatures, J. Appl. Polym. Sci. 48 (1993) 443–451. https://doi.org/10.1002/app.1993.070480309.

[68] J.R. Campanelli, D.G. Cooper, M.R. Kamal, Catalyzed hydrolysis of polyethylene terephthalate melts, J. Appl. Polym. Sci. 53 (1994) 985–991. https://doi.org/10.1002/app.1994.070530801.

[69] Y. Wang, Y. Zhang, H. Song, Y. Wang, T. Deng, X. Hou, Zinc-catalyzed ester bond cleavage: Chemical degradation of polyethylene terephthalate, J. Clean. Prod. 208 (2019) 1469–1475. https://doi.org/10.1016/j.jclepro.2018.10.117.

[70] L. Zhang, Kinetics of hydrolysis of poly(ethylene terephthalate) wastes catalyzed by dual functional phase transfer catalyst: A mechanism of chain-end scission, Eur. J. Pharmacol. 742 (2014) 1–5. https://doi.org/10.1016/j.eurpolymj.2014.08.007.

[71] D.C. Cooper, Catalyzed Hydrolysis of Polyethylene Terephthalate Melts, (n.d.) 985–991.

[72] T. Yoshioka, T. Motoki, A. Okuwaki, Kinetics of hydrolysis of poly(ethylene terephthalate) powder in sulfuric acid by a modified shrinking-core model, Ind. Eng. Chem. Res. 40 (2001) 75–79. https://doi.org/10.1021/ie000592u.

[73] M.N. Siddiqui, D.S. Achilias, H.H. Redhwi, D.N. Bikiaris, K.A.G. Katsogiannis, G.P. Karayannidis, Hydrolytic depolymerization of PET in a microwave reactor, Macromol. Mater. Eng. 295 (2010) 575–584. https://doi.org/10.1002/mame.201000050.

[74] G.D. Yadav, In Pursuit of The Net Zero Goal and Sustainability : Hydrogen Economy , (2023).

[75] Greyer, No Title, World Bank Gr. Basel Conv. Plast. (2021).

[76] T. Thiounn, R.C. Smith, Advances and approaches for chemical recycling of plastic waste, J. Polym. Sci. 58 (2020) 1347–1364. https://doi.org/10.1002/pol.20190261.

[77] R. Darzi, Y. Dubowski, R. Posmanik, Hydrothermal processing of polyethylene-terephthalate and nylon-6 mixture as a plastic waste upcycling treatment: A comprehensive multi-phase analysis, Waste Manag. 143 (2022) 223–231. https://doi.org/10.1016/j.wasman.2022.03.002.

[78] T. Iwaya, M. Sasaki, M. Goto, Kinetic analysis for hydrothermal depolymerization of nylon 6, Polym. Degrad. Stab. 91 (2006) 1989–1995. https://doi.org/10.1016/j.polymdegradstab.2006.02.009.

[79] C. Gong, K. Zhang, C. Yang, J. Chen, S. Zhang, C. Yi, Simple process for separation and recycling of nylon 6 and polyurethane components from waste nylon 6/polyurethane debris, Text. Res. J. 91 (2020) 18–27. https://doi.org/10.1177/0040517520931893.

[80] I. Kikic, Polymer-supercritical fluid interactions, J. Supercrit. Fluids. 47 (2009) 458–465. https://doi.org/10.1016/j.supflu.2008.10.016.

[81] H. Bockhorn, A. Hornung, U. Hornung, J. Weichmann, Kinetic study on the non-catalysed and catalysed degradation of polyamide 6 with isothermal and dynamic methods, Thermochim. Acta. 337 (1999) 97–110. https://doi.org/10.1016/s0040-6031(99)00151-3.

[82] A. Kamimura, Y. Oishi, K. Kaiso, T. Sugimoto, K. Kashiwagi, Supercritical secondary alcohols as useful media to convert polyamide into monomeric lactams, ChemSusChem. 1 (2008) 82–84. https://doi.org/10.1002/cssc.200700024.

[83] M. Goto, Chemical recycling of plastics using sub- and supercritical fluids, J. Supercrit. Fluids. 47 (2009) 500–507. https://doi.org/10.1016/j.supflu.2008.10.011.

[84] G.D. Yadav, B.G. Motirale, Ionic Liquid as Catalyst for Solid−Liquid Phase Transfer Catalyzed Synthesis of p-Nitrodiphenyl Ether, Ind. Eng. Chem. Res. 47 (2008) 9081–9089. https://doi.org/10.1021/ie800340j.

[85] G.D. Yadav, Insight into Green Phase Transfer Catalysis, Top. Catal. 29 (2004) 145–161. https://doi.org/10.1023/B:TOCA.0000029797.93561.cd.

[86] P. Application, Patent Application Publication (10) Pub . No .: US 2022/0089536 A1, 2022.

[87] A. Kamimura, K. Ikeda, S. Suzuki, K. Kato, Y. Akinari, T. Sugimoto, K. Kashiwagi, K. Kaiso, H. Matsumoto, M. Yoshimoto, Efficient Conversion of Polyamides to ω-Hydroxyalkanoic Acids: A New Method for Chemical Recycling of Waste Plastics, ChemSusChem. 7 (2014) 2473–2477. https://doi.org/10.1002/cssc.201402125.

[88] W. Wang, L. Meng, K. Leng, Y. Huang, Hydrolysis of waste monomer casting nylon catalyzed by solid acids, Polym. Degrad. Stab. 136 (2017) 112–120. https://doi.org/10.1016/j.polymdegradstab.2016.12.017.

[89] J. Chen, Z. Li, L. Jin, P. Ni, G. Liu, H. He, J. Zhang, J. Dong, R. Ruan, Catalytic

hydrothermal depolymerization of nylon 6, J. Mater. Cycles Waste Manag. 12 (2010) 321–325. https://doi.org/10.1007/s10163-010-0304-y.

[90] Y. Tian, H. Qin, X. Yang, C. Chi, S. Liu, Influence of ionic liquids on the structure of polyamide 6, Mater. Lett. 180 (2016) 200–202. https://doi.org/10.1016/j.matlet.2016.05.151.

[91] R. Geyer, J.R. Jambeck, K.L. Law, Production, use, and fate of all plastics ever made, Sci. Adv. 3 (2017) e1700782.

[92] R. Geyer, J.R. Jambeck, K.L. Law, Production, use, and fate of all plastics ever made, Sci. Adv. 3 (2022) e1700782. https://doi.org/10.1126/sciadv.1700782.

[93] K.L. Law, Plastics in the Marine Environment., Ann. Rev. Mar. Sci. 9 (2017) 205–229. https://doi.org/10.1146/annurev-marine-010816-060409.

[94] J.R. Westlake, M.W. Tran, Y. Jiang, X. Zhang, A.D. Burrows, M. Xie, Biodegradable biopolymers for active packaging: demand, development and directions, Sustain. Food Technol. 1 (2023) 50–72. https://doi.org/10.1039/d2fb00004k.

[95] K.L. Law, R. Narayan, Reducing environmental plastic pollution by designing polymer materials for managed end-of-life, Nat. Rev. Mater. 7 (2022) 104–116. https://doi.org/10.1038/s41578-021-00382-0.

[96] N. Mulchandani, R. Narayan, Redesigning Carbon–Carbon Backbone Polymers for Biodegradability–Compostability at the End-of-Life Stage, Molecules. 28 (2023). https://doi.org/10.3390/molecules28093832.

[97] K.H. Paek, S.G. Im, Synthesis of a series of biodegradable poly(butylene carbonate-: co - isophthalate) random copolymers derived from CO2-based comonomers for sustainable packaging, Green Chem. 22 (2020) 4570–4580. https://doi.org/10.1039/d0gc01549k.

[98] R.W. Hartel, The crystalline state, 2008. https://doi.org/10.1007/978-0-387-71947-4_4.

[99] T. Burford, W. Rieg, S. Madbouly, Biodegradable poly(butylene adipate-co-terephthalate) (PBAT), Phys. Sci. Rev. (2021) 1–30. https://doi.org/10.1515/psr-2020-0078.

[100] B. Dietrich, [BASF] US20110187029A1 (Older), 1 (2011).

[101] M. Chanda, Introduction to Polymer Science and Chemistry: A Problem-Solving Approach: SECOND EDITION, 2013. https://doi.org/10.1201/b14577.

[102] A. Rudin, P. Choi, Chapter 7 - Step-Growth Polymerizations, in: A. Rudin, P.B.T.-T.E. of P.S.& E. (Third E. Choi (Eds.), Academic Press, Boston, 2013: pp. 305–339. https://doi.org/https://doi.org/10.1016/B978-0-12-382178-2.00007-9.

[103] T.E. Long, Modern Polyesters: Chemistry and Technology of Polyesters and Copolyesters, 2004. https://doi.org/10.1002/0470090685.

[104] R.A. Mashelkar, Review Polyethylene Article, Rev. Lit. Arts Am. 41 (1986) 2969–2987.

[105] K. Tomita, H. Ida, Studies on the formation of poly(ethylene terephthalate): 2. Rate of transesterification of dimethyl terephthalate with ethylene glycol, Polymer (Guildf). 14 (1973) 55–60. https://doi.org/10.1016/0032-3861(73)90096-7.

[106] T. Formation, P. Terephthalate, E. Interchange, The Formation, (1959) 123–137.

[107] J. Jian, Z. Xiangbin, H. Xianbo, An overview on synthesis, properties and applications of poly(butylene-adipate-co-terephthalate)–PBAT, Adv. Ind. Eng. Polym. Res. 3 (2020) 19–26. https://doi.org/10.1016/j.aiepr.2020.01.001.

[108] U. Witt, [BASF] US9040639 | Method for the continuous production of biodegradable polyesters, 2 (2015). https://patents.google.com/patent/US9040639.

[109] I.E. Nifant'ev, V. V. Bagrov, P.D. Komarov, V.I. Ovchinnikova, P. V. Ivchenko, Aryloxy 'biometal' complexes as efficient catalysts for the synthesis of poly(butylene adipate terephthalate), Mendeleev Commun. 32 (2022) 351–353. https://doi.org/10.1016/j.mencom.2022.05.020.

[110] Denial Mahata, S. Karthikeyan, R. Godse, V.K. Gupta, Poly(butylene adipate-co-terephthalate) Polyester Synthesis Process and Product Development, Polym. Sci. - Ser. C. 63 (2021) 102–111. https://doi.org/10.1134/S1811238221010045.

[111] US2009117013A1_Original_document_20230423021739.pdf, (n.d.).

[112] C. Polymers, Standard Practice for Dilute Solution Viscosity of Polymers 1, Annu. B. ASTM Stand. i (2001) 1–6. https://doi.org/10.1520/D2857-22.2.

[113] A. Conix, On the Molecular Weight Determination of Poly (et hylene t erepht halat e), Makromolecular Chem. Phys. 49 (1958) 226–235.

[114] R.N. Shroff, I. Corporution, Single-Point Determination, 9 (1965) 1547–1551.

[115] P.E.T. Yarns, Standard Test Method for Carboxyl End Group Content of Polyethylene Terephthalate, i (2015) 1–3. https://doi.org/10.1520/D7409-15.2.

[116] W. Tian, Z. Zeng, W. Xue, Y. Li, T. Zhang, Kinetics of the mono-esterification between terephthalic acid and 1,4-butanediol, Chinese J. Chem. Eng. 18 (2010) 391–396. https://doi.org/10.1016/S1004-9541(10)60236-4.

[117] R.T. Haug, The practical handbook of compost engineering, Routledge, 2018.

[118] K. Law, R. Narayan, Reducing environmental plastic pollution by designing polymer materials for managed end-of-life, Nat. Rev. Mater. 7 (2021) 1–13. https://doi.org/10.1038/s41578-021-00382-0.

APPENDIX A2: CHAPTER 2

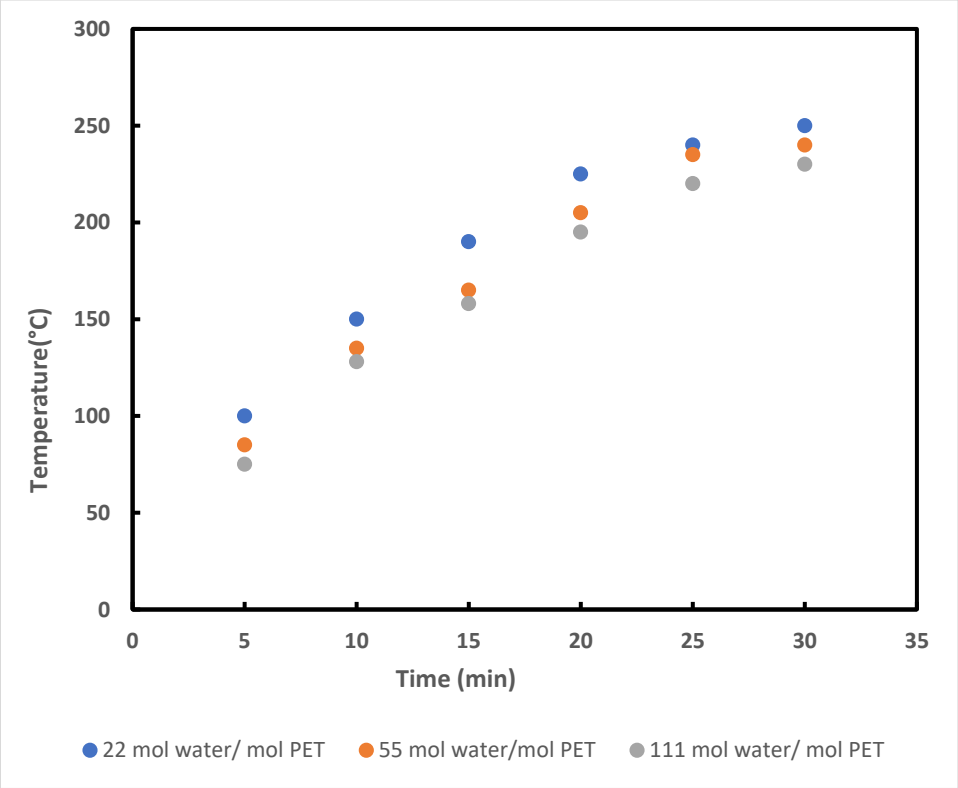

Figure A2.1. Temperature profile in autoclave for various initial W/P ratio.

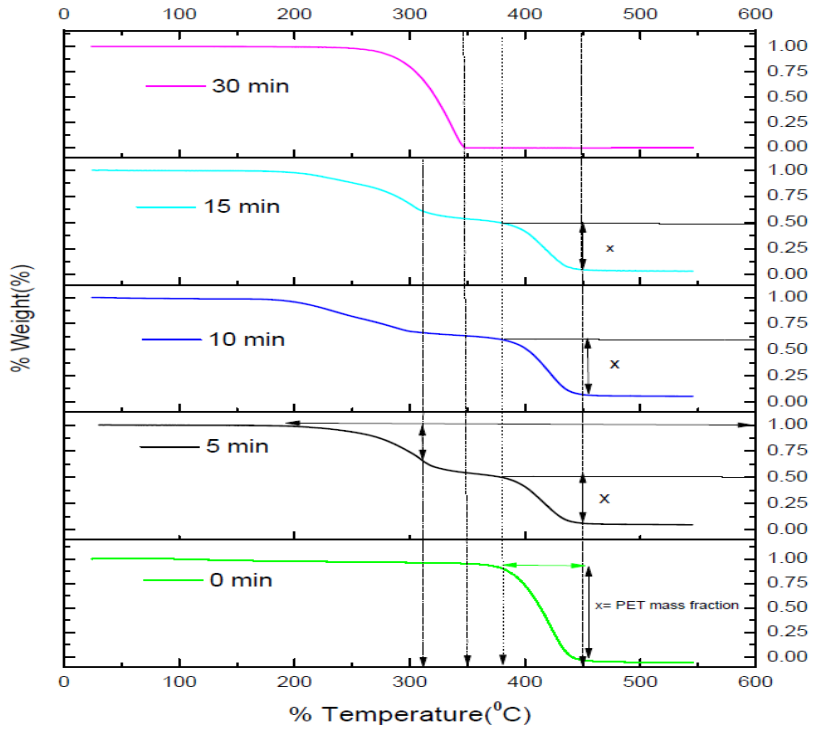

Figure A2.2. TGA plot variation of PET with PEG-400 treatment time.

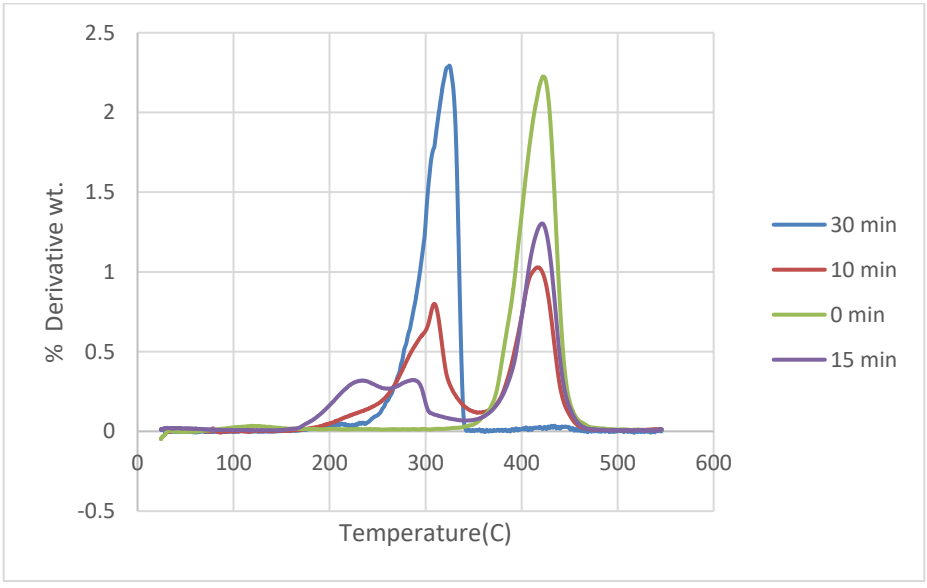

Figure A2.3. TGA plot variation of PET with PEG-400 treatment time.

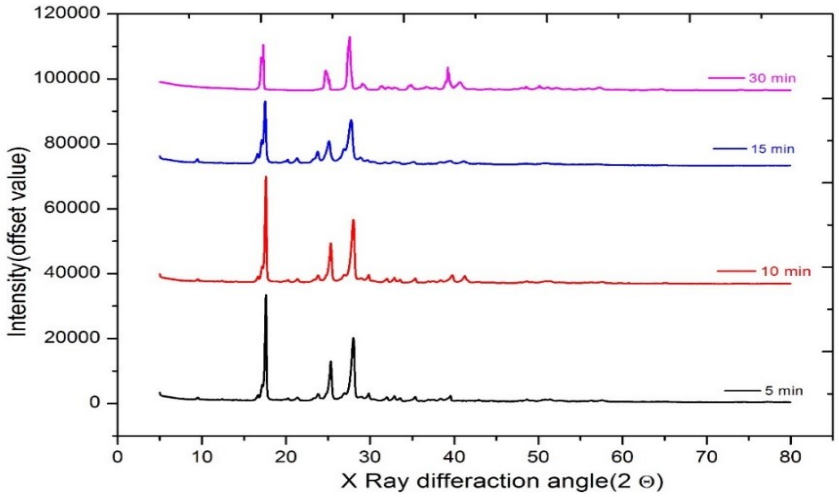

Figure

A2.4. XRD plot variation of PET with PEG-400 treatment time.

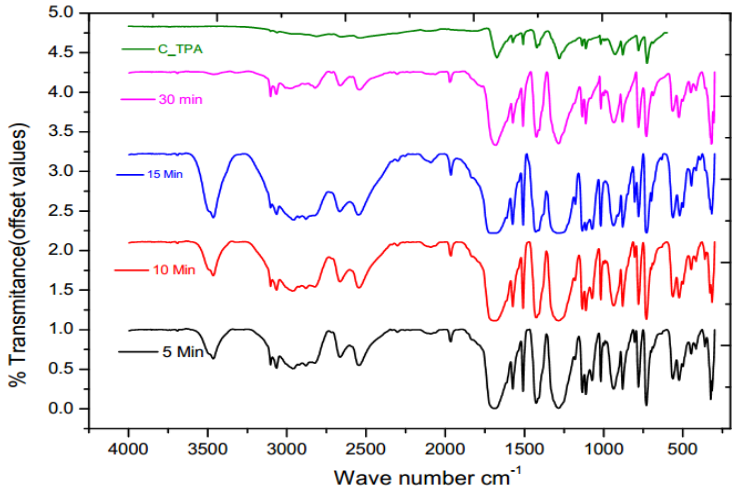

Figure A2.5. FTIR of standard TPA and PET with PEG-400 at various reaction times.

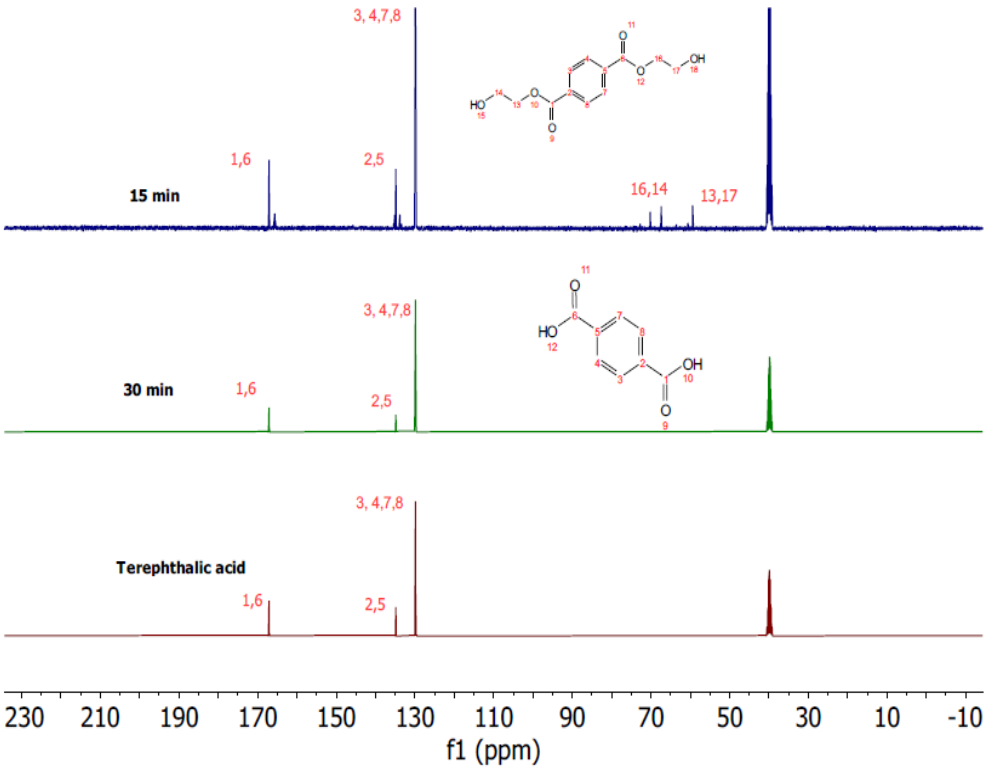

Figure A2.6. NMR^{13}C spectra of standard TPA and PET with PEG 400 at various reaction times.

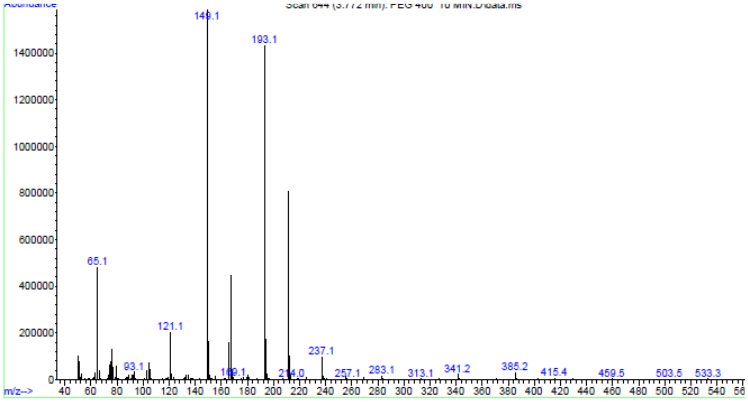

(a)

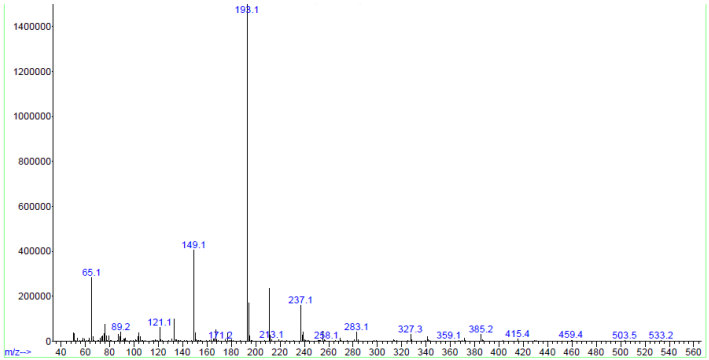

(b)

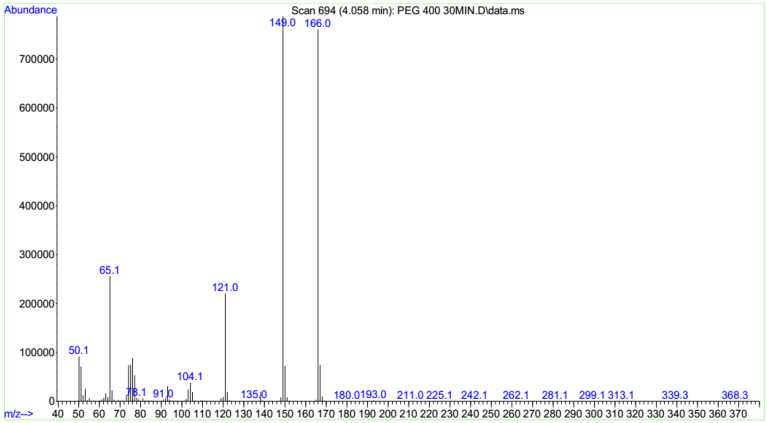

(c)

Figure A2.7. Mass spectra (a) 3 min; (b) 10 min (c) 30 min reaction time hydrolytic sample with PEG 400.

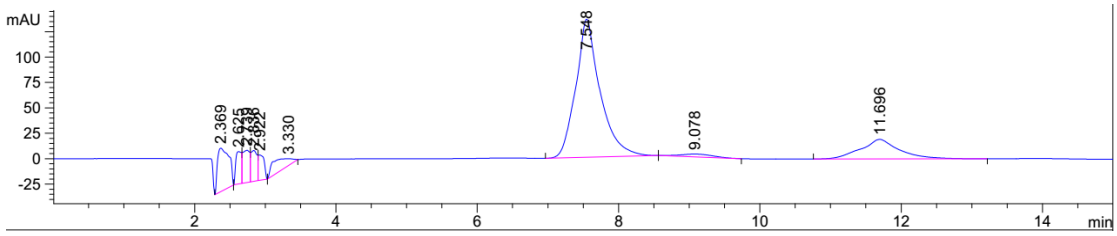

(a)

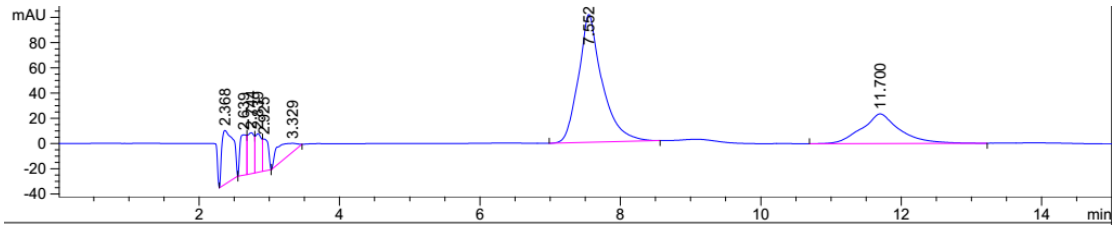

(b)

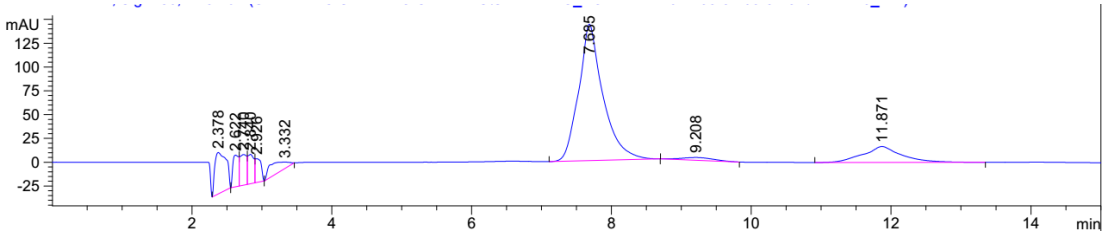

(c)

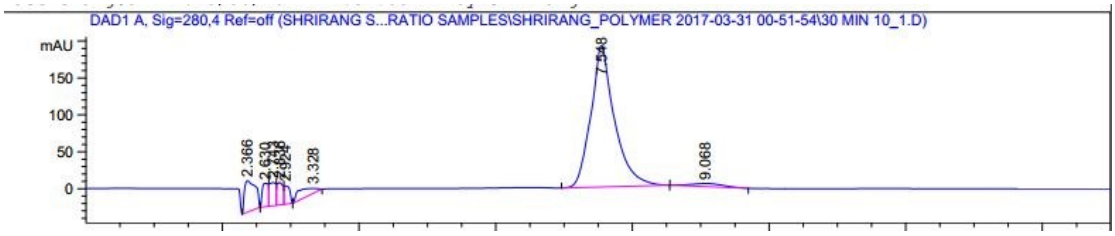

(d)

Figure A2.8. HPLC analysis spectrum for product mixture with PEG-400 treatment time:(a) 3min;(b) 5 min; (c) 10 min; (d) 30 min.

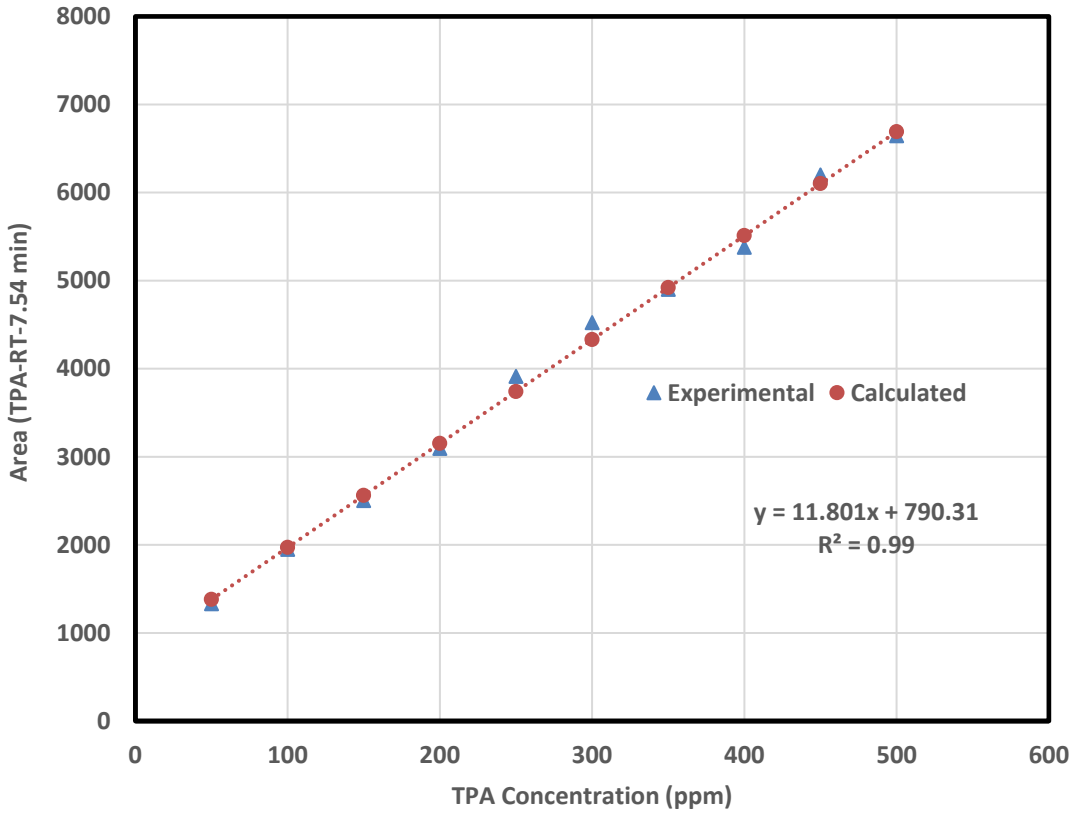

Figure A2.9. HPLC analysis calibration curve for terephthalic acid: Experimental and calculated values for retention time of 7.54 $\pm$0.10 min.

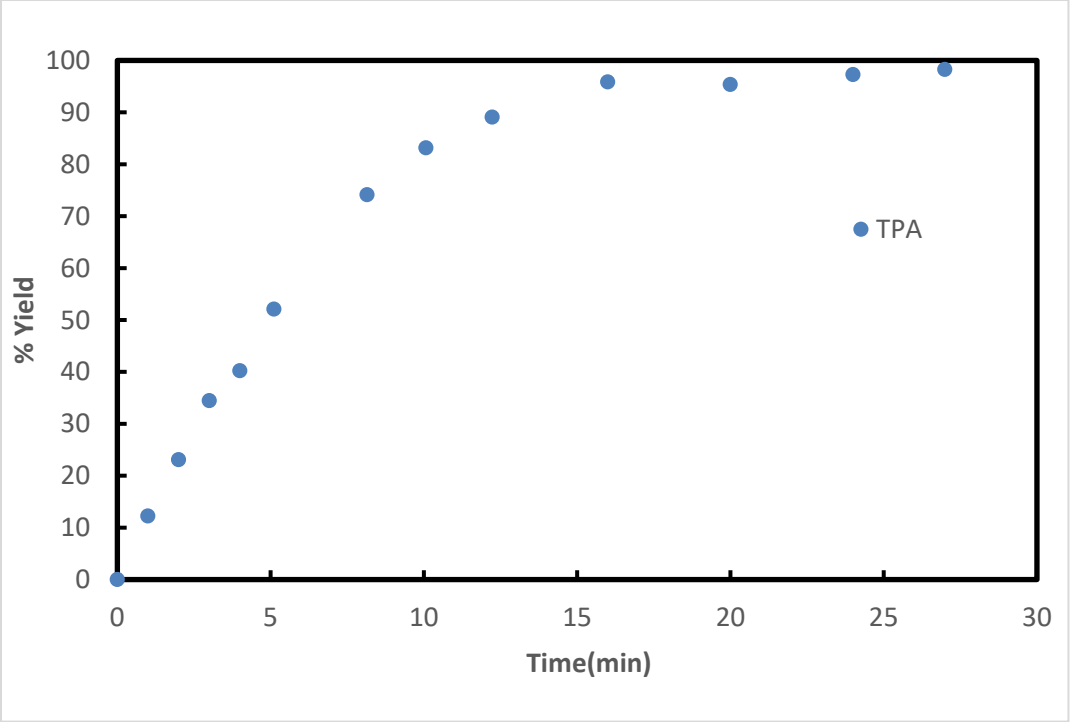

Figure A2.10. Concentration profile for % yield of TPA for time at 240 °C with PEG 400 catalytic effect. (Reaction condition- Temperature: 240°C; Catalyst concentration:2.11×10^{-5} mol/cm^3; PET concentration: 5.27×10^{-4} (mol/cm^3); Water: 100 cm^3; Speed of agitation: 650 rpm) (Analysis based on HPLC Method).

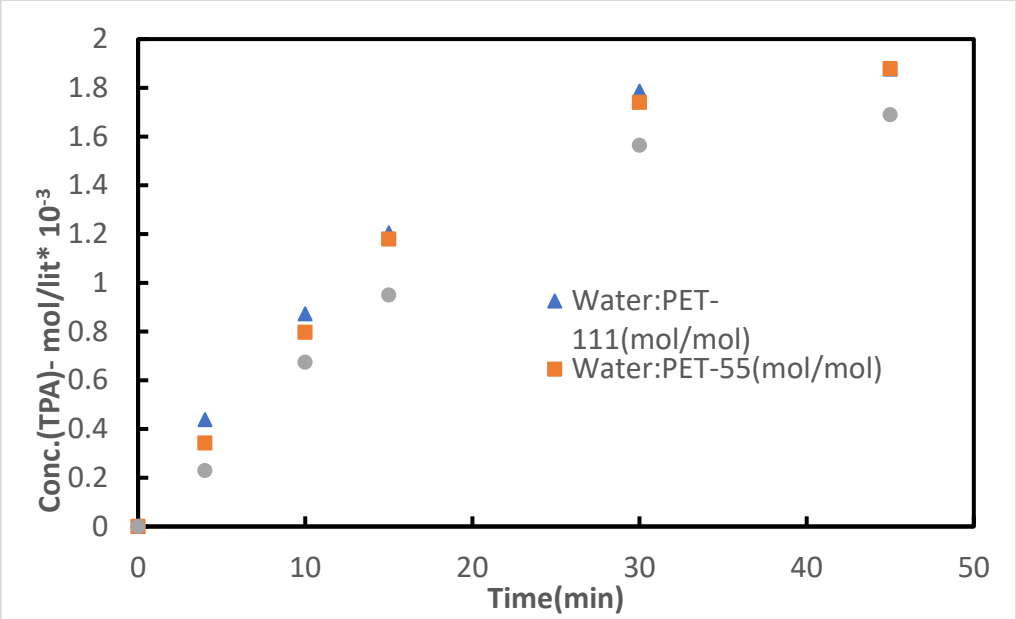

Figure A2.11. Terephthalic acid concentration with time for three different Initial charge ratios. (Reaction condition- Temperature: 240°C; Reaction time: 30 min; Catalyst concentration: 2.11×10^{-5} mol/cm^3; Speed of agitation: 650 rpm) (Analysis based on HPLC Method).

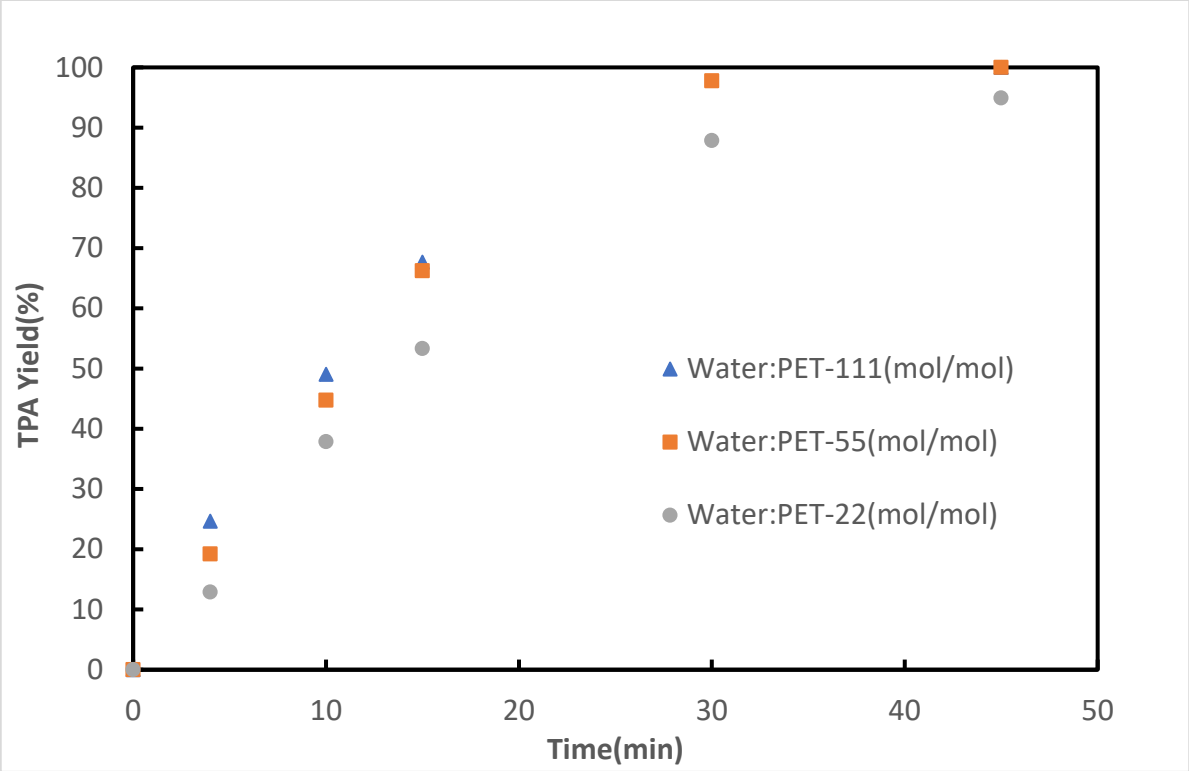

Figure A2.12. TPA yield as function of initial water concentration. (Reaction condition- Temperature: 240 °C; Catalyst concentration: 2.11×10^{-5} mol/cm^3; Speed of agitation: 650 rpm) (Analysis based on HPLC Method).

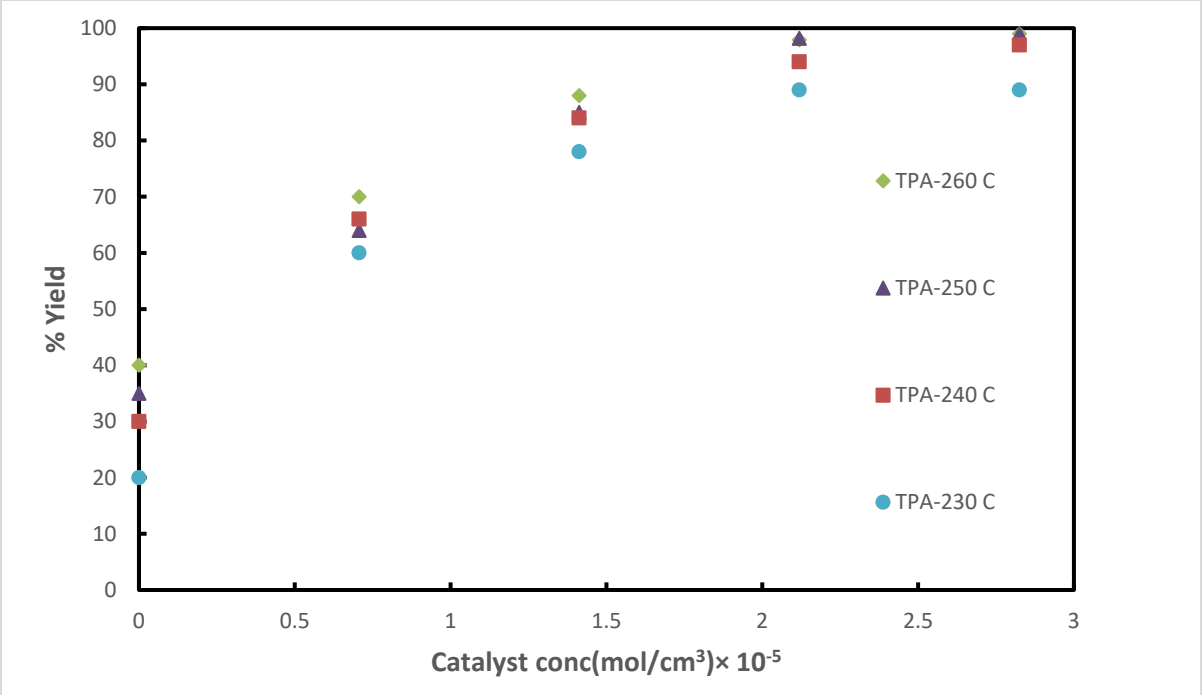

Figure A2.13. Effect of catalyst concentration on TPA yield at different temperature in presence of PEG 400. (Reaction condition- Temperature: 240°C; Reaction time: 30 min; PET concentration: 5.27×10^{-4} (mol/cm^3); Water: 100 cm^3 Speed of agitation: 650 rpm) (Analysis based on HPLC Method).

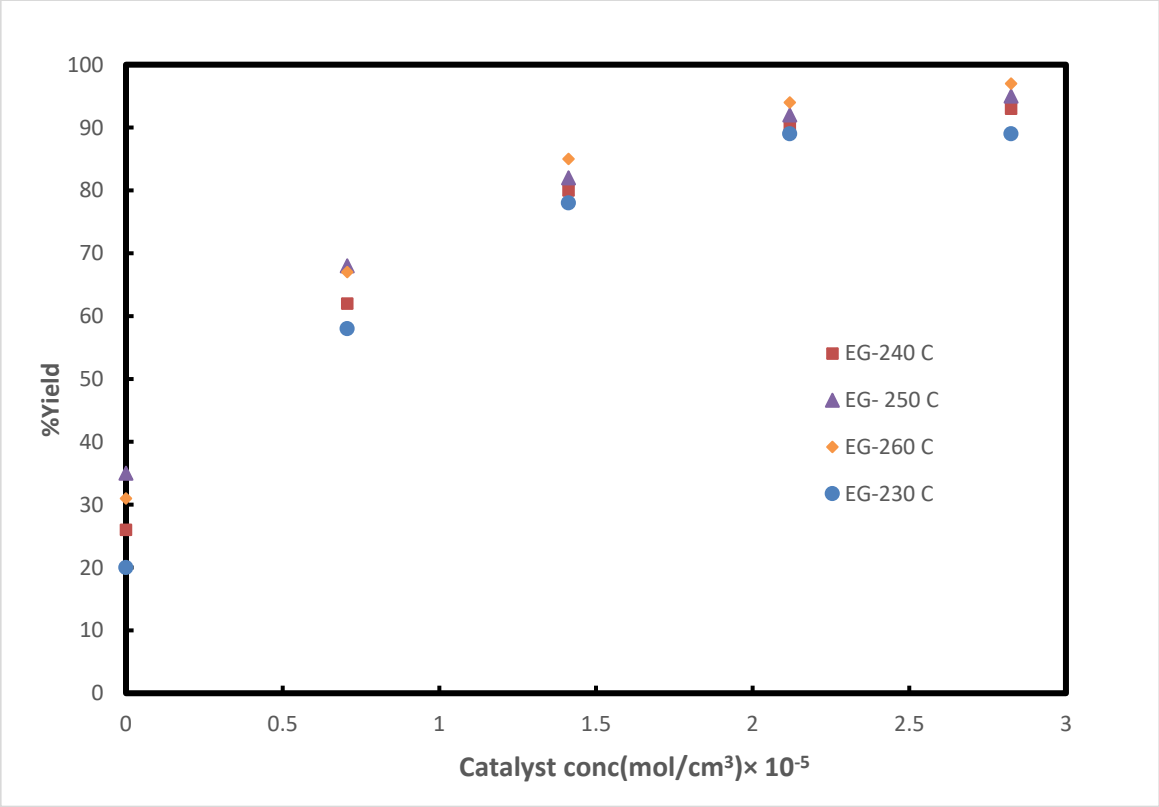

Figure A2.14. Effect catalyst concentration on EG yield at different temperature. (Reaction condition- Temperature: 240℃; Reaction time: 30 min; PET concentration: 5.27×10^{-4} (mol/cm^3); Water: 100 cm^3 Speed of agitation: 650 rpm) (Analysis based on HPLC Method).

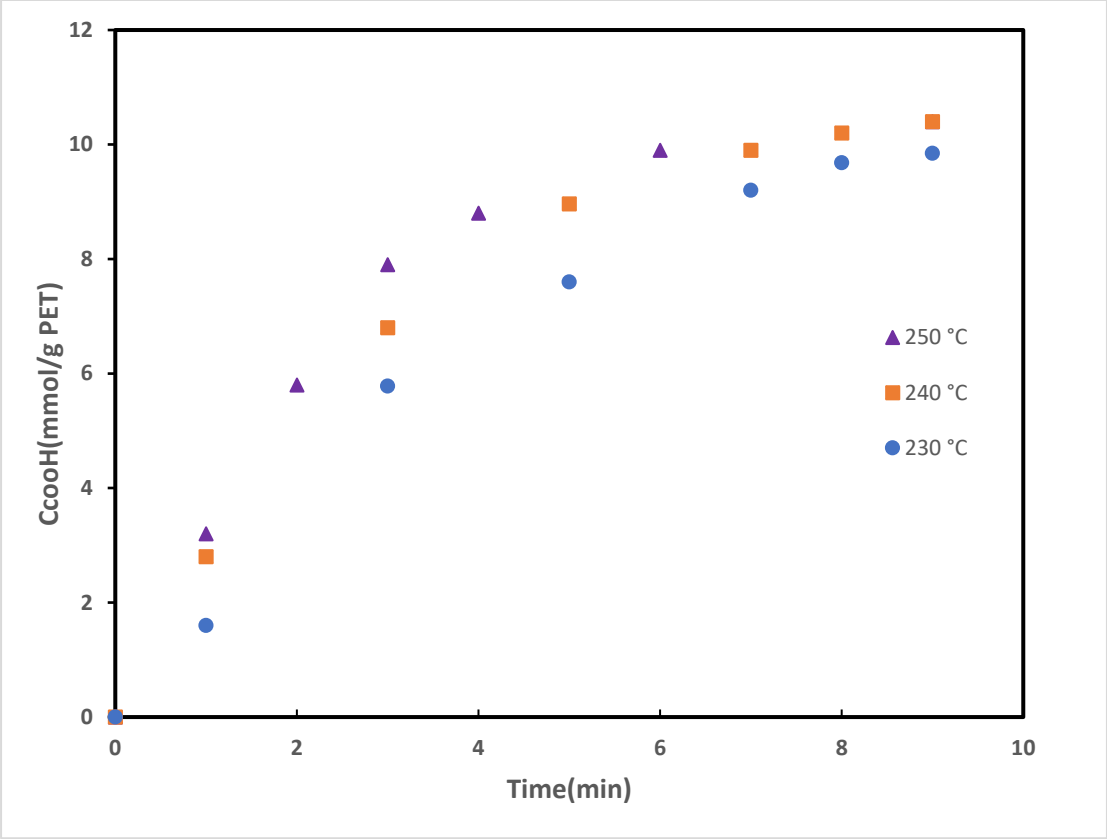

Figure A2.15. Effect of Temperature carboxylic group concentration for short reaction time. (Reaction condition- Catalyst concentration: 2.11× 10^{-5} mol/cm^3; PET concentration: 5.27×10^{-4}(mol/cm^3); Water: 100 cm^3; Speed of agitation: 650 rpm). (Analysis based on end group).

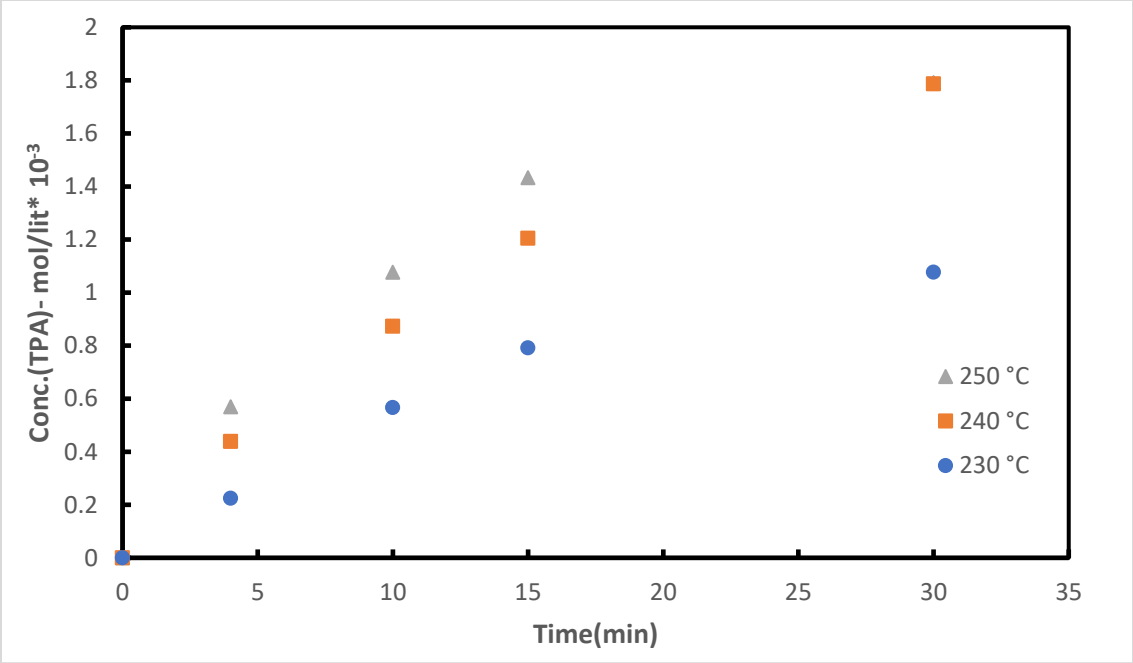

Figure A2.16. Effect of Temperature terephthalic acid concentration for short reaction time. (Reaction condition- Catalyst concentration: 2.11×10^{-5} mol/cm^3; PET concentration: 1.786×10^{-4} (mol/cm^3); Water: 100 cm^3; Speed of agitation: 650 rpm) (Analysis based on HPLC Method).

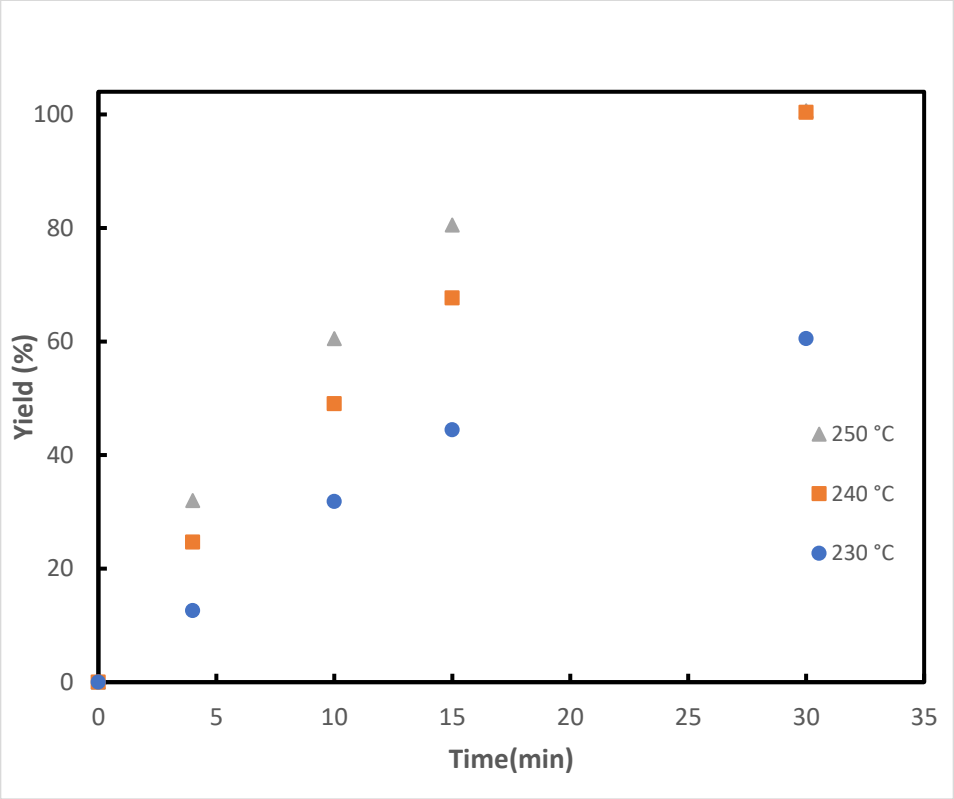

Figure A2.17. Effect of Temperature TPA yield for reaction short reaction time. (Reaction condition- Catalyst concentration: 2.11×10^{-5} mol/cm^3; PET concentration: 1.786×10^{-4} (mol/cm^3); Water: 100 cm^3; Speed of agitation: 650 rpm) (Analysis based on HPLC Method).

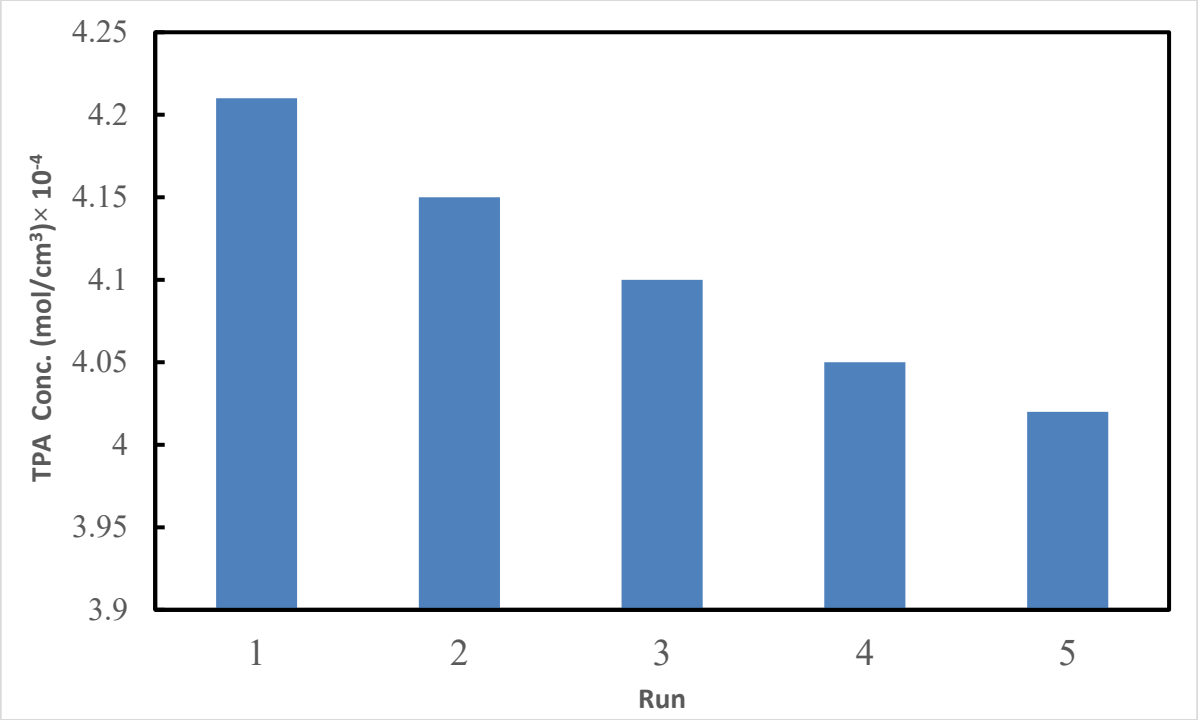

Figure A2.18. Reusability of PEG 400 (Reaction condition- Temperature: 240℃; Catalyst concentration: 2.11× 10^{-5} mol/cm^3; PET concentration: 1.786×10^{-4} (mol/cm^3); Water: 100 cm^3; Reaction time: 30 min; Speed of agitation: 650 rpm) (Analysis based on HPLC Method).

Table A2.1 Thermal properties of PET samples at various reaction times

Reaction time (min)	Glass transition temperature (°C)	Crystallization temperature (°C)	Melting Temperature (°C)	Enthalpy of Crystallization ΔH_C (J/g)	Enthalpy of melting ΔHm (J/g)	% Crystallinity		
						$\Delta H_C / \Delta H_{lit}$	$\Delta Hm / \Delta H_{lit}$	$(\Delta H_C / \Delta H_{lit}) – (\Delta Hm / \Delta H_{lit})$
0	75	160	230	13.25	32	9.04	22.3	13.26
5	70	160	225	20	30	14.13	21.43	7.3
10	65	NA	220	22	30	15.31	21.42	6.11
15	NA	NA	210	NA	5	-	-	
20	NA	NA	NA	NA	NA	-	-	
30	NA	NA	NA	NA	NA	-	-	

APPENDIX A4: CHAPTER 4

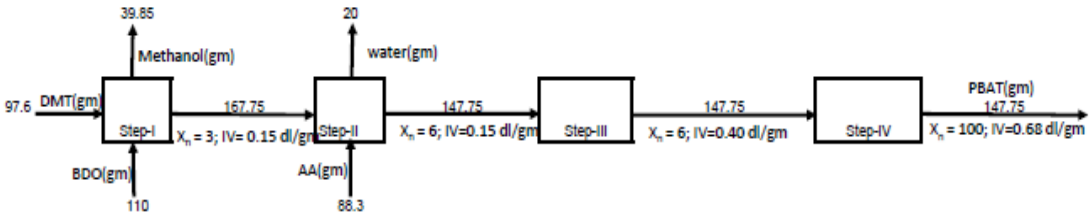

Figure A4.1. PBAT synthesis mass balance for different stages.

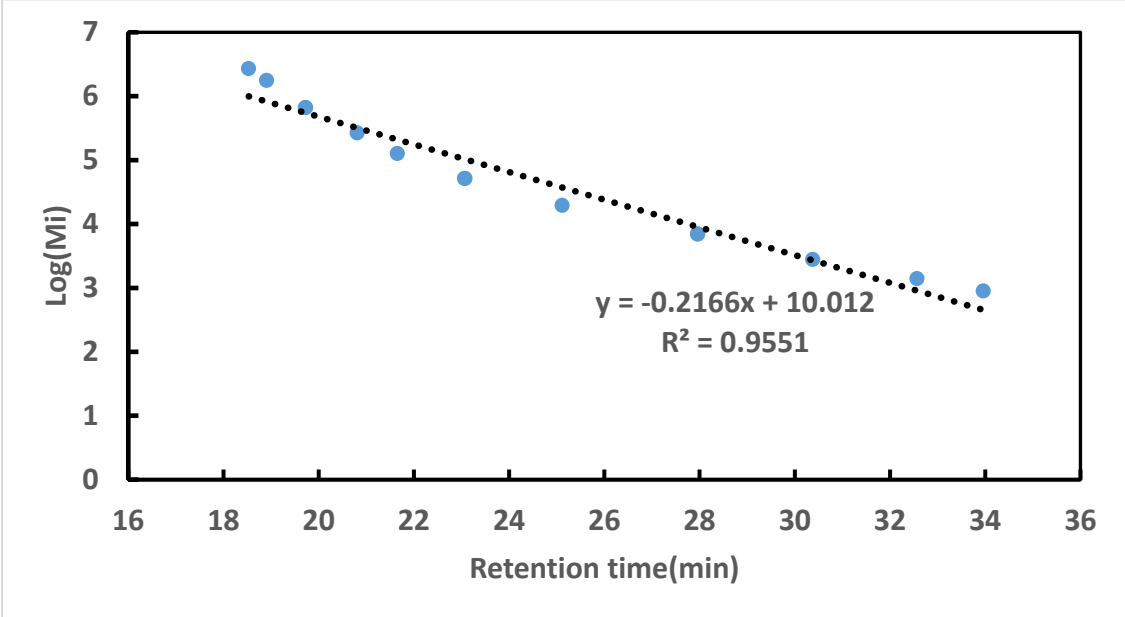

Figure A4.2. Polystyrene calibration curve log (Mi) versus retention time.

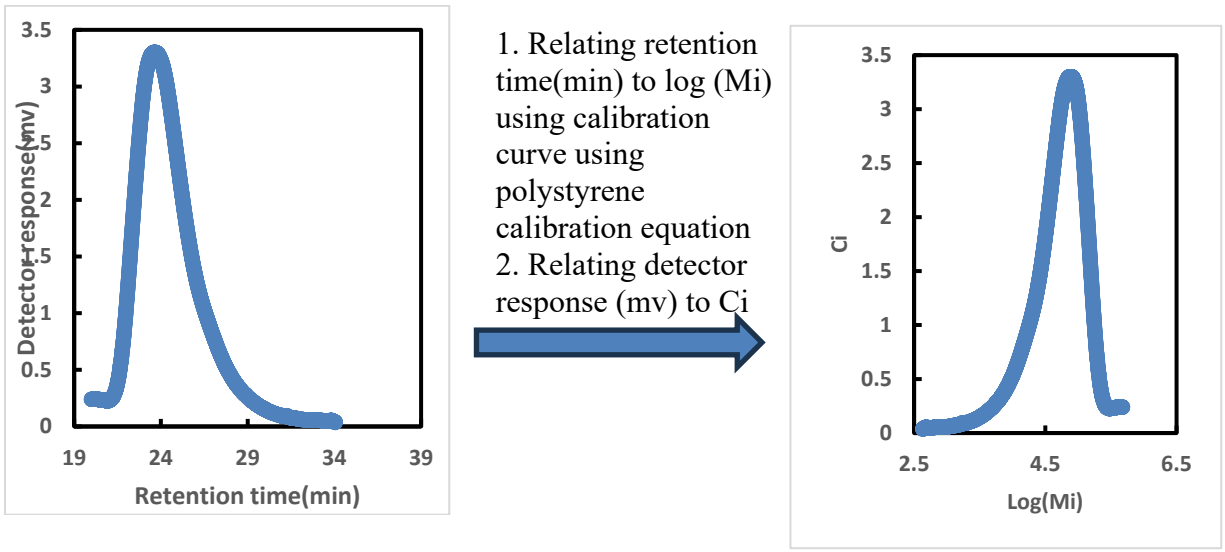

(a) (b)

Figure A4.3. PBAT Gel permeation chromatography data processing (a) raw data, (b) processed by relating retention time to log(Mi) and detector response to concentration.

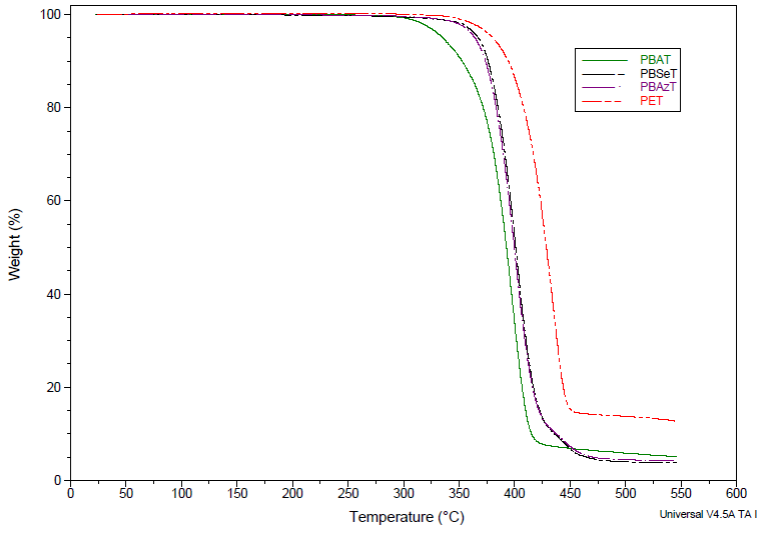

Figure A4.4. TGA plot after stage-IV (polycondensation-II) for polymer varying for aliphatic acid carbon content (cooling cycle).

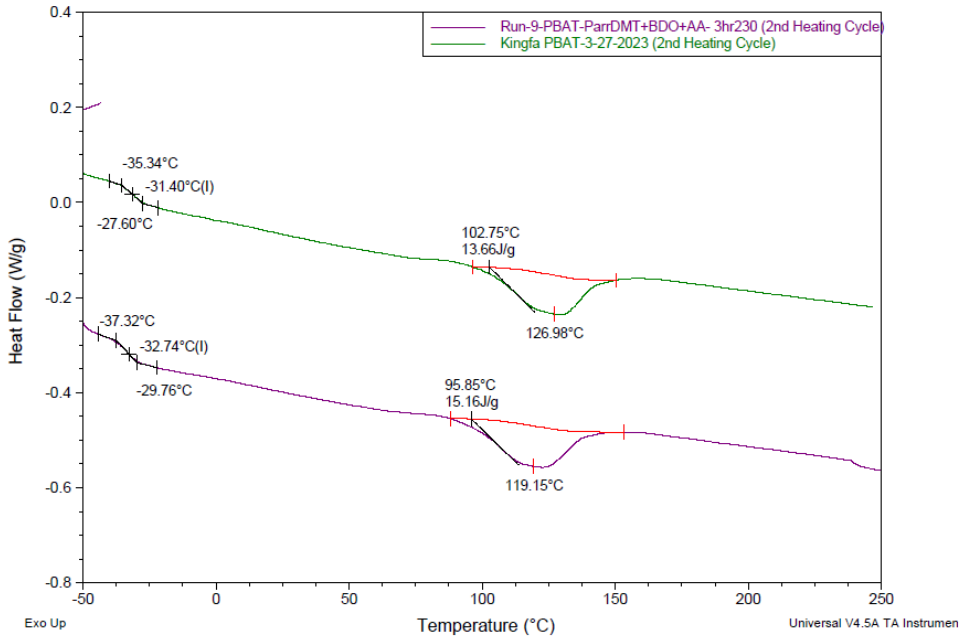

Figure A4.5. DSC overlay plot for Run-9-3 hr @230C and kingfa polymer.

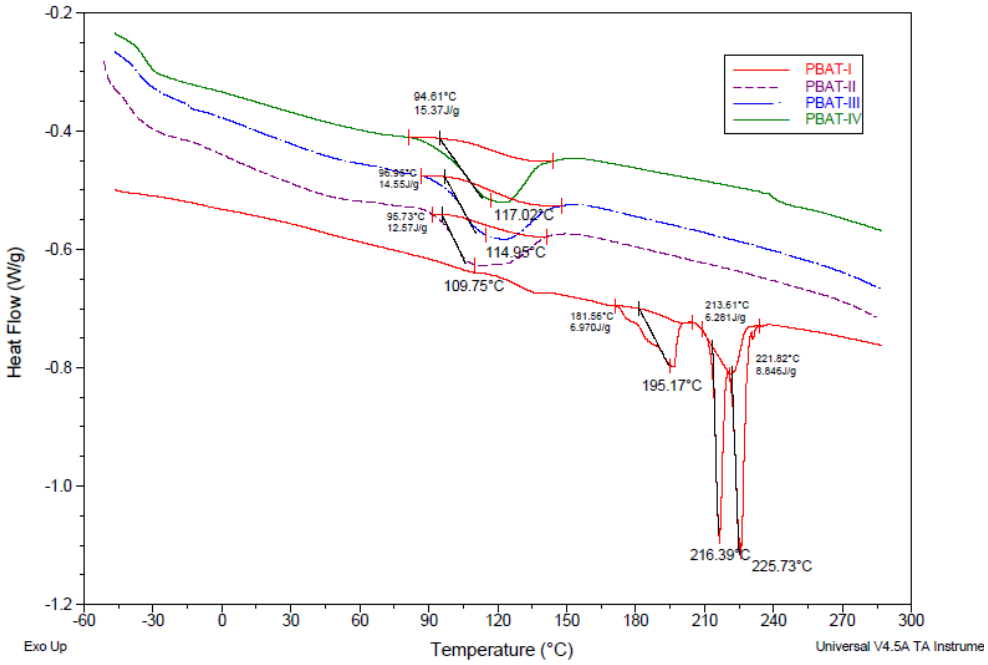

Figure A4.6. DSC plot for PBAT polymer for different stages (second heating cycle).

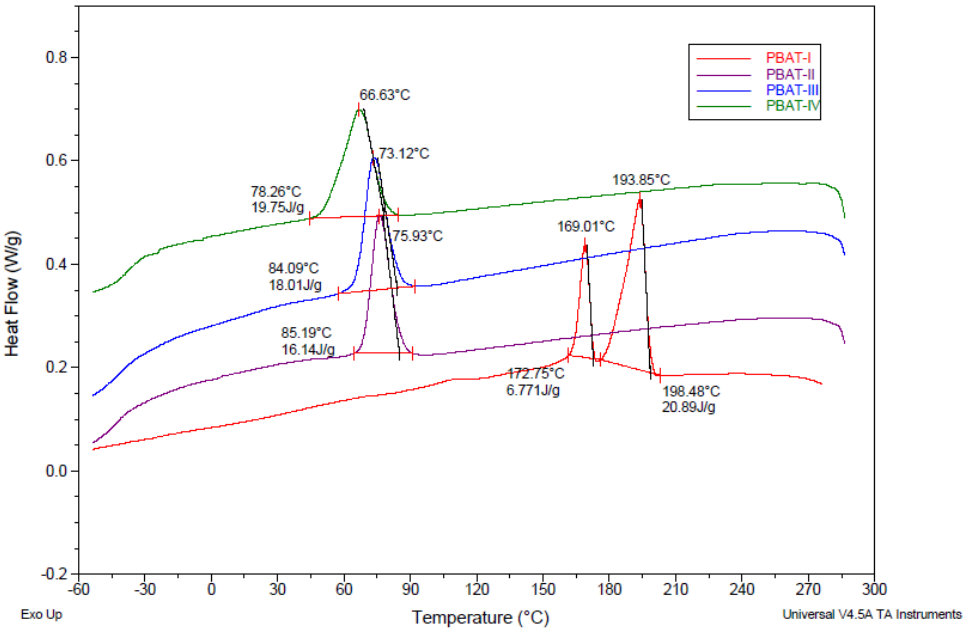

Figure A4.7. DSC plot for PBAT polymer for at different stages of reaction (cooling cycle).

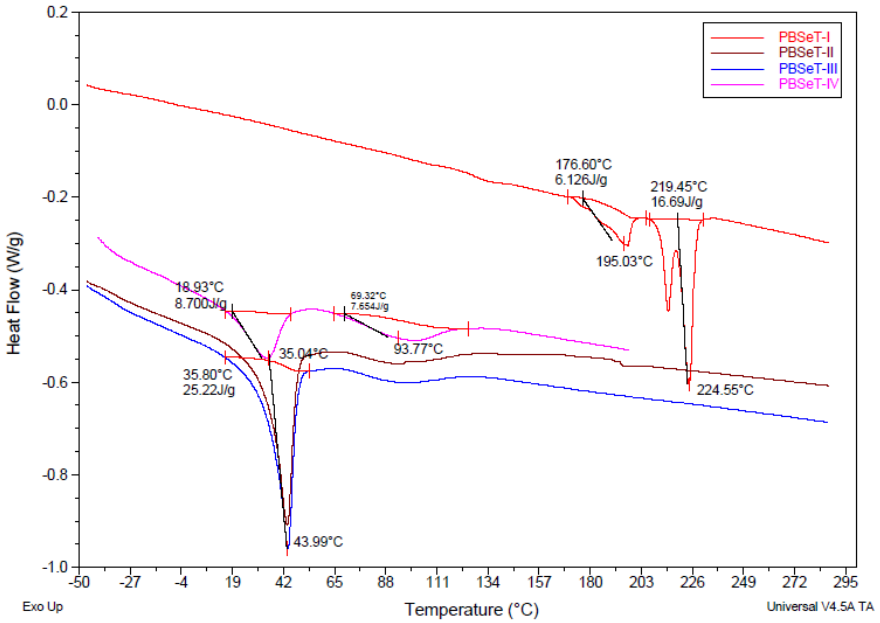

Figure A4.8. DSC plot for PBSeT polymer for different stages (second heating cycle).

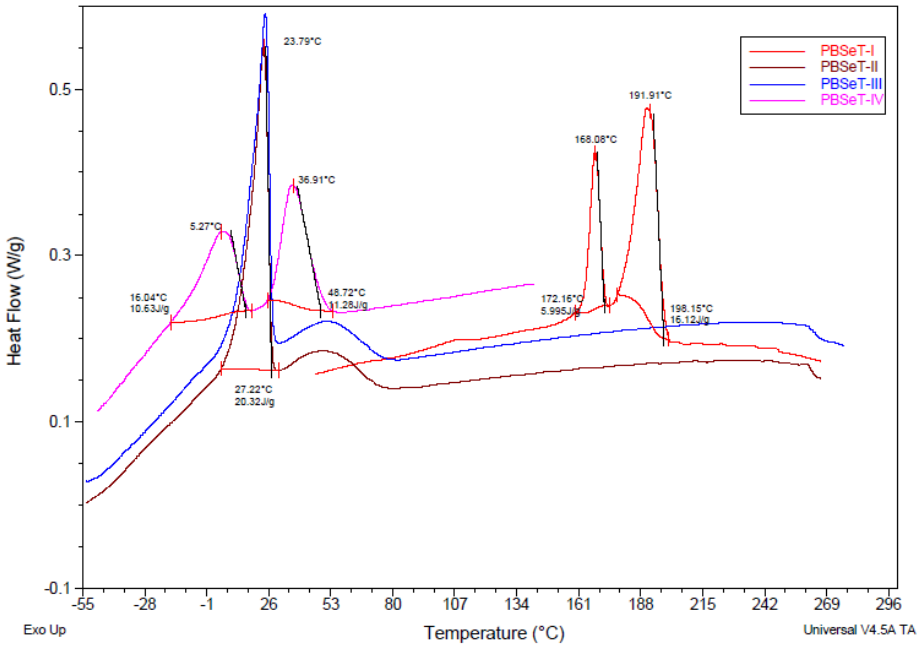

Figure A4.9. DSC plot for PBSeT polymer for different stages (cooling cycle).

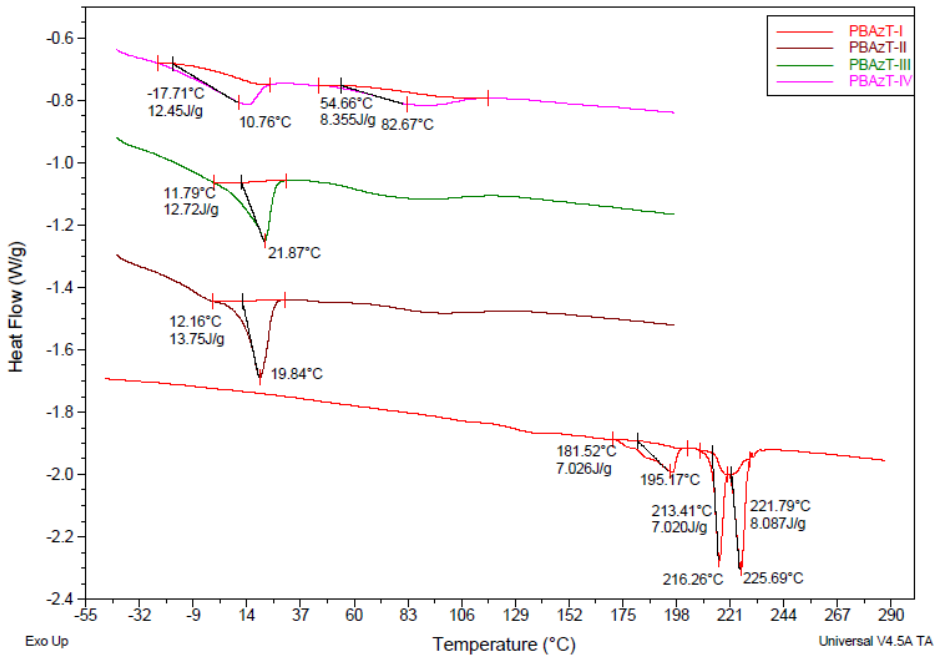

Figure A4.10. DSC plot for PBAzT polymer for different stages (heating cycle).

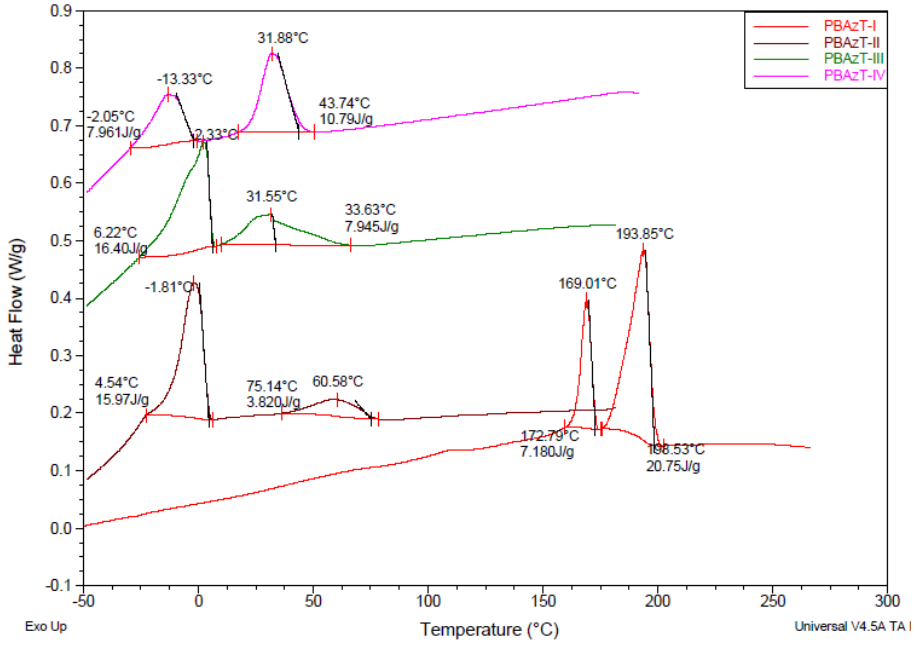

Figure A4.11. DSC plot for PBAzT polymer for different stages (cooling cycle).

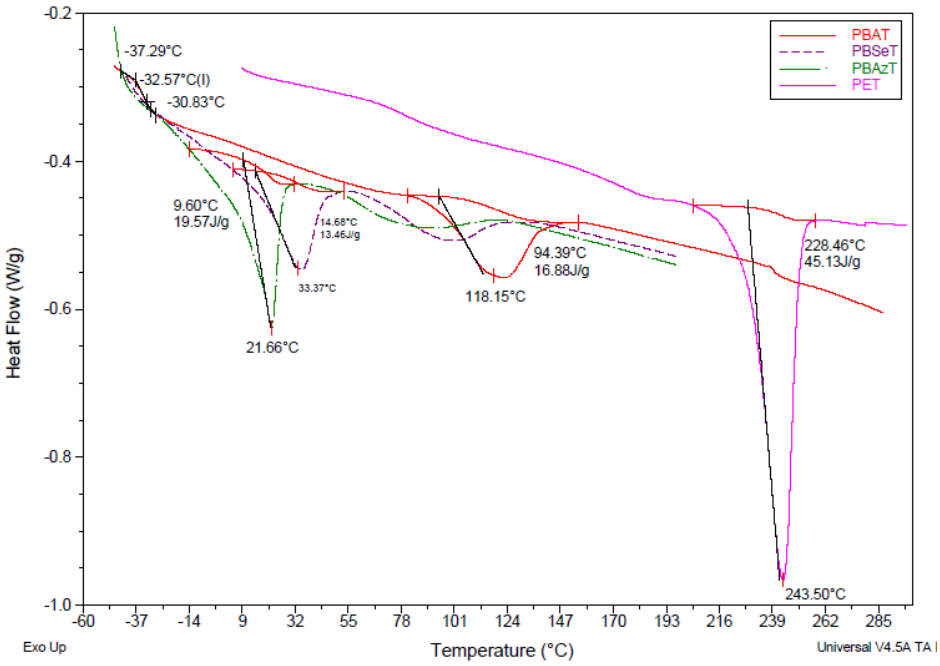

Figure A4.12. DSC plot after stage-IV (polycondensation-II) for polymer varying for aliphatic acid carbon content (second heating cycle).

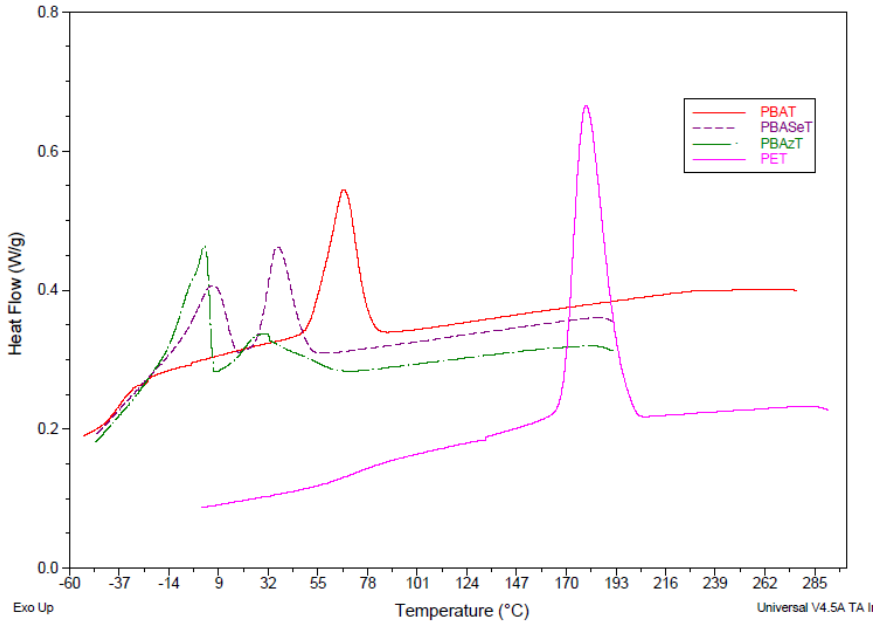

Figure A4.13. DSC plot after stage-IV (polycondensation-II) for polymer varying for aliphatic acid carbon content (cooling cycle).

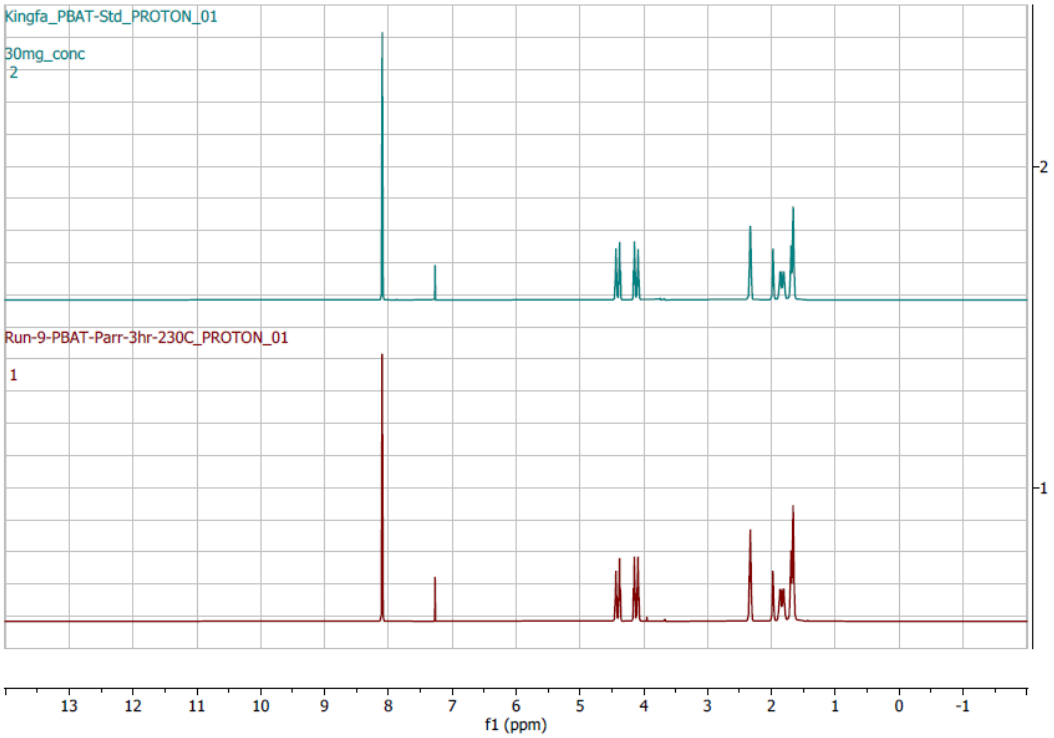

Figure A4.14. [1]H NMR of PBAT sample after stage-IV (polycondensation-II) and commercial sample.

APPENDIX A5: CHAPTER 5

Table A5.1 Review of commercial technologies for compost operation

Company	Prcoess	Product- Claimed	Process time and demand for utility
Harp renewables	Feed- organic waste+ microorganism+ compostable waste Digester convert food waste into soil amendment product	Solid- soil amendment product	24 hr 38KWh/day
Ecosafe/ Bio-material digester	Digester convert food waste into gray water	Liquid- gray water directly discharged into drain	NA
LFC digester	Digester convert food waste into gray water	Liquid- gray water directly discharged into drain	24 hr 1.85KWh/day (for 9-75kg capacity machine)
Lomi	Feed- organic waste+ microorganism+ compostable polymers Convert food waste into soil amendment product	Solid- soil amendment product	3-5 h 0.75KWh/ 5h(one cycle)
Airtheral	Feed- organic waste+ microorganism convert food waste into soil amendment product	Solid- soil amendment product	2-7 h
Reencle	Feed- organic waste+ microorganism	Solid- soil amendment product	24 h/1kg waste 1.25KWh/day
Dailydump	Feed- organic waste+ microorganism+ neem leaves	Solid- Compost	30 days No electricity required
Tero	Feed- Food waste	Soil nutrient rich fertilizer	24 hr

Figure A5.1. Picture of compost bioreactor for visual observation of compostable bags.